INFORMATION TO USERS

This manuscript has been reproduced from the microfilm master. UMI films the text directly from the original or copy submitted. Thus, some thesis and dissertation copies are in typewriter face, while others may be from any type of computer printer.

The quality of this reproduction is dependent upon the quality of the copy submitted. Broken or indistinct print, colored or poor quality illustrations and photographs, print bleedthrough, substandard margins, and improper alignment can adversely affect reproduction.

In the unlikely event that the author did not send UMI a complete manuscript and there are missing pages, these will be noted. Also, if unauthorized copyright material had to be removed, a note will indicate the deletion.

Oversize materials (e.g., maps, drawings, charts) are reproduced by sectioning the original, beginning at the upper left-hand corner and continuing from left to right in equal sections with small overlaps.

Photographs included in the original manuscript have been reproduced xerographically in this copy. Higher quality 6" x 9" black and white photographic prints are available for any photographs or illustrations appearing in this copy for an additional charge. Contact UMI directly to order.

Bell & Howell Information and Learning
300 North Zeeb Road, Ann Arbor, MI 48106-1346 USA
800-521-0600

UMI®

The role of the renal sodium-dependent phosphate cotransporter genes, NPT1 and NPT2, in inherited hypophosphatemias.

by

Claudine H. Kos

Department of Biology
McGill University
Montreal, Quebec
January 1998

A thesis submitted to the Faculty of Graduate Studies and Research in partial fulfilment of the requirements of the degree of Ph.D.

Dedicated with love to
Helen Rita Szczygiel-Kos
and in memory of
Mary Ann Gavin-Farrell
Stephanie Elizabeth Morse
and
Zarka Leigh Smith

Abstract

This thesis includes three studies examining the role of the type I (NPT1) and type II (NPT2) renal sodium (Na^+)-phosphate (Pi) cotransporter genes in inherited hypophosphatemias. In the first study, the chromosomal locations of the NPT1 and NPT2 genes in human and rabbit are determined by physical mapping techniques. The NPT1 and NPT2 genes map respectively to human chromosomes 6p22 and 5q35 and to rabbit chromosomes 12p11 and 3p11. The localization of the two cotransporter genes to autosomes excludes them as candidate genes for X-linked hypophosphatemia. In addition, these assignments agree with the previously reported homology between rabbit chromosome 12 and human chromosome 6 and provide the basis for the establishment of a conserved syntenic group between rabbit chromosome 3 and human chromosome 5.

The goal of the second study was to clone, sequence and characterize the structure of the human NPT2 gene in order to design intronic primers to amplify NPT2 exons from patient DNA. Parallel experiments were performed on the mouse *Npt2* gene, so that a vector could be designed to knockout the mouse *Npt2* gene. In both species, the type II renal Na^+-Pi cotransporter gene is approximately 16kb in length and is comprised of 13 exons and 12 introns. This work provides a basis for the study of the regulation of NPT2 transcription and facilitates the screening of DNA samples from patients with autosomally inherited disorders of renal Pi reabsorption for mutations in the NPT2 gene.

In the third study, polymorphic markers flanking the NPT1 and NPT2 genes were typed in members of a Bedouin kindred segregating the autosomal disorder Hereditary hypophosphatemic rickets with hypercalciuria (HHRH). Genotype data were examined for excess homozygosity and allele sharing among affected pedigree members. Data did not reveal excess allele sharing on either chromosome 6 or 5, where the NPT1 and NPT2 genes are located, but suggested chromosome 3p as a site for further investigation. Identification of a HHRH locus is the first step toward identifying a gene involved in the pathophysiology of this disorder.

Résumé

Cette thèse comprend trois études sur le rôle du gène cotransporteur rénal de type I et II dans l'hypophosphatémie héréditaire. Dans la première étude, on détermine par des techniques de cartographie physique que les gènes NPT2 et NPT1 sont localisés chez l'homme sur les chromosomes 6p22 et 5q35 respectivement, et sur les chromosomes 12p11 et 3p11 chez le lapin. Localisés sur des autosomes, ces deux gènes ne sont pas susceptibles d'être responsables de l'hypophosphatémie liée au chromosome X. En plus de confirmer l'homologie déjà connue entre le chromosome 12 du lapin et 6 de l'homme, ce résultat fournit la base pour l'établissement d'une section de correspondances chromosomiques entre les chromosomes 3 du lapin et 5 de l'homme.

L'objectif de la seconde étude est de cloner, séquencer et caractériser la structure du gène humain NPT2 afin de déterminer ultérieurement les amorces introniques qui amplifieront les exons NPT2 dans l'ADN du patient. Chez la souris, des expériences similaires ont été faites dans le but de concevoir un vecteur qui détruise le gène *Npt2*. Les gènes NPT2 et *Npt2* ont une longueur approximative de 16 kb et sont composés de 13 exons et de 12 introns. Ces connaissances sont d'une part nécessaires pour l'étude de la régulation de la transcription du gène NPT2; et d'autre part elles facilitent la recherche de mutations de ce gène dans l'ADN des patients atteints de l'hypophosphatémie héréditaire.

Dans la troisième partie, on dispose des échantillons de l'ADN de 61 membres d'une famille bédouine, dont certains qui souffrent de la maladie autosomale appelée le rachitisme héréditaire hypophosphatémique avec hypercalciurie (RHHH). Après détermination de la taille des allèles des marqueurs polymorphiques qui entourent les gènes NPT1 et NPT2, les données du génotype ont permis de détecter une homozygosité excessive et l'allèle commun (sharing) chez les membres atteints. Il s'est avéré que les chromosomes 5 et 6, qui contiennent les gènes NPT1 et NPT2, ne présentaient pas de l'allèle commun, contrairement au chromosome 3p qui requiert une recherche plus approfondie. La localisation du RHHH sur un chromosome permettrait d'identifier un des gènes responsables de la pathophysiologie de cette maladie.

Table of Contents

Index of Figures and Tables

Chapter 1. General Introduction

Chapter 2. Chromosomal localization of the NPT1 and NPT2 genes

Localization of a renal sodium-phosphate cotransporter gene to human chromosome 5q35

High resolution mapping of the renal sodium-phosphate cotransporter gene (NPT2) confirms its localization to human chromosome 5q35

Comparative mapping of Na^+-phosphate cotransporter genes, NPT1 and NPT2, in human and rabbit

Chapter 3. NPT2 Gene Structure

Sructure of murine and human renal type II Na^+-phosphate cotransporter genes (Npt2 and NPT2)

Chapter 4. A search for the gene responsible for HHRH

List of Abbreviations

ADHR	Autosomal dominant vitamin D resistant rickets
ADH	Autosomal dominant hypocalcemia
ABHHRH	one of three small pedigrees made from portions of the large Bedouin kindred
AHHRH	one of eight small pedigrees made from portions of the large Bedouin kindred
BBM	brush border membrane
BHHRH	one of eight small pedigrees made from portions of the large Bedouin kindred
BLM	basolateral membrane
bp	basepair
Ca^{2+}	calcium
cDNA	complementary DNA
CGR	Center for Genome Research (at the WIBR at MIT)
CHHRH	one of eight small pedigrees made from portions of the large Bedouin kindred
CLCN5	chloride channel gene mutated in X-linked hypercalciuric nephrolithiasis
cM	centiMorgan (genetic mapping unit)
cR	centiRay (radiation hybrid mapping unit)
DHHRH	one of eight small pedigrees made from portions of the large Bedouin kindred
DEGHHRH	one of three small pedigrees made from portions of the large Bedouin kindred
DIG	deoxygenin
diphor-1	dietary Pi-regulated RNA-1
ECE	endothelin converting enzyme gene
EHHRH	one of eight small pedigrees made from portions of the large Bedouin kindred
FHHRH	one of eight small pedigrees made from portions of the large Bedouin kindred
FISH	fluorescent *in situ* hybridization
GHHRH	one of eight small pedigrees made from portions of the large Bedouin kindred
Glvr-1	cell surface receptor for gibbon ape leukemia virus which function as a Na^{+}-Pi cotransporter
Gy	X-linked hypophosphatemia-gyrorotory (mouse disorder)
HBD	Hypophosphatemic bone disease
HHHRH	one of the small pedigrees made from portions of the large Bedouin kindred
HHRH	Hereditary hypophosphatemic rickets with hypercalciuria
HSA	*Homo sapien*
Hyp	X-linked hypophosphatemia (mouse disorder)
IBD	identity or identical by descent
IBS	identity by state
ID	identification number
kb	kilobase
kD	kiloDalton
LGMD2A	Limb girdle muscular dystrophy (inherited human disorder)
Mb	megabase
min	minutes

MIT	Massachusetts Institute of Technology
Na^+	sodium
NEP	neutral endopeptidase gene
NPT1, *Npt1*	type I renal sodium-phosphate cotransporter gene symbol in human and mouse
NPT2, *Npt2*	type II renal sodium-phosphate cotransporter gene symbol in human and mouse
Npt2$^{-/-}$	homozygous *Npt2* knock-out mouse
OCU	*Oryctolagus cuniculus* (Latin name for domestic rabbit)
OHO	Oncogenic hypophosphatemic osteomalacia (acquired human disorder)
PCR	polymerase chain reaction
PCT	proximal convoluted tubule
PEX	phosphate regulating gene with homology to endopeptidases, on the X-chromosome
Pi	inorganic phosphate
PIC	polymorphic information content
PST	proximal straight tubule
PT	proximal tubule
PTH	parathyroid hormone
Ram-1	cell surface receptor for rat amphotropic virus which functions as a Na^+-Pi cotransporter
RFLP	restriction fragment length polymorphism
RH	radiation hybrid
SCH	somatic cell hybrid
s	seconds
STR	short tandem repeat
WIBR	Whitehead Institute for Biomedical Research
VNTR	variable number of tandem repeat
XLH	X-linked hypophosphatemia (human disorder)
XLHN	X-linked hypercalciuric nephrolithiasis
XLRHR	X-linked recessive hypophosphatemic rickets
µl	microliter
µM	micromolar
^oC	temperature units degrees Celsius
$1,25(OH)_2D$	1,25-dihydroxyvitamin D

Preface

In compliance with the Faculty of Graduate Studies and Research, the following excerpt from the "Guidelines for Thesis Preparation" is cited below:

> *"Candidates have the option of including, as part of the thesis, the text of one or more papers submitted or to be submitted for publication, or the clearly-duplicated text of one or more published papers. These texts must be bound as an integral part of the thesis.*
>
> *If this option is chosen, connecting texts that provide logical bridges between the different papers are mandatory. The thesis must be written in such a way that it is more than a mere collection of manuscripts; in other words, results of a series of papers must be integrated.*
>
> *The thesis must still conform to all other requirements of the "Guidelines for Thesis Preparation". The thesis must include: a table of contents, an abstract in English and French, an introduction which clearly states the rationale and objectives of the study, a review of the literature, a final conclusion and summary, and a thorough bibliography or reference list.*
>
> *Additional material must be provided where appropriate (e.g. in appendices) and in sufficient detail to allow a clear and precise judgment to be made of the importance and originality of the research reported in the thesis.*
>
> *In the case of manuscripts co-authored by the candidate and others, the candidate is required to make an explicit statement in the thesis as to who contributed to such work and to what extent. Supervisors must attest to the accuracy of such statements at the doctoral oral defense. Since the task of the examiners is made more difficult in these cases, it is in the candidate's interest to make perfectly clear the responsibilities of all the authors of the co-authored papers."*

This dissertation includes four published articles. Three of these articles are presented in chapter 2 and a fourth in chapter 3. All four manuscripts were co-authored by my supervisor Dr. H.S. Tenenhouse. I performed the work described in the four manuscripts with the exception of the following contributions made by co-authors.

Contributions by co-authors

Chapter 2.

Localization of a renal sodium-phosphate cotransporter gene to human chromosome 5q35 ,Genomics volume 19: 176-177 1997. Kos, C.H., Tihy, F., Murer, H. Lemieus, N., Tenenhouse, H.S.

The somatic cell hybrid mapping was done in the laboratory of M. Econs at Duke University. The rabbit NPT1 and NPT2 and human NPT2 cDNA probes were gifts of H. Murer of Zurich, Switzerland. The fluorescent *in situ* hybridization was done with the assistance of F. Tihy in the laboratory of N. Lemieux.

High resolution mapping of the renal sodium-phosphate cotransporter gene (NPT2) confirms its localization to human chromosome 5q35, Pediatric Research volume 41: 632-634 1997. McPherson, J., Wagner-McPherson, C.B., Krane, M.C., Kos, C.H., Tenenhouse, H.S.

The somatic cell hybrid-, radiation hybrid-, and fluorescent *in situ* hybridization mapping were done by M.C Krane and C.B. Wagner-McPherson in the laboratory of J. McPherson at University of California-Irvine.

Comparative mapping of Na^+-phosphate cotransporter genes, NPT1 and NPT2, in human and rabbit, Cytogenetics and Cell Genetics volume 75: 22-24 1996. Kos, C.H., Tihy, F., Murer, H. Lemieus, N., Tenenhouse, H.S.

H. Murer provided three of the cDNA probes. The fluorescent *in situ* hybridization was done with the assistance of F. Tihy in the laboratory of N. Lemieux.

Chapter 3.

Structure of murine and human renal type II Na^+-phosphate cotransporter genes (Npt2 and NPT2), Proceedings of the National Academy of Sciences USA volume 93: 7409-7414 1996. Hartman, C., Hewson, S., Kos, C.H., Hilfiker, H., Murer, H., Tenenhouse, H.S.

C.M Hartmann and H. Hilfiker performed the mouse promoter studies in the laboratory of H. Murer. A.S. Hewson screened the mouse library and characterized the mouse *Npt2* intron exon boundaries. Y. Soumounou assisted in confirming the intron/exon boundary sequences.

Acknowledgments

I would like to extend my gratitude to my two thesis supervisors, Dr. Susie Tenenhouse and Dr. Ken Morgan, for their assistance and guidance during my doctoral training. Having me as a student was not always easy. I commend them for their perseverance. Susie and Ken introduced me to several other talented scientists and provided me with many opportunities for collaboration. I would also like to thank the three 'de facto' supervisors that looked after me during my various stages (French meaning of the word). They are Dr. Nicole Lemieux, Dr. Andrew Karaplis, and Dr. Thomas Hudson. These three people shared with me their laboratories, their scientific expertise and numerous chocolate moments.

I had several unusual supervisory committee meetings including one that lasted only 15 minutes. I thank my supervisory committee members, Dr. C.R Scriver, Dr. R. Rozen, and Dr. D.M. Green for finding the time to run all over Montreal to meet with me and of course, for their insightful questions and support. David Green gets a special thank you for allowing me to participate in his course and for spending so many hours talking with me in his office.

Since I worked in so many laboratories, it would be impossible to thank all the people who have helped me with my experiments and made me laugh. I would like to thank my fellow students and the staff in the departments of biochemical genetics and cytogenetics at the Montreal Children's Hospital, Annie Bilodeao and Louise Laquerre at the Université de Montréal for helping me make my slides when my mother was sick, Michelle Gschwend, Melanie Mahatani, John Rioux, Christinia Vestergaard, and the countless other people at the Center for Genome Research at MIT's Whitehead Institute for Biomedical Research who taught me a great deal in a short time, Danielle Frappier and all of the members of Ken's and Tom's team for incorporating me into the new lab at the MGH, Lynda McNeil for her help during the writing and submission of my thesis and Fran Langton of Human Genetics Dept. for consistently exceeding her responsibilities and doing everything that everyone else was either unable or unwilling to do.

I also would like to thank Dr. Virginia Hayssen and Dr. Jeanne Powell for their inspiration and good stories and Jean B., Mark W., Suzanne C., Don C., Tara H., Dan F., Emily T., Andrew T., Francois L., Benoit O., Valerie Y., Tanya K., Paul M., Kevin N., Stacy H., Elizabeth B., Rick H., Judy L., Kathryn G., Aude J., David B., Pierre L., Chantal D., Rob S., Pierre B., Kevin C., Charles F., Cristyn W., Giovanni G., David T., Sarah H., Carl A., Raj A., Peter A., Jodi F., Olivier R., Lisa F., Scott M., Martin K., Brad G., Jamie E., Daniel P., Andrea G., Sylvain M., Dave T., Phil T., Tom M., Amber S., Mary Jane P., Peter H., Greg M. and Silvia V. for making Montreal memorable. And to Nicolas M.

I extol my deepest personal gratitude to Alan Levin, Frédérique Tihy, Laurent Beck, and Maite Maldonado. They assisted me in numerous professional ways, but it is for making my life special that I love them.

Merci beaucoup à mon Riri, un homme spécial (signification anglaise), pour la traduction de mon résumé.

Mostly, I want to thank to my mother, my father, my sisters Shannon and Lauren, Babci, Jennie, Connie and my cat Sam for being incredible people (except for Sam) and sharing their lives with me.

Chapter 1. General Introduction

Background

Phosphorus plays a fundamental role in many aspects of cellular metabolism. It participates in energy provision and transfer in the form of ATP. It is involved in the regulation of enzyme activity via phosphorylation and dephosphorylation reactions and its concentration influences metabolic pathways such as glycolysis, and the formation of 1,25-dihydroxyvitamin D. It also is a component of DNA, RNA, membrane phospholipids and bone.

In combination with calcium (Ca^{2+}), phosphorus forms hydroxyapatite, the major mineral component of bone. The total phosphorus content of a 70kg man is about 700g (Chan and Bell, 1990), approximately 80-85% of which is deposited in the skeleton (Schrier and Gottschalk, 1988). The remainder is widely distributed throughout the body with roughly 14% intracellular and 1% in the extracellular fluid (Knochel and Agarwal, 1996). Serum phosphorus exists primarily as inorganic phosphate (Pi) with some organic phosphate found bound to proteins and in phospholipids. At physiological pH, serum Pi is present in two forms, HPO_4^{-2} and $H_2PO_4^{-1}$, at a ratio of 4:1. Serum Pi concentrations vary both with age and time of day, but are generally maintained in adults between 2.5 and 4.5 mg/dl (Knox and Haramati, 1985). Adequate levels of serum Pi, especially during the growth period, are necessary for normal bone formation.

Serum Pi concentration is determined by dietary phosphorus intake, intestinal phosphorus absorption and reabsorption of phosphorus by the kidney. The US Food and Drug Administration recommends that 1gm of phosphorus be ingested daily. Although, the bioavailability of phosphorus varies depending on the type of food, meeting this recommendation is easily achieved by eating a balanced diet rich in protein. The phosphorus content of the average US diet ranges between 800-1600mg per day (Rasmussen and Tenenhouse, 1995). Dietary phosphate deficiency is unlikely to develop except under conditions of extreme starvation or as a consequence of the administration of therapeutic phosphate binders (Rasmussen and Tenenhouse, 1995).

The major portion of ingested organic phosphate is broken down into Pi which is absorbed in the intestinal tract. There are two mechanisms for intestinal Pi absorption. The first is concentration dependent, passive diffusion. The second process is active sodium (Na^+)-dependent Pi transport, which is upregulated by the hormone 1,25-dihydroxyvitamin D ($1,25(OH)_2D$). Under normal conditions, intestinal Pi absorption

occurs principally by passive diffusion and the amount of phosphate absorbed in the intestine exceeds the body's requirements. Hormonal regulation of Pi absorption plays a minor role in maintaining phosphate homeostasis, functioning only under conditions of dietary Pi deprivation. The highest rate of intestinal Pi absorption occurs in the jejunum, followed by the duodenum and the ileum (Chan and Bell, 1990; Schrier and Gottschalk, 1988; Walling, 1977).

Renal phosphorus reabsorption

It is the kidney that plays the most important role in maintaining Pi homeostasis, and therefore, is important for proper bone mineralization and growth. Most of the Pi in serum (90-95%) is freely filtered at the glomerulus (Schrier and Gottschalk, 1988). Renal handling of Pi consists of regulated reabsorption from the glomerular filtrate. Once in the kidney, the proximal tubule (PT) is the major site of filtered Pi reabsorption and its regulation. In the normal subject, up to 85% of filtered Pi is reabsorbed in the PT, with 60% in the proximal convoluted tubule (PCT) and 15-20% in the proximal straight tubule (PST) (Chan and Bell, 1990; Rasmussen and Tenenhouse, 1995; Tenenhouse, 1997). The epithelial cells lining the PT are polarized with an apical brush border membrane (BBM) and a basolateral membrane (BLM). The two cell membranes are structurally and functionally different allowing for unidirectional transepithelial transport of Pi (Berry, 1987). Epithelial cells of the proximal tubule reabsorb Pi from the lumen by transporting it across the BBM, through the PT cell, and out across the BLM into the blood (Murer, 1992) (Figure 1).

Pi uptake across the BBM is the rate-limiting step in the overall process of Pi reabsorption. The transport of Pi across the BBM occurs by a Na^+-dependent process. The driving force of Pi transport, which occurs against its electrochemical gradient, is a Na^+ gradient maintained at the BLM by a Na^+/potassium ATPase (Figure 1). The binding of Na^+ to the apical surface of the cotransporter facilitates binding of Pi and the dissociation of Na^+ signals dissociation of Pi at the intracellular surface. Two kinetically distinct Na^+-dependent Pi transport systems in the kidney have been defined (Walker et al., 1987); a high-capacity low-affinity system in the PCT believed to reabsorb the bulk of filtered Pi and a low-capacity high-affinity system in both the PCT and PST that reclaims the residual Pi (Murer et al., 1991; Walker et al., 1987).

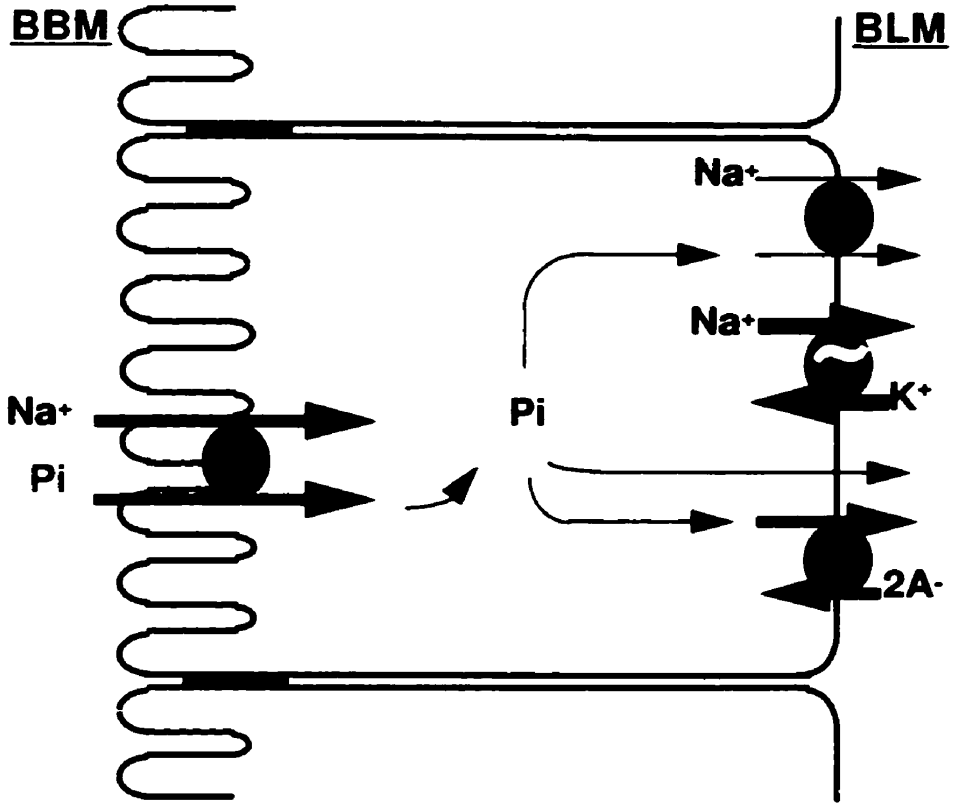

Figure 1. Transepithilal transport of inorganic phosphate (Pi) in a mammalian renal proximal tubule cell. Pi entry at the brush border membrane (BBB) occurs against an electrochemical gradient. The driving force is the sodium (Na^+) gradient maintained by the Na^+/potassium (K^+) ATPase at the basolateral membrane (BLM). It is postulated that Pi is transported out of the cell across the BLM via one of three mechanisms: diffusion, Na^+-Pi cotransport, or anion (A-) exchange.

Regulation of renal BBM Na^+-Pi cotransport

The major regulators of renal Na^+-Pi cotransport are parathyroid hormone (PTH) and dietary phosphate intake (Pi availability) (Murer and Biber, 1996; Murer et al., 1991). The primary physiological role of PTH is the maintenance of Ca^{2+} homeostasis. When serum Ca^{2+} levels are low, PTH stimulates 25-hydroxyvitamin-D-1-α-hydroxylase (1-α-hydroxylase) activity. The enzyme 1-α-hydroxylase converts 25-hydroxyvitamin D into $1,25(OH)_2D$, the most biologically active of the vitamin D metabolites (Reichel et al., 1989). The increase in serum levels of $1,25(OH)_2D$ induces bone resorption which results in an increase in both serum Ca^{2+} and Pi levels. $1,25(OH)_2D$ also acts on the intestine to increase the absorption of Ca^{2+} and Pi. In the kidney, PTH stimulates renal Ca^{2+} reabsorption, thereby further increasing serum Ca^{2+} levels. To prevent extracellular Ca^{2+} and Pi from exceeding their solubility product, PTH inhibits renal Pi reabsorption.

PTH action decreases the Vmax of both the low-affinity, high-capacity and high-affinity, low-capacity Na^+-Pi cotransport systems without changing the affinity of the transport systems for phosphate (Quamme, 1990; Rasmussen and Tenenhouse, 1995). This inhibition of renal Na^+-Pi cotransport systems by PTH occurs via both protein kinase A and protein kinase C signaling pathways and is independent of protein synthesis (Cole et al., 1987; Murer et al., 1991). It was shown that the inhibitory action of PTH on renal Pi transport is blocked by disrupting the microtubule network and preventing endocytosis (Kempson et al., 1989). Although an active endocytic pathway is necessary for the full inhibitory effect of PTH on apical Na^+-Pi cotransport activity, PTH does not increase the overall level of endocytosis in the cell (Paraiso et al., 1995). It is believed that PTH stimulates the preferential shuttling of Na^+-Pi cotransporters into endocytic vesicles (Murer and Biber, 1996). In this way, endocytic removal of Na^+-Pi cotransporters can be increased without increasing the overall rate of endocytosis of the cell. Endocytic internalization of the cotransporters from the plasma membrane is followed by rapid lysosomal proteolysis (Pfister et al., 1997) and recovery of Na^+-Pi cotransport activity requires de novo protein synthesis (Murer et al., 1996; Paraiso et al., 1995).

Like PTH, Pi deprivation stimulates the activity of 1-α-hydroxylase activity in the PT of the kidney. This increases serum levels of $1,25(OH)_2D$ which promotes bone resorption and increases intestinal absorption of Ca^{2+} and Pi in an effort to raise serum concentrations. The effect of dietary Pi deprivation on renal Pi reabsorption is opposite

to that of PTH. Dietary Pi deprivation stimulates an acute increase in the overall capacity of the renal PT to reabsorb Pi that occurs within 4 hours of a decrease in serum Pi levels (Levine et al., 1986; Trohler et al., 1976). The rapid adaptive increase in renal PT BBM Na^+-Pi cotransport activity and BBM Na^+-Pi cotransporter protein abundance is independent of protein synthesis. Similar to the response of the renal PT to PTH, the acute response of the renal PT to dietary Pi restriction is mediated by microtubule-dependent translocation of Na^+-Pi cotransporter proteins (Lotscher et al., 1997). The acute increase in Na^+-Pi cotransport activity is due to insertion of presynthesized Na^+-Pi cotransporter proteins into the BBM (Levi et al., 1994; Lotscher et al., 1997). Only after prolonged Pi deprivation is protein synthesis required to increase Na^+-Pi cotransport activity (Levi et al., 1994; Lotscher et al., 1997).

In addition to PTH and dietary Pi, there are many other hormonal and non-hormonal regulators of Na^+-Pi cotransport (Knox and Haramati, 1985; Ritz et al., 1980). Although the mechanisms are not fully understood, hormones which stimulate Pi reabsorption include insulin (Abraham et al., 1990), insulin-like growth factor-I (Caverzasio and Bonjour, 1989), and thyroid hormone (Noronha-Blob et al., 1988). Factors which inhibit renal Pi reabsorption are PTH-related peptide (Pizurki et al., 1988), calcitonin (Yusufi et al., 1987), atrial natriuretic factor (Nakai et al., 1988), epidermal growth factor (Arar et al., 1995), transforming growth factor-α (Pizurki et al., 1990) and gluccocorticoids (Levi et al., 1995).

Isolation and characterization of renal Na^+-Pi cotransporters

Since renal Na^+-Pi cotransporters are of low abundance and are imbedded within cellular membranes, they are difficult to purify by traditional methods without inactivating them. A group in Switzerland recently isolated, by expression cloning in *Xenopus* oocytes, several renal-specific high-affinity Na^+-Pi cotransporter cDNAs (Magagnin et al., 1993; Verri et al., 1995; Werner et al., 1991). The cDNAs encode for two distinct types of renal Na^+-Pi cotransporters, type I, NPT1 and type II, NPT2 (Table 1). The two types demonstrate only 20% homology. The 2.1kb NPT1 mRNA encodes a ~50kD protein, where as the larger 2.7kb NPT2 mRNA encodes a ~70kD protein. Both have been localized to the renal BBM (Biber et al., 1993; Custer et al., 1993).Two other membrane proteins, Ram-1 and Glvr-1, originally described as cell-surface viral receptors, have been shown to mediate Na^+-Pi cotransport (Kavanaugh et al., 1994). These proteins are expressed in the kidney as well as in a wide variety of

Table 1. Renal Na+ -Pi cotransporter types

	NPT1	NPT2
• Cloned cDNAs	human (NPT1) rabbit (NaPi-1) mouse (*Npt1*)	human (NaPi-3) rabbit (NaPi-6) mouse (NaPi-7) rat (NaPi-2) opossum (NaPi-4) flounder (NaPi-5)
• mRNA size	~ 2.5 kb	~ 2.7 kb
• Protein size	~ 467 aa	~ 639 aa
• Homology between groups	20%	
• Regulation	not pH dependent not affected by dietary Pi intake not a target for PTH action	pH dependent regulated by dietary Pi intake target for PTH action

cell types including brain, liver, muscle and bone morrow (Kavanaugh and Kabat, 1996). Although their transport activity is increased by Pi deprivation, they are unlikely to be important for the maintenance of serum Pi levels. It is more likely that Ram-1 and Glvr-1 have a role to play in the maintenance of intracellular Pi levels necessary for normal cellular functions. Characterization of the transport properties revealed that the NPT2 cotransporter is the only known Na^+-Pi cotransporter with activity that is regulated like the renal PT by PTH and dietary Pi intake (Murer and Biber, 1997).

Inherited disorders of Pi homeostasis

The maintenance of appropriate extracellular Pi levels is vital for achieving proper skeletal mineralization. While bone abnormalities are associated with several disorders of altered phosphate homeostasis, little is known about the role of renal Pi transport in the etiology of bone disease. The McKusick catalogue of Mendelian inheritance in man (McKusick et al., 1992) lists 5 inherited disorders of phosphate homeostasis where the primary defect is thought to disturb renal Pi transport (Table 2). All of the disorders are rare.

The two disorders that I will focus on are X-linked hypophosphatemia (XLH) (Winters et al., 1958), also known as both familial hypophosphatemic rickets and Vitamin D resistant rickets, and hereditary hypophosphatemic rickets with hypercalciuria (HHRH) (Tieder et al., 1985). Less is known about the other three disorders, all of which show autosomal transmission. Hypophosphatemic bone disease has been described in 5 patients and is characterized by modest short stature, nonrachitic bone abnormalities and hypophosphatemia. Autosomal dominant vitamin D resistant rickets was first shown in 5 members of a three generation pedigree. Two of these 5 cases exhibit autosomal dominant transmission. Examination of a larger pedigree revealed extensive phenotypic variability (Econs and McEnery, 1997). Autosomal recessive hypophosphatemic rickets was diagnosed in two offspring of a first cousin mating.

XLH was the first of the inherited disorders of Pi homeostasis to be described (Albright et al., 1937). It is the most prevalent of the 5 disorders with an incidence of approximately 1:20,000 births and displays X-linked dominant transmission (Winters et al., 1958). HHRH was described in a large Bedouin kindred by Tieder in 1985. HHRH is thought to be very rare. Only a small number of sporadic cases (Chen et al., 1989; Glorieux et al., 1986; Nishiyama et al., 1986) and two other

Table 2. Inherited Hypophosphatemias

X-linked Hypophosphatemia (XLH)	307800, 307810
Hereditary Hypophosphatemic Rickets with Hypercalciuria (HHRH)	241530
Hypophosphatemic Bone Disease	146350
Autosomal Dominant Vitamin D Resistant Rickets	193100
Autosomal Recessive Hypophosphatemic Rickets	241520

Taken from McKusick et al. 1992

Israeli families (Arie et al., 1982; Tieder et al., 1992) have been reported with HHRH. HHRH displays autosomal inheritance which has been described as both autosomal recessive (Tieder et al., 1985) and autosomal dominant (Rasmussen and Tenenhouse, 1995; Tieder et al., 1987).

X-linked hypophosphatemia (XLH)

In addition to hypophosphatemia, the clinical manifestations of XLH include decreased renal phosphate reabsorption, growth retardation, femoral and tibial bowing, impaired bone mineralization and radiologic and histomorphometric evidence of rickets and osteomalacia (Table 3). Rickets and osteomalacia are metabolic disorders of bone in which the mineralization of the epiphyseal cartilage and organic bone matrix is impaired. The epiphyseal region of bone is an area of high mitotic activity responsible for bone elongation. This abnormality results in a decrease in the amount of mineralized bone and an increase in the amount of osteoid (cartilage or organic component of bone, which is secreted by osteoblasts), leading to decreased bone strength. Bones become soft, bend easily and are liable to deformities and pseudofractures (Van De Graaf and Fox, 1992). Serum $1,25(OH)_2D$ levels are normal in spite of hypophosphatemia indicating that XLH patients fail to respond to hypophosphatemia with an appropriate increase in renal 1-α-hydroxylase activity. They do not show an increase in serum $1,25(OH)_2D$ or an increase in urinary Ca^{2+} excretion.

There is an acquired, rare, tumor-induced disease called oncogenic hypophosphatemic osteomalacia (OHO) with symptoms very similar to XLH. Patients with OHO have hypophosphatemia, resulting from impaired renal reabsorption of filtered Pi, inappropriately low serum levels of $1,25(OH)_2D$ and osteomalacia (Weidner, 1991). The symptoms are reversed upon removal of the tumor. Of interest is the finding that conditioned medium obtained from OHO cultured cells inhibits Na^+-Pi cotransporter activity in kidney cell lines (Cai et al., 1994). Since substances that have a role in normal physiologic processes are frequently secreted by tumors in an upregulated fashion, these findings suggest that the tumor secretes a phosphaturic factor which normally controls Pi reabsorption (Econs and Drezner, 1994). Scientists have named this putative phosphate regulating hormone "phosphatonin" (Econs and Drezner, 1994).

Table 3. Comparison of the disorders XLH and HHRH

XLH (*Hyp*)	HHRH
- Clinical -	
Growth retardation	
Bowing of lower limbs	
Shortened stature	
Rickets / Osteomalacia	
- Biochemical -	
Hypophosphatemia	
Decreased renal Pi reabsorption	
Failure to increase serum $1,25(OH_2)D$ in response to low serum Pi	Appropriate increase in serum 1,25(OH)D in response to low serum Pi
No hypercalciuria	Hypercalciuria
- Inheritance -	
X-linked dominant	autosomal ? - unclear

Mouse homologues of XLH

There are two mouse models for XLH, hypophosphatemic *Hyp* (Eicher et al., 1976; Tenenhouse and Scriver, 1992) and gyrorotory *Gy* (Lyon et al., 1986). The *Hyp* mouse arose spontaneously at the Jackson laboratories. The *Gy* mouse was the offspring of a pregnant mouse exposed to radiation at day 17 of gestation. Both *Hyp* and *Gy* mice display rachitic bone disease, reduced growth rate, short stature, hypophosphatemia and decreased renal Na^+-Pi cotransport. Although earlier studies suggested that these mice exhibited differences in the regulation of vitamin D (Davidai et al., 1990), it has recently been shown that dietary Pi induces similar responses in both PTH and $1,25(OH)_2D$ levels in the two mice (Meyer et al., 1996; Tenenhouse et al., 1992) . However, *Gy* mice do exhibit inner ear abnormalities, extreme hyperactivity and circling behavior not seen in *Hyp* mice (Lyon et al., 1986). *Hyp* and *Gy* mice were originally described as closely linked on the X chromosome. Due to a single recombination event they were not considered to be allelic (Lyon et al., 1986).

Much of what is know about the pathophysiology of XLH comes from studies in *Hyp* mice. These mice have an intact low-affinity, high-capacity Na^+-Pi cotransport system. Although the affinity for Pi is similar in normal and Hyp mice, the Vmax of the high-affinity, low-capacity Na^+-Pi cotransporter in *Hyp* mice is half that of normal mice (Tenenhouse et al., 1989). These data suggest that the number of high-affinity Pi transport sites may be decreased in *Hyp* renal BBM. Renal mRNA from *Hyp* mice injected into *Xenopus* oocytes results in 50% lower Na^+-Pi cotransport activity than an equivalent amount of mRNA from normal littermates (Tenenhouse et al., 1994). Murine type II renal Na^+-Pi cotransporter (*Npt2*) cDNA and antibodies raised to synthetic *Npt2* -COOH terminal peptide, were used to examine the effect of the *Hyp* mutation on renal expression of Na^+-Pi cotransporter mRNA and protein. The study demonstrated that *Hyp* mice have a reduction in the abundance of *Npt2* mRNA and protein compared to the levels observed in normal mice (Tenenhouse et al., 1994), suggesting that *Npt2* may be the mutated gene responsible for XLH. Recent studies have concluded that the reduction in renal Na^+-Pi cotransport activity in *Gy* mice is also associated with a proportional decrease in *Npt2* mRNA and protein (Beck et al., 1996; Tenenhouse and Beck, 1996). In order to determine if either the NPT2 or NPT1 gene was a candidate for XLH, I established the chromosomal location of these genes by fluorescent in situ hybridization (Kos et al., 1994; Kos et al., 1996) (See Chapter 2,

Chromosomal Localization). By mapping the NPT1 and NPT2 genes to autosomes, I excluded them as candidates for XLH.

PEX

Soon afterwards, the HYP Consortium identified by positional cloning the mutant gene responsible for XLH at Xp22.1 (The Hyp Consortium, 1995). The gene exhibits homology to a family of endopeptidase genes (Turner and Tanzawa, 1997), including neutral endopeptidase (NEP) (Shipp et al., 1991), Kell blood group antigen (Lee et al., 1991) and endothelin converting enzyme (ECE) (Shipp et al., 1991; Xu et al., 1994) and was thus designated PEX (phosphate regulating gene with homology to endopeptidases, on the X-chromosome) (The Hyp Consortium, 1995). (Please note that the symbol PEX is also used as nomenclature for multiple peroxisomal proteins (peroxins) e.g., PEX5).

Mammalian endopeptidases are cell-surface proteins believed to be involved in the postsecretory activation or inactivation of a variety of peptide hormones. NEP is widely distributed on mammalian cells and terminates the actions of a variety of peptides, including some involved in cardiovascular regulation, inflammatory response and synaptic neuropeptide metabolism, by cleaving peptide bonds on the amino side of hydrophilic amino acid residues (Turner and Tanzawa, 1997). ECE converts the inactive, 38-residue, big endothelin-1 peptide into endothelin, a 21-residue vasoactive peptide by cleavage at specific amino acid residues (Xu et al., 1994).

Various types of PEX mutations including deletions, frameshift and point mutations were detected in XLH patients. These mutations likely result in a loss of normal PEX function and not activation of an aberrant function (Dixon et al., 1996; Holm et al., 1996; Mokrycki et al., 1996; Rowe et al., 1997) . Mutations in the murine homologue of human PEX have been detected in both the *Hyp* and *Gy* mouse (Beck et al., 1997; Strom et al., 1997).

Surprisingly, Northern blot, RNAse protection and RT-PCR analysis of murine and human tissues were unable to demonstrate Pex expression in normal kidneys (Beck et al., 1997; Du et al., 1996) Of seven tissues examined by Northern blot, only bone showed detectable Pex expression (Du et al., 1996). Therefore the defect in bone mineralization seen in XLH patients is likely a consequence of a primary defect in the PEX gene, expressed in bone, and not low plasma Pi levels to which it was originally attributed.

It is postulated that the PEX enzyme processes one or more hormones that are part of a cascade of proteins involved in regulating renal Na^+-Pi cotransporter gene expression, such as the putative phosphate regulating hormone phosphatonin. This is consistent with studies demonstrating that a humoral factor underlies the inhibition of renal Pi transport in *Hyp* mice. Parabiosis experiments showed that normal mice surgically joined to *Hyp* mice developed hypophosphatemia, decreased renal Pi reabsorption and decreased Na^+-Pi cotransport activity at the BBM (Meyer et al., 1989). Transplantation studies in which kidneys from normal mice were transplanted into *Hyp* mice demonstrated a persistence of hypophosphatemia and decreased Pi reabsorption (Nesbitt et al., 1992). The results of these experiments suggest that the renal Na^+-Pi cotransport defect is not intrinsic to the kidney, but dependent on an extrarenal phosphaturic factor.

This concept of an extrarenal factor being responsible for the renal Na^+-Pi cotransport defect conflicts with the results of earlier experiments (Bell et al., 1988) which showed that primary renal epithelial cell cultures from *Hyp* mice display reduced Pi uptake and abnormal vitamin D metabolism after several days in culture. Based on what is known regarding the regulation of Na^+-Pi cotransporter activity by PTH and dietary Pi restriction, an explanation for the earlier observation may be that insufficient time had passed to allow the primary cell cultures to synthesize new Na^+-Pi cotransporter proteins or that Na^+-Pi cotransporter proteins were not being properly shuttled to the BBM. Nevertheless, the defect in Pi uptake observed in *Hyp* culture was not as profound as it is in *Hyp* mice.

Hereditary hypophosphatemic rickets with hypercalciuria (HHRH)

HHRH shares many characteristics with XLH, including growth retardation, femoral and tibial bowing, impaired bone mineralization, radiologic and histomorphometric evidence of rickets and osteomalacia, hypophosphatemia and decreased renal phosphate reabsorption (Gazit et al., 1991; Tieder et al., 1985; Tieder et al., 1987) (Table 3). HHRH is distinguished from XLH by the following biochemical differences. HHRH patients respond appropriately to hypophosphatemia and show an increase in serum $1,25(OH)_2D$ levels. The increased serum $1,25(OH)_2D$ levels cause an increase in intestinal absorption of Pi and Ca^{2+} in HHRH patients. The excess Ca^{2+} absorption is compensated for by increasing urinary Ca^{2+} excretion (hypercalciuria). This suggests that the regulation of vitamin D metabolism is intact in HHRH patients, but altered in XLH patients (Tieder et al., 1985; Tieder et al., 1987). HHRH patients also differ

from XLH patients in their response to treatment. Complete remission of the HHRH phenotype is seen after therapy with phosphate alone (Tieder et al., 1992), whereas treatment with both phosphate and vitamin D is necessary to ameliorate the symptoms of XLH (Rasmussen and Tenenhouse, 1995).

Subsequent examination of the Bedouin kindred where HHRH was first described revealed that many presumed normal individuals display idiopathic hypercalciuria (IH). IH is defined as hypercalciuria without an identifiable systemic cause and is common in the general population. It can occur in a variety of forms and is believed to have a genetic component (Scheinman, 1998). In the Bedouin HHRH kindred, IH is thought to be due to increased intestinal Ca^{2+} absorption, secondary to mild hypophosphatemia and stimulation of $1,25(OH)_2D$ production, and to represent the mild, heterozygotic form of HHRH.

Overview of gene mapping

The goal of mapping is to find the relative locations of genes, markers, or disease loci on a given chromosome (Hudson et al., 1995; Schuler et al., 1996). In general, there are two types of gene maps. Physical or syntenic maps assign the location of a gene to a specific chromosome or chromosome segment by assaying for the presence of genes or their products (O'Brien et al., 1988). Genetic maps, also known as meiotic or linkage maps, assign genes relative to other loci. These maps are based on measuring the number of times two or more markers recombine during gamete formation or the number of times they are inherited together (O'Brien et al., 1988). Both types of maps provide information on the chromosome location, order and distance between markers.

Physical maps

There are many techniques for creating physical maps such as, cloning and sequencing (Smith and Cantor, 1986), somatic cell hybrid mapping, radiation hybrid mapping (Cox et al., 1990; Hudson et al., 1995) and cytogenetic mapping. All physical mapping techniques require either an enzyme activity, antibody, probe or polymerase chain reaction (PCR) product to assay the location of the marker. The latter three physical mapping techniques, somatic cell hybrid (Kos et al., 1994; McPherson et al., 1997), radiation hybrid (McPherson et al., 1997) , and cytogenetic mapping (Kos et al., 1994; Kos et al., 1996; McPherson et al., 1997),were used to localize the NPT1 and NPT2 genes in Chapter 2.

Somatic Cell Hybrid Mapping

The resolution of somatic cell hybrid (SCH) mapping is usually limited to the level of a chromosome. Human and rodent cells are cultured together and treated with agents that induce membrane fusion (D'Eustachio and Ruddle, 1983). These hybrid cells retain the entire complement of rodent chromosomes but lose human chromosomes in different combinations. Mapping data is collected by monitoring the loss or presence of a marker (D'Eustachio and Ruddle, 1983). Concordant association of 2 human markers in a hybrid cell line is interpreted as evidence for synteny (O'Brien et al., 1988).

Radiation Hybrid Mapping

Radiation hybrid (RH) mapping is a regional somatic cell hybrid technique with a resolution of ~500kb (Cox et al., 1990). Instead of using normal human cells, cells are subjected to a lethal dose of x-rays, which breaks the chromosomes into fragments, before fusion with rodent cells (Goss and Harris, 1975). Hybrid cells randomly retain one or more fragments of human chromosomes. Increasing the dose of radiation will lead to more breakage and decrease the size of the retained fragments, thereby increasing the mapping resolution that can be achieved with RH cell lines. The unit of measurement in RH mapping is the centiRay (cR). A distance of 1cR corresponds to 1% frequency of breakage between two markers after a given exposure to X-rays. The further apart markers are on a chromosome, the more likely they are to be separated by a break and be found on different fragments. RH cell lines are scored like SCH cell lines for the presence of markers and the data are analyzed statistically to yield information about the relative order and distance of the markers.

Cytogenetic Mapping

Cytogenetic banding techniques are often used to characterize the rescued chromosomal material in somatic cell and radiation hybrid cell lines. As a result, the accuracy of these hybrid cell mapping techniques is dependent on the quality of the cytogenetic characterization of the cells. The field of cytogenetics has also made many direct contributions of the construction of physical maps. One of the greatest advances in cytogenetics has been the development of fluorescent in situ hybridization (FISH) (Lichter et al., 1991; Lichter and Ward, 1990; Trask, 1991).

FISH represents the most direct approach for determining the location, order and orientation of genomic clones. The wide range of resolution and the applicability of the FISH technique to several areas of genome research is currently not possible with any other mapping technique (Heiskanen et al., 1996). Probes of various types and sizes (genomic DNA , cDNA or RNA, PCR products, plasmids, cosmids etc.) are labeled with biotin or deoxygenein (DIG), hybridized to template DNA, and visualized directly with a microscope after incubation with fluorochrome conjugated antibodies to biotin or DIG.

The resolution obtained by FISH depends on the method used to prepare the template genomic DNA. The less condensed the DNA template, the higher the resolution. Metaphase chromosomes provide the lowest resolution of the DNA templates: in order for two loci to be distinguished they must be separated by greater than 1 megabase (Mb). Therefore, metaphase chromosomes are not generally used as a template for ordering probes. However, metaphase chromosomes are the best templates for determining chromosome assignment and detecting homologous regions. During metaphase, chromosomes condense and display distinct, reproducible banding patterns, when stained with fluorochromes or dyes. These bands are due to differences in gene density, replication time, base composition, repeat number and chromatin structure and are unique to each chromosome and species (Hsu, 1979). Chromosome nomenclature defines obvious morphological features, such as the ends of chromosome arms, the centromere, the bands and the subbands. The bands are numbered consecutively from the centromere outward along each chromosome arm. Consequently, when using metaphase chromosomes as a template for FISH, cytogenetists are able to identify the telomere/centromere orientation and to localize a probe to a specific chromosome band.

Other DNA templates for FISH include mechanically stretched chromosomes, interphase nuclei and DNA fibers. These templates provide higher resolution than that seen when metaphase chromosomes are used as a template, but lack some other qualities that enable chromosome orientation and identification. For instance, the stretching of metaphase chromosomes by centrifugation before fixation increases their length by 5-20 times, allowing for the resolution of probes separated by 200kb. While the telomere/centromere orientation remains discernible, the procedure distorts the morphology and banding of the chromosome necessary for its identification (Laan et al., 1995). The chromosomal mapping of the NPT1 and NPT2 genes in Chapter 2 was accomplished by FISH of labeled NPT1 and NPT2 cDNA probes to metaphase chromosomes (Kos et al., 1994; Kos et al., 1996; McPherson et al., 1997).

Genetic map

The creation of a genetic map was first described in 1913 by Sturtevant who determined the order of 6 sex-linked markers in Drosophilia (Sturtevant, 1913). He observed that during meiosis certain segments of chromosomes recombine while others remain intact, and that the frequency of recombination between any two markers serves as an index of the distance between them (Sturtevant, 1913). According to Mendel's law of independent assortment, markers that are not allelic assort independently of one another. However, it is only when markers are on different chromosomes or far apart on the same chromosome that the law of independent assortment holds true. Markers on the same chromosome only assort independently when they are separated by a crossover event. A crossover is the breakage and exchange of genetic material between the strands of homologous chromosomes. If the probability of breakage is equal along the length of a chromosome, then markers separated by a large distance will have more places for breaks to occur and a greater frequency of crossover events than markers situated very close to one another (Ott, 1991).

Crossovers are recognized by looking at the haplotypes passed from parents to children. Markers situated very close together on the same chromosome will not recombine and assort independently, but will be transmitted together to the gamete. By counting how often markers have recombined or conversely, how often they have been transmitted together, one can deduce the order and distance between markers for mapping purposes. Independently inherited markers are expected to produce equal numbers of recombinant and nonrecombinant haplotypes. Thus, when markers are found together more than 50 percent of the time they are said to be linked (Ott, 1991). The term syntenic means "on the same thread" and refers to genes located on the same chromosome whether or not they are physically close enough together that the recombination frequency suggests linkage.

Recombinant individuals arise due to crossovers. However, not all crossovers result in an identifiable recombinant. A parent must be doubly heterozygous for the haplotypes produced to be distinguished. The pedigree in Figure 2 is an example of a case where recombinant and nonrecombinant haplotypes produced by a parent cannot be distinguished. The father's haplotype is AB/ab. The mother has the haplotype A*b/ab. The haplotypes of the children are Ab/ab and A*b/ab. One child is scored as a recombinant Ab/ab, having received from the father alleles that were present on

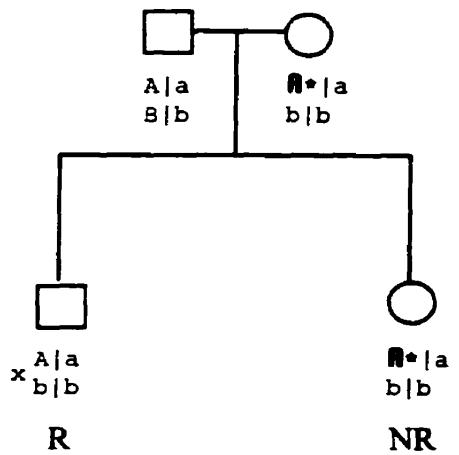

Figure 2. Family with genotypes at two loci showing one recombinant (R) and one nonrecombinant (NR) offspring. Recombination is determined based on the paternal haplotypes only. The maternal haplotype is noninformative for linkage. An x marks the site of crossing over.

different chromosomes (A/b). The second child is scored as a non-recombinant A*b/ab, because the alleles are the same as found in the parents. It is clear that the father's chromosome did not undergo recombination. Because the mother is homozygous for b alleles, it is not possible to tell whether or not a crossover occurred between a and b. In this example, the maternal haplotype is uninformative for linkage analysis. A mating is potentially informative when at least one of the parents is a double heterozygote, but ideally one wants both parents to be doubly heterozygous.

To obtain informative data one must be able to trace a crossover event. To increase the chances of getting informative data, it is best to use genetic markers that are highly polymorphic among the population. A marker is considered polymorphic if it has two or more alleles, and the rarest allele has a frequency greater than 0.01 in the population. The degree of informativeness or polymorphism of a genetic marker depends on the number of alleles at the marker locus and their relative frequencies in the population. In general, highly polymorphic markers have many alleles that are of equal frequency. The two units used to measure the degree of marker polymorphism are the polymorphic information content (PIC) (Botstein et al., 1980) and heterozygosity (Shugart, 1995) values.

With the exception of genes localized to the X-chromosome, which are relatively easy to identify by their pedigree pattern, few genes were genetically mapped in humans before the 1980s. One reason for this is that unlike experimental organisms, such as Drosophilia and mice, where breeding times are short and offspring numbers large, human matings can not be arranged to suit experimental purposes. A second reason is that before the 1980s few genetic markers had been found in humans which were polymorphic enough to allow existing mating in natural populations to be informative for linkage analysis (Lander, 1988).

Up until the 1980s, human genetic markers consisted mainly of protein isoforms, chromosome variants, blood groups, or phenotypes which had low polymorphic values. For instance, the most common allele for three erythrocyte markers, Lutheran, Kell, and adenylate kinase, was found at a frequency of greater than 0.95 in European individuals (Renwick, 1969). Consequently, the construction of human genetic maps lagged behind the maps of other organisms. The advent of recombinant DNA technology provided the means to detect new types of markers and brought about rapid advances in human genetic mapping. The first novel polymorphic DNA markers to be

described were the restriction fragment length polymorphisms (RFLPs)(Botstein et al., 1980). These markers arise by point mutations in DNA sequence which remove or create restriction enzyme cut sites, or by insertion, duplication or deletions in DNA which change the size of a restriction fragment. Although usually only biallelic, the frequency of each of the two RFLP alleles is close to 0.50. RFLPs are found throughout the genome at approximately every one thousand base pairs (Botstein et al., 1980). This means they are common enough to be used for the construction of a true linkage map of the human genome (Botstein et al., 1980; Lander, 1988).

Other markers were soon discovered that were comprised of repeated DNA sequences which vary in length among individuals; variable number of tandem repeats (VNTRs) (Nakamura et al., 1987) or minisatellites (Jeffereys et al., 1985) and short tandem repeats (STRs) also known as simple sequence repeats or microsatellites (Weber and May, 1989). Although VNTRs have higher polymorphic values than RFLPs, they cluster in the telomeric region of chromosomes decreasing their usefulness for making genetic maps (Royle et al., 1988). However, STRs have very high polymorphic values (http://gdbwww.gdb.org) and are scattered throughout the genome at about every 50-100Kb (30-60Kb) (Stallings et al., 1991). The STRs can be strings of dinucleotide, (for example strings of repeated cytosine and adenine nucleotides), trinucleotide (Gastier et al., 1995), or tetranucleotide repeats. These markers are easily typed by PCR using primers specific for the regions flanking the repeated sequence. Most recently, single nucleotide polymorphisms (SNPs) that can be typed using high-throughput DNA chip technology have been identified (Wang et at., 1998). The markers used for the genetic mapping in my thesis research were STRs.

Conversion and integration of the maps

All of the mapping techniques provide information about marker order and the relative distances between markers, but the actual physical distance between markers is often very different (Ott, 1991). The unit of measurement for genetic maps is a centiMorgan (cM). By definition, 1cM is the distance within which recombination occurs 1% of the time. Assuming that the total human genetic map is 3,600cM and there are 3.1×10^9 bp in the haploid genome (Dib et al., 1998), a genetic distance of 1cM corresponds to approximately 1,000kb or 1 megabase (Mb). Although recombination is assumed to occur at a constant rate randomly throughout the genome, in reality there are recombination hot spots and areas of repressed recombination. There are also differences in the rate of recombination between the sexes. Consequently, 1cM may

correspond to a 1Mb separation of two markers, to a 10Mb separation in an area of repressed recombination or to a 0.1Mb separation in an area of increased recombination. The RH mapping unit, cR, (see above) is analogous to the cM in that it corresponds to a 1% frequency of breakage between two markers, but is dependent on the dosage of X-rays administered. As part of the international project to sequence the human genome, efforts are being made to combine markers previously localized and ordered using the different mapping techniques into an integrated map (Hudson et al., 1995).

Methods of detecting linkage

In addition to a genetic map of localized markers, linkage analysis requires a statistical method to determine the probability that two markers are linked. One of the best known methods is the LOD score method (Ott, 1991). To perform linkage analysis marker parameters such as the allele frequencies in the population need to be specified. When one of the markers is a disease locus, additional parameters such as mode of inheritance, disease frequency, phenocopy frequency and penetrance values need to be specified. For single gene disorders, the genetic model, the disease frequency, phenocopy frequency and penetrance values are usually available. To perform linkage studies, investigators first collect DNA samples from families while carefully and accurately documenting the pedigree structure and each individual's affection status. Then the DNA samples are genotyped for polymorphic markers. Finally, statistical assessment of linkage is performed. Once a chromosomal location is determined, additional markers in the region are genotyped to identify markers that flank the disease gene more closely.

LOD score method

The LOD score method is used to determine the odds in favor of two loci being linked versus being unlinked (Ott, 1994). The base 10 logarithm of this ratio is the LOD score ($Z(\theta)$), which stands for "logarithm of the odds favoring linkage". The logarithm of the likelihood ratio is taken so that the scores from different meioses can be added. LOD scores > 3.0 indicate significant evidence (1000:1 odds in favor) of linkage while scores < -2.0 lead to the conclusion of non-linkage. It is usually necessary to combine LOD scores from different families to achieve a LOD score above 3.0.

The formula for calculating a LOD score is:

$$Z\ (\theta) = \log_{10} \frac{L(\theta)}{L(0.50)}$$

In words:

$$Z\ (\theta) = \log_{10} \frac{\text{(probability of the data if loci are linked with a recombination fraction of } \theta<0.50)}{\text{(probability of the data if loci are unlinked } \theta= 0.50)}$$

The recombination fraction, θ, is related to the genetic distance between the disease gene and marker locus. The larger the value of θ the more likely that a gametic haplotype is a recombinant. θ can range from zero for markers showing complete linkage with no recombination, to 0.50 for unlinked loci. The numerator of this equation is based on the numbers of recombinant and nonrecombinant progeny observed in the family. The denominator of this equation is the probability that the data were observed assuming independent segregation of loci.

Many factors complicate the search for disease genes using the LOD score approach. These include uncertainties about the genetic model, locus heterogeneity, and misdiagnosis of phenotype. Complex disorders, such as insulin-dependent diabetes or Alzheimer's disease, are defined as such because the disease trait does not follow a simple dominant or recessive inheritance pattern. These diseases are thought to be caused by several genes acting together to increase the risk of disease expression. A lack of knowledge about the genetic model, the ways in which the genes interact, and the effects of environmental variables can decrease the power of the LOD score method to such an extent that it is impossible to detect linkage in complex disorders. Therefore, investigators have come up with other model-independent, non-parametric approaches to assess where disease loci map (Econs and Speer, 1996).

Non-parametric methods to map disease genes often rely on allele sharing or identity by descent (IBD) measurements between affected pedigree members to determine where a disease locus may lie. When two people possess alleles of the same type which were not inherited from a common ancestor, the alleles are said to be identical by state (IBS) (Figure 3). If two individuals possess alleles of the same type which were inherited from a common ancestor they are considered to be identical by descent (IBD) (Figure 3) (Schork and Chakravarti, 1996). When performing IBD mapping, one assumes that a common ancestor brought an allele which predisposes for either a simple or complex

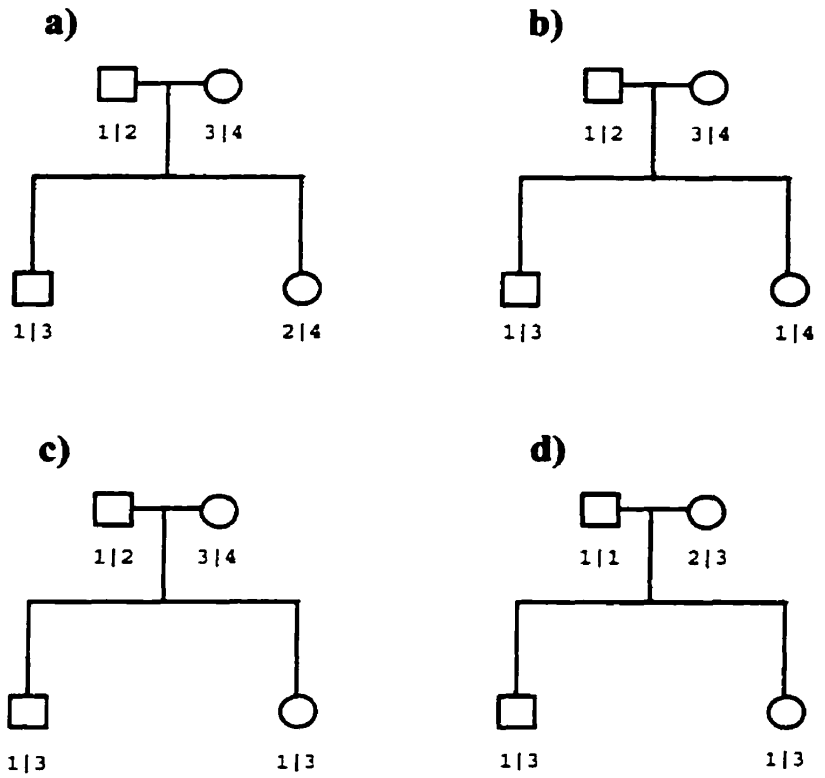

Figure 3. Examples of situations in which IBD and IBS information can and can not be determined. The numbers represent alleles (genotypes) at a single locus. For situation a), the two offspring share no alleles IBS or IBD. For situation b), the two offspring share a single allele (1)both IBS and IBD. For situation c), the two offspring share both alleles IBS and IBD. For situation d), the two offspring share both alleles IBS, but only a single allele (3) is unambiguously shared IBD (modified from Schork and Chakravarti, 1996).

disease into the family or population. No assumptions need to be made regarding the mode of inheritance or frequency of the disease allele. Over time, recombination and random segregation reduce the amount of allele sharing among the affected members, except in the region containing the shared disease allele. Therefore, linkage of a disease to a locus is detected by virtue of the fact that affected relatives will have inherited the same alleles on one or both chromosomes more often than expected under random segregation. After combining the number of shared alleles (0, 1 or 2) between affected relatives, a test is applied to determine if the observed results are significantly different from the expected results.

A subset of IBD mapping is homozygosity by descent mapping (homozygosity mapping) (Lander and Botstein, 1987). When performing homozygosity mapping one assumes that an ancestor, common to all the affected individuals, brought an allele which predisposes for a rare, recessive disease into the family or population (Figure 4). A consanguineous mating increases the chance that the offspring will inherit two copies of a disease allele identical and homozygous by descent. Linkage of a rare, recessive disorder to a locus is detected by locating overlapping regions of homozygosity in affected individuals from inbred pedigrees. Inbred affected individuals from unrelated pedigrees will be homozygous at the same markers more often than expected under random segregation, while closely related inbred affected individuals will be homozygous for the same allele at the same markers more often than expected under random segregation (Figure 4b). The homozygosity mapping approach does not work well if more than one disease allele is segregating in the family, because of the presence of affected individuals that are compound heterozygotes and not homozygotes at the disease locus (Figure 5). Both IBD and homozygosity mapping approaches were used to analyze the genotype data for the large Bedouin HHRH kindred in an effort to map a HHRH disease gene.

The role of the NPT1 and NPT2 genes in inherited hypophosphatemias and the aims of my thesis.

The efforts of many scientists over the past 20 years have highlighted the importance of renal Pi reabsorption, and more specifically Na^+-Pi cotransport, in maintaining sufficient serum Pi levels to achieve proper bone development. My thesis centered on ascertaining whether the NPT1 and NPT2 genes are candidates for inherited disorders of Pi homeostasis. The laboratory obtained five renal Na^+-Pi cotransporter cDNA

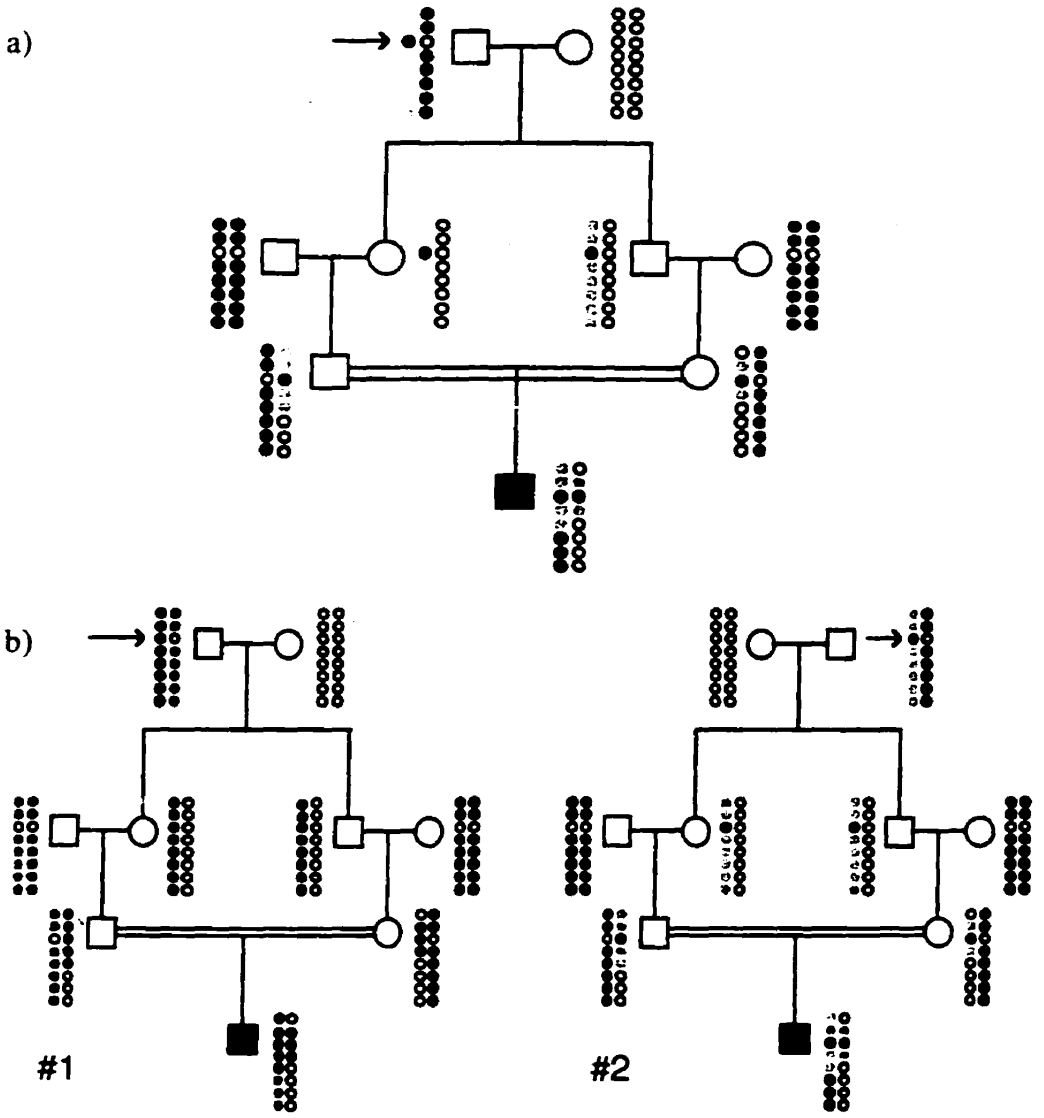

Figure 4. Homozygosity mapping. The small circles represent linked marker loci. The colors and shading refer to the alleles at each locus. The arrows point to the founding mutant allele at the third gene in the eight marker haplotype of the great grandfather. Part a) depicts a recessively inherited trait segregating in an inbred family. Portions of the great grandfather's chromosome, including the mutant allele and flanking portions of the great grandfather's haplotype, are passed on to each of his children and grandchildren. The union of two first cousins resulted in an affected male offspring who is homozygous by descent for the same mutant allele. Part b) depicts two other inbred families with mutations at the same gene. Although the alleles are different in these families, the markers that show homozygosity are the same.

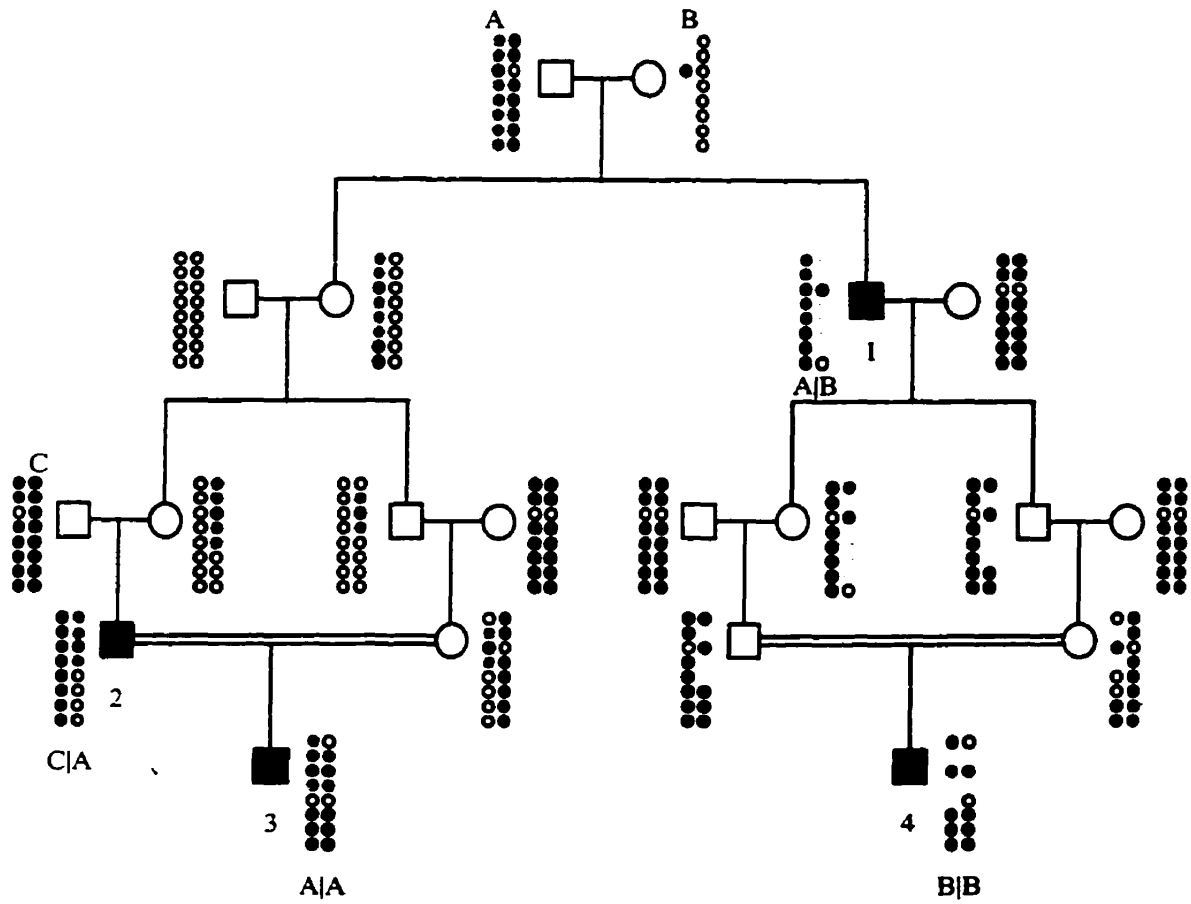

Figure 5. Allelic heterogeneity in an inbred family. This picture depicts a recessively inherited trait segregating in an inbred pedigree. Disease alleles of independent origin have entered the pedigree on three different haplotypes (A, B, C). There are four affected individuals. Affected individual 1 is a compound heterozygote of haplotypes A and B. Affected individual 2 is a compound heterozygote of haplotypes C and A. Affected individual 3 is homozygous for haplotype A and affected individual 4 is homozygous for haplotype B.

clones: rabbit (Werner et al., 1991) and human (Chong et al., 1993) NPT1 and rabbit (Verri et al., 1995), rat and human (Magagnin et al., 1993), NPT2 (Table 1). My first goal focused on the physical chromosomal mapping of the NPT1 and NPT2 genes in human and rabbit to determine if they were potential candidates for X-linked or autosomally inherited hypophosphatemias. My second goal was to sequence the promoter and characterize the structure of the NPT2 gene so that primers could be designed to amplify NPT2 exons from patient's DNA. This was necessary since NPT2 expression is kidney-specific and it was not feasible to obtain kidney biopsies from patients for RT/PCR of cellular RNA. Finally, I used genetic mapping methods to determine whether there was evidence for linkage of HHRH to either the NPT1 or NPT2 genes.

The following three chapters contain the results of the laboratory experiments and data analysis conducted while registered as a graduate student in the Department of Biology at McGill University. My research work was conducted in three McGill teaching hospitals: the Montreal Children's Hospital, the Jewish General Hospital and the Montreal General Hospital (MGH), as well as in the Department of Pathology at the University of Montreal and at the Center for Genome Research at the Whitehead Institute for Biomedical Research of Massachusetts Institute of Technology (WICGR).

Chapter 2. Chromosomal localization of the NPT1 and NPT2 genes

This chapter includes three published manuscripts that focus on the physical mapping of the NPT1 and NPT2 genes. The FISH technique was used in each of the manuscripts presented.

"Localization of a renal sodium-phosphate cotransporter gene to human chromosome 5q35", Genomics volume 19: 176-177 1997.

Experiments in mice showed that renal *Npt2* gene expression was decreased in *Hyp* mice relative to normal littermates, suggesting that the NPT2 gene could be the mutant gene responsible for X-linked hypophosphatemia in mice and human. The purpose of this study was to localize the human NPT2 gene in order to determine whether it was a candidate gene for X-linked hypophosphatemia.

Localization of a Renal Sodium-Phosphate Cotransporter Gene to Human Chromosome 5q35

Claudine H. Kos,* Frédérique Tihy,† Michael J. Econs,‡ Heini Murer,§ Nicole Lemieux,† and Harriet S. Tenenhouse*,¶,1

*Departments of *Biology and ¶Pediatrics, McGill University, Montreal, Quebec H3H 1P3, Canada, †Departement de Pathologie, Université de Montréal, Montreal, Quebec H3C 3J7, Canada, ‡Department of Medicine, Duke University, Durham, North Carolina 27710; and §Institute of Physiology, University of Zurich, CH-8057 Zurich, Switzerland*

Received July 22, 1993, revised September 28, 1993

Several Mendelian disorders of renal phosphate reabsorption, associated with hypophosphatemia and bone disease, have been described (6). These include X-linked hypophosphatemia (XLH), hereditary hypophosphatemic rickets with hypercalciuria, hypophosphatemic bone disease, and autosomal dominant and autosomal recessive hypophosphatemic rickets. The underlying mechanisms for renal phosphate wasting in these disorders remain unknown. The proximal tubule is the major site of renal phosphate reabsorption (1). Thus, mutations in genes that participate in the transepithelial transport of phosphate in this segment of the nephron may be responsible for these disorders. Recently, a cDNA encoding a renal proximal tubular, brush-border membrane Na^+-phosphate cotransporter (NaP_i-3) was cloned from human kidney cortex (5). As a first step in establishing whether mutations in the NaP_i-3 gene are the cause of inherited disorders in phosphate homeostasis, we sought to determine its chromosomal localization.

To establish whether NaP_i-3 was a candidate gene for XLH, the most prevalent of the Mendelian hypophosphatemias (9), we performed Southern analyses of digests of genomic DNA from XY, XX, and XXX human fibroblast cell lines, using a ^{32}P-labeled NaP_i-3 cDNA probe. A gene dose effect was not observed, thereby providing evidence for autosomal localization of the NaP_i-3 gene.

To determine on which autosome the NaP_i-3 gene lies, we amplified DNA from the NIGMS Human/Rodent Cell Hybrid Mapping Panel No. 2 (3), using human-specific PCR primers that were based on the NaP_i-3 sequence (5) (sense, ^{32}P-labeled GGAGGTGAGCTCTGCCATC; antisense, CAGTTAAAG-CAGTCATGCACC). The PCR products were electrophoresed

[1] To whom correspondence should be addressed at the Montreal Children's Hospital, 2300 Tupper Street, Montreal, Quebec H3H 1P3, Canada. Telephone: (514) 934-4417. Fax: (514) 934-4329.

The HGMW-approved symbol for this locus is NPT2.

FIG. 1. Fluorescence *in situ* hybridization of a 2.7-kb biotinylated NaP_i-3 cDNA probe to human metaphase and prometaphase chromosomes localizes the renal Na^+-P_i cotransporter gene to chromosome 5q35.

GENOMICS **19**, 176–177 (1994)
0888-7543/94 $6.00

on a standard polyacrylamide sequencing gel and visualized by autoradiography. Human genomic DNA gave a band at 269 bases, indicating that the primers flanked an intron of 122 bases. Amplification occurred with only one cell line in the panel. This cell line, No. 10114, contains human chromosome 5. The primers did not amplify DNA in either the murine or hamster controls.

To determine the precise localization of the NaP_i-3 gene on human chromosome 5, we performed high-resolution fluorescence *in situ* hybridization using a method for mapping genes directly on banded chromosomes (4). Metaphase and prometaphase chromosomes were obtained from cultures of normal human peripheral blood lymphocytes that were synchronized with thymidine and treated with 5-bromodeoxyuridine (4). Before use, chromosome spreads were treated with RNase and denatured for 2 min in 70% formamide/2× SSC at 70°C. A 2.7-kb NaP_i-3 cDNA in pSPORT (5) was CsCl purified, biotin labeled by nick-translation (Bionick, BRL), and denatured at 95°C for 10 min. After overnight hybridization at 37°C (2), the slides were washed and incubated with immunofluorescent reagents to produce a signal at the site of hybridization (4). Direct banding of hybridized chromosomes was achieved by counterstaining with propidium iodide. The slides were viewed using a Leitz Aristoplan epifluorescent microscope with a filter combination appropriate for fluorescent labeling. Localization of the NaP_i-3 gene was established by analysis of 67 randomly selected metaphase and prometaphase spreads. Fifty percent exhibited a signal on both chromatids, and 85% exhibited at least one signal, on band q35 of chromosome 5 (Fig. 1).

The present results rule out the NaP_i-3 gene as a candidate gene in XLH (9). These findings are consistent with the demonstration that in the murine X-linked *Hyp* homologue of the human disease, the renal defect in brush-border membrane Na^+-phosphate cotransport is not intrinsic to the kidney but rather depends on a circulating humoral factor for its expression (7, 8). Further work is necessary to establish whether mutations in the NaP_i-3 gene are responsible for autosomally inherited disorders of phosphate homeostasis with impaired renal phosphate reabsorption (6).

ACKNOWLEDGMENTS

This work was supported by grants from the Medical Research Council of Canada (MRC Genetics Group Grant to H.S.T.), the National Institutes of Health (MO1-RR-30, AR27032, and AR42228 to M.J.E.), and the Swiss National Funds (32-30785.91 to H.M.). We thank Dr. P. Eydoux and the Cytogenetics Department at the Montreal Children's Hospital for technical help, M. Jean Léveillé for photographic work, Dr. C. R. Scriver for his continued interest, and Lynne Prevost for preparation of the manuscript.

REFERENCES

1. Berndt, T. J., and Knox, F. G. (1992). Renal regulation of phosphate excretion. *In* "The Kidney, Physiology and Pathophysiology" (D. W. Seldin and G. Giebisch, Eds.), pp. 2511–2532, Raven, New York.
2. Drouin, R., Lemieux, N., and Richer, C. L. (1988). High-resolution R-banding at the 1250-band level. 1. Technical considerations on cell synchronization and R-banding (RHG and RBG). *Cytobios* **56:** 107–125.
3. Dubois, B. L., and Naylor, S. L. (1993). Characterization of NIGMS human/rodent somatic cell hybrid mapping panel 2 by PCR. *Genomics* **16:** 315–319.
4. Lemieux, N., Dutrillaux, B., and Viegas-Péquignot, E. (1992). A simple method for simultaneous R- or G-banding and fluorescence in situ hybridization of small single-copy genes. *Cytogenet. Cell Genet.* **59:** 311–312.
5. Magagnin, S., Werner, A., Markovich, D., Sorribas, V., Stange, G., Biber, J., and Murer, H. (1993). Expression cloning of human and rat renal cortex Na/Pi cotransport. *Proc. Natl. Acad. Sci. USA* **90:** 5979–5983.
6. McKusick, V. A. (1992). "Mendelian Inheritance in Man," 10th ed., Johns Hopkins Univ. Press, Baltimore, MD.
7. Meyer, R. A., Jr., Tenenhouse, H. S., Meyer, M. H., and Klugerman, A. H. (1989). The renal phosphate transport defect in normal mice parabiosed to X-linked hypophosphatemic mice persists after parathyroidectomy. *J. Bone Min. Res.* **4:** 523–532.
8. Nesbitt, T., Coffman, T. M., Griffiths, R., and Drezner, M. K. (1992). Cross-transplantation of kidneys in normal and *Hyp* mice: Evidence that the *Hyp* phenotype is unrelated to an intrinsic renal defect. *J. Clin. Invest.* **89:** 1453–1459.
9. Rasmussen, H., and Tenenhouse, H. S. (1989). Hypophosphatemias. *In* "The Metabolic Basis of Inherited Disease" (C. R. Scriver, A. L. Beaudet, W. S. Sly, and D. Valle, Eds.), pp. 2581–2601, McGraw-Hill, New York.

"High resolution mapping of the renal sodium-phosphate cotransporter gene (NPT2) confirms its localization to human chromosome 5q35", Pediatric Research volume 41: 632-634 1997.

Subsequent to our localization of the NPT2 gene to 5q35, another group published that the NPT2 gene localized to 5q13 (Ghishan et al., 1994). This is a significant discrepancy since efforts to map autosomal hypophosphatemias by linkage analysis require the selection of polymorphic markers that map close to the candidate gene of interest. This study was undertaken to confirm the localization of the NPT2 gene to 5q35 and to identify polymorphic markers flanking the NPT2 gene.

High Resolution Mapping of the Renal Sodium-Phosphate Cotransporter Gene (NPT2) Confirms Its Localization to Human Chromosome 5q35

JOHN D. McPHERSON, MARY CAROL KRANE, CARYN B. WAGNER-McPHERSON, CLAUDINE H. KOS, AND HARRIET S. TENENHOUSE

Department of Genetics, Washington University School of Medicine, St. Louis, Missouri 63108 [J.D.M., C.B.W.-M.]; Department of Biological Chemistry, University of California, Irvine, California 92717 [J.D.M., M.C.K.]; and Departments of Biology and Pediatrics, McGill University, Montreal, Quebec H3H 1P3, Canada [C.H.K., H.S.T.]

ABSTRACT

The precise chromosomal localization of the type II renal-specific Na^+-phosphate (P_i) cotransporter (NPT2) gene (gene symbol SLC17A2) is necessary for the identification of closely linked polymorphic markers to determine whether NPT2 is a candidate gene for inherited disorders of renal P_i reabsorption. Recent studies by two different groups localized NPT2 to human chromosome 5q35 and 5q13, respectively. To resolve this discrepancy, we used three independent methods. The results using a human chromosome 5/rodent somatic cell hybrid deletion panel, fluorescence *in situ* hybridization with a PAC clone containing the NPT2 locus, and analysis of a chromosome 5-specific radiation hybrid panel were all consistent with the 5q35 assignment of the NPT2 gene. The radiation hybrid results placed NPT2 between polymorphic microsatellite markers D5S498 and D5S469. These findings will allow the initiation of linkage analysis to determine if NPT2 has a causative role in Mendelian disorders of renal P_i wasting. (***Pediatr Res* 41: 632–634, 1997**)

Abbreviations

NPT2, type II renal sodium-phosphate cotransporter
P_i, inorganic phosphate
PCR, polymerase chain reaction
FISH, fluorescence *in situ* hybridization

The mammalian kidney is an important arbiter of extracellular phosphate (P_i) homeostasis. Renal reabsorption of filtered P_i occurs predominantly in the proximal tubule where concentrative Na^+-gradient dependent P_i transport across the brush-border membrane is the rate limiting step in the overall P_i reabsorptive process and the major site for its regulation (1, 2). Recently, homologous cDNAs encoding high affinity, renal-specific, brush-border membrane Na^+-P_i cotransporters (NPT2 type, Genome Data Base symbol SLC17A2) were cloned from several mammalian species (3–6), thereby providing useful probes to study the regulation of renal NPT2 gene expression and determine whether NPT2 is a candidate gene for Mendelian disorders of renal P_i reabsorption (7, 8).

We demonstrated that renal NPT2 gene expression is significantly reduced in X-linked *Hyp* mice, a murine homologue of human X-linked hypophosphatemia (9). We also showed that the NPT2 gene maps to human chromosome 5q35 (10) and mouse chromosome 13B (X. Zhang, H. S. Tenenhouse, A. S. Hewson, H. Murer, and P. Eydoux, manuscript submitted for publication) by FISH, using the corresponding NPT2 cDNAs as probes. These findings indicate that mutations in NPT2 are not responsible for the homologous human and murine X-linked hypophosphatemias and suggest that the gene at the X-linked hypophosphatemia (*Hyp*) locus is involved in the regulation of renal NPT2 gene expression. A candidate gene for X-linked hypophosphatemia has recently been identified (11).

To determine whether NPT2 is a candidate gene for autosomal disorders of renal P_i wasting (7, 8), polymorphic markers mapping close to the NPT2 gene on chromosome 5q35 (10) are required for linkage analysis. However, the application of this approach has been complicated by a second report which localized the NPT2 gene to human chromosome 5q13 (12). The present study was undertaken to resolve this discrepancy. We used NPT2-specific primers to PCR amplify genomic DNA from a panel of human-hamster somatic cell hybrids which either contain or lack DNA in regions q13 and q35 of chro-

Received July 29, 1996; accepted January 6, 1997.
Correspondence: Dr. Harriet S. Tenenhouse, McGill University-Montreal Children's Hospital Research Institute, 2300 Tupper Street, Montreal, Quebec H3H 1P3, Canada.
Supported by a Medical Research Council of Canada MRC Genetics Group Grant (H.S.T.) and National Institutes of Health Grant HG00834 (J.D.M.).

mosome 5 (13, 14) and a panel of chromosome 5 radiation hybrids (J. D. McPherson, unpublished data). In addition, we identified polymorphic microsatellite markers that flank the NPT2 locus on human chromosome 5 using the radiation hybrid panel and confirmed the localization of the NPT2 gene to chromosome 5q35 by FISH using an NPT2 genomic clone as probe.

METHODS

Deletion panel mapping. NPT2-specific oligonucleotide primers (forward 1405: 5′-CCGCTCACACTGGGTTCCAA-3′; reverse 1667: 5′-AGTGAGGGCAGCAGCAGGAA-3′) were used to amplify DNA isolated from somatic cell hybrids obtained from a chromosome 5 deletion panel (13, 14). The NPT2 primers are numbered according to their position in the NPT2 cDNA [NaP_i-3 in (3)]. The PCR amplification conditions were 1.5 mM $MgCl_2$, 0.4 μM of each primer, 200 μM of each dNTP and 1 unit of *Taq* polymerase (Boehringer Mannheim) with the supplied buffer. The PCR cycling parameters were 94°C, 3 min (94°C, 30 s/64°C, 5 s/72°C, 30 s) × 33; 72°C, 7 min with an MJ Research PTC200 Thermocycler. PCR products and DNA Molecular Weight Marker VI (Boehringer Mannheim, Indianapolis, IN) were separated on 6% acrylamide gels.

Radiation hybrid mapping. NPT2-specific oligonucleotide primers (forward 618: 5′-GGAGGTGAGCTCTGCCATC-3′; reverse 764: 5′-CAGTTAAAGCAGTCATGCACC-3′) were used to amplify DNA isolated from 180 chromosome 5-specific radiation hybrids (J. D. McPherson, unpublished data). PCR conditions were essentially the same as above with the following cycling parameters: 94°C, 1 min (94°C, 30 s/60°C, 30 s/72°C, 30 s) × 35; 72°C, 10 min. PCR products and DNA Molecular Weight Markers (Boehringer Mannheim) were separated on 3% agarose gels and the hybrids scored for the presence or absence of the NPT2 locus. The position of NPT2 relative to previously ordered chromosome 5 markers was determined using the rh2pt and RHMAXLIK programs with the SAVMAX value of the latter set to 8 (15).

FISH. A human PAC clone (203K6) containing the NPT2 locus was isolated from an arrayed library (generously provided by Pieter de Jong) using the NPT2-specific primers (forward 618 and reverse 764) described above. DNA from the PAC 203K6 clone was direct labeled with fluorescein-dUTP (Prime-It Fluor, Stratagene, La Jolla, CA) as recommended by the supplier and hybridized to human metaphase chromosomes, and images were collected as previously described (16). Over 30 metaphase spreads were examined.

RESULTS

Figure 1 depicts the results of PCR amplification of DNA isolated from a human chromosome 5 natural deletion panel, selected from human/hamster somatic cell hybrids (13, 14). An NPT2 PCR product of the expected size (962 bp) was generated with DNA from all cell lines containing the distal portion of the long arm of chromosome 5 (HHW105, HHW1064, HHW1421, HHW1499, and HHW1600) but not with DNA from HHW1138, a cell line lacking the region of interest (Fig. 1). These findings localize NPT2 to 5q33.2-qter. Moreover, the demonstration that a PCR product was obtained with DNA from HHW1064, a cell line lacking the 5q13 region (Fig. 1), indicates that NPT2 does not map to this locus as reported by Ghishan *et al.* (12). No PCR product was detected in negative controls run in the absence of DNA or in the presence of hamster (UCW56) DNA (Fig. 1). A PCR product of the expected size was obtained with human (46XY) DNA as template (Fig. 1).

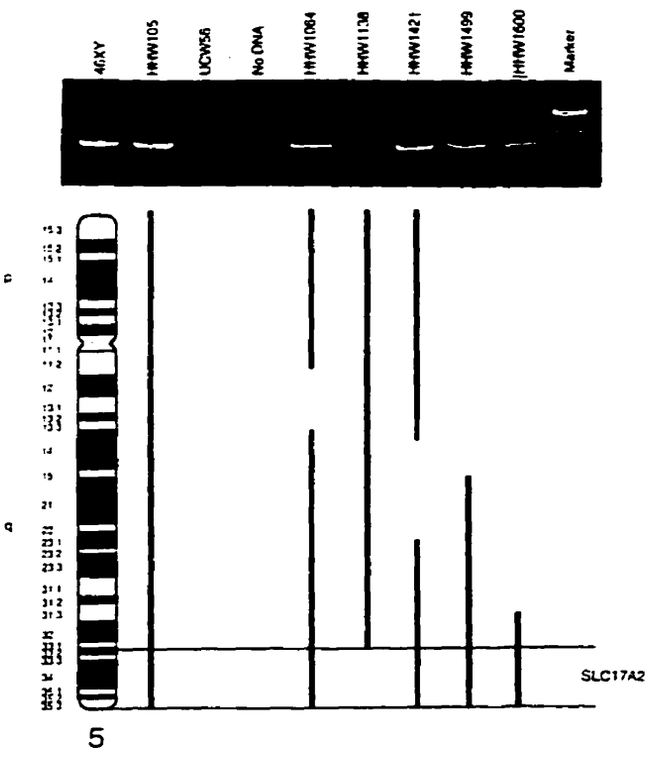

Figure 1. Regional mapping of NPT2 by PCR amplification of DNA from a panel of human-hamster somatic cell hybrids. Solid lines below the lanes indicate the portion of human chromosome 5 present in the indicated hybrids. The PCR conditions were 1.5 mM $MgCl_2$, 0.4 μM of each primer (forward 1405: 5′-CCGCTCACACTGGGTTCCAA-3′; reverse 1667: 5′-AGTGAGGGCAGCAGCAGGAA-3′), 200 μM of each dNTP and 1 unit of *Taq* polymerase (Boehringer Mannheim). The PCR cycling parameters were 94°C, 3 min; (94°C, 30 s/64°C, 5 s/72°C, 30 s) × 33; 72°C, 7 min with an MJ Research PTC200 thermocycler. PCR products were separated on 6% acrylamide gels. Visible fragments of 2176 and 1766 bp (doublet), 1230, 1033, 653, and 517 bp were obtained with DNA Molecular Weight Marker VI (Boehringer Mannheim).

Radiation hybrid mapping was performed by PCR analysis using NPT2-specific primers and DNA isolated from 180 chromosome 5-specific radiation hybrids. The hybrids were scored for the presence or absence of the NPT2 locus by the presence or absence of a 269 bp NPT2 PCR product. The position of NPT2 was determined relative to 248 markers previously ordered on human chromosome 5 by radiation hybrid mapping (J. D. McPherson, unpublished data). The NPT2 locus was localized between D5S498 and D5S469 using the RHMAXLIK program (15) at a log likelyhood > 10E-3. The calculated distance between NPT2 and D5S469 was 32.2

centiRays (cR) and between NPT2 and D5S498 was 65.9 cR, with associated LOD scores of 16.02 and 8.08, respectively. Calibration of the chromosome 5 radiation map, using both the chromosome size and sequence-tagged sites generated from the end clones of an 850-kb YAC, yielded an approximate value of 40 kb/cR, in agreement with that of a previous study (17). Thus, NPT2 is estimated to be 2.6 Mb distal to D5S498 and 1.3 Mb proximal to D5S469. The known localization of the dinucleotide repeat markers D5S498 and D5S469 to distal 5q is consistent with the data from the chromosome 5 deletion mapping panel shown in Figure 1.

The localization of NPT2 to human chromosome 5q35 was also confirmed by hybridization of human metaphase chromosomes with fluorescein-labeled, denatured genomic DNA from a human PAC clone (203K6) containing the NPT2 locus (data not shown). The genomic probe hybridized only to the q35 region of chromosome 5. Of all chromosomes examined with hybridization to 5q35, greater than 90% showed a signal on both chromatids. No signal was observed on any other chromosome.

DISCUSSION

We demonstrate by three independent methods that the gene encoding the high affinity, renal-specific brush-border membrane Na^+-P_i cotransporter (NPT2, gene symbol SLC172A) maps to human chromosome 5q35. The methods include PCR amplification of genomic DNA from a panel of human-hamster somatic cell hybrids that either lack or contain DNA in regions 5q13 and 5q35 (13, 14) and a chromosome 5 radiation hybrid panel (J. D. McPherson, unpublished data), using NPT2-specific primers. In addition, FISH was performed with an NPT2 genomic clone as probe. The present findings are consistent with our previous mapping data in which a human NPT2 cDNA was used as a probe for FISH (10). We suggest that the localization of NPT2 to chromosome 5q13 (12) was likely the result of nonspecific hybridization (only nine cells of 50 examined gave a positive signal) (12). Moreover, improper chromosomal assignment may have occurred since hybridization was not performed directly on banded chromosomes (12).

Using the radiation hybrid panel, we were able to confirm the localization of NPT2, to position NPT2 relative to other chromosome 5 loci, and to identify flanking polymorphic microsatellite markers D5S498 and D5S469. These data provide a basis for linkage analysis to determine whether the Na^+-P_i cotransporter is a candidate gene for several autosomal disorders of renal phosphate wasting (7, 8).

The NPT2-specific primers used in the present study were designed from the cDNA sequence (3). Each of the NPT2-specific primer pairs spans an intron, generating a PCR product that is larger than that expected from the cDNA sequence. The size of NPT2 introns was derived by cloning and characterization of the human NPT2 gene (18). Primer pairs "forward 618/reverse 764" and "forward 1405/reverse 1667" amplify introns 6 and 12 which are 122 and 700 bp, respectively (18). Because NPT2 is renal-specific and not expressed in white blood cells or skin fibroblasts, a knowledge of the intron/exon boundaries of the NPT2 gene is necessary for mutation analysis of the NPT2 coding sequence in genomic DNA samples. This information is relevant to patients with autosomal disorders of renal P_i wasting once linkage to polymorphic markers flanking NPT2 on human chromosome 5q35 is established.

Acknowledgments. The authors thank Drs. Michael Boehnke for the rh2pt and RHMAXLIK programs and Pieter de Jong for the arrayed library of human PAC clones.

REFERENCES

1. Berndt TJ, Knox FG 1992 Renal regulation of phosphate excretion. In: Seldin DW, Giebisch G (eds) The Kidney. Physiology and Pathophysiology. Raven Press, New York, pp 2511–2532
2. Murer H, Biber J 1996 Molecular mechanisms of renal apical Na phosphate cotransport. Annu Rev Physiol 58:607–618
3. Magagnin S, Werner A, Markovich D, Sorribas V, Stange G, Biber J, Murer H 1993 Expression cloning of human and rat renal cortex Na/P_i cotransport. Proc Natl Acad Sci USA 90:5979–5983
4. Sorribas V, Markovich D, Hayes G, Stange G, Forgo J, Biber J, Murer H 1994 Cloning of a Na/P_i cotransporter from opossum kidney cells. J Biol Chem 269:6615–6621
5. Verri T, Markovich D, Perego C, Norbis F, Stange G, Sorribas V, Biber J, Murer H 1995 Cloning of a rabbit renal Na-P_i cotransporter, which is regulated by dietary phosphate. Am J Physiol 268:F626–F633
6. Hartmann CM, Wagner CA, Busch AE, Markovich D, Biber J, Lang F, Murer H 1995 Transport characteristics of a murine renal Na/P_i-cotransporter. Pflügers Arch 430:830–836
7. McKusick VA 1992 Mendelian Inheritance in Man. Johns Hopkins University Press, Baltimore
8. Rasmussen H, Tenenhouse HS 1995 Mendelian hypophosphatemias. In: Scriver CR, Beaudet AL, Sly WS, Valle D (eds) The Metabolic and Molecular Basis of Inherited Disease. McGraw-Hill, New York, pp 3717–3745
9. Tenenhouse HS, Werner A, Biber J, Ma S, Martel J, Roy S, Murer H 1994 Renal Na^+-phosphate cotransport in murine X-linked hypophosphatemic rickets: molecular characterization. J Clin Invest 93:671–676
10. Kos CH, Tihy F, Econs MJ, Murer H, Lemieux N, Tenenhouse HS 1994 Localization of a renal sodium phosphate cotransporter gene to human chromosome 5q35. Genomics 19:176–177
11. The HYP Consortium 1995 A gene (PEX) with homologies to endopeptidases is mutated in patients with X-linked hypophosphatemic rickets. Nat Genet 11:130–136
12. Ghishan FK, Knobel S, Dasuki M, Butler M, Phillips J 1994 Chromosomal localization of the human renal sodium phosphate transporter to chromosome 5: implications for X-linked hypophosphatemia. Pediatr Res 35:510–513
13. Iozzo RV, Naso MF, Cannizzaro LA, Wasmuth JJ, McPherson JD 1992 Mapping of the versican proteoglycan gene (CSPG2) to the long arm of human chromosome 5 (5q12–5q14). Genomics 14:845–851
14. McPherson JD, Morton RA, Ewing CM, Wasmuth JJ, Overhauser J, Nagafuchi A, Tsukita S, Isaacs WB 1994 Assignment of the human α-catenin gene (CTNNA1) to chromosome 5q21–q22. Genomics 19:190
15. Boehnke M, Lange K, Cox DR 1991 Statistical methods for multipoint radiation hybrid mapping. Am J Hum Genet 49:1174–1188
16. Carpten JD, DiDonato CJ, Ingraham SE, Wagner-McPherson C, Nieuwenhuijsen BW, Wasmuth JJ, Burghes AMH 1994 A YAC contig of the region containing the spinal muscular atrophy gene (SMA): identification of an unstable region. Genomics 24:351–356
17. Warrington JA, Bengtsson U 1994 High-resolution physical mapping of human 5q31–q33 using three methods: radiation hybrid mapping, interphase fluorescence *in situ* hybridization, and pulsed-field gel electrophoresis. Genomics 24:395–398
18. Hartmann CM, Hewson AS, Kos CH, Hilfiker H, Soumounou Y, Murer H, Tenenhouse HS 1996 Structure of murine and human renal type II Na^+-phosphate cotransporter genes (*Npt2* and NPT2). Proc Natl Acad Sci USA 93:7409–7414

"Comparative mapping of Na^+-phosphate cotransporter genes, NPT1 and NPT2, in human and rabbit", Cytogenetics and Cell Genetics volume 75: 22-24 1996.

A great deal can be learned about the evolutionary history of related species by comparing their chromosomes and, when possible their gene maps (Mange and Mange, 1990). It has often been observed that closely related species have similar chromosomes and gene maps. Conserved chromosomal segments can serve as phylogenetic characters for tracking rearrangements resulting in evolution and speciation and for reconstruction of ancestral genomes (O'Brien et al., 1997).

Comparative gene mapping in mammals was first performed early in the history of genetics (Womack, 1987). The first linkage group reported in a mammalian species was between the loci albino and pink eye in mice (Haldane et al., 1915), a linkage conservation later demonstrated in both rats (Castle and Wachter, 1924) and deermice (Clark, 1936). The gene map of the laboratory mouse was essentially the sole reference for the organization of genes on mammalian autosomes up until the 1970's. Its relationship to the maps of others species was unknown simply because maps of other species did not exist (Womack, 1987). When Ohno postulated the conservation of the mammalian X chromosome (Ohno, 1967), the paucity of mapping data in mammalian species other than the mouse prohibited scientists from generating models of autosomal conservation (Womack, 1987). The complete synteny conservation of greater than 14 genes on the X chromosome in mouse and man supports Ohno's hypothesis that chromosomal rearrangements involving the X chromosome and autosomes are strongly selected against. Similarly, complete synteny conservation is found for all genes mapped to the Y chromosome (Nadeau, 1989).

In addition to providing tools for studying evolution and speciation, comparative gene mapping and knowledge of the gene maps of other species have applications to the study of human disease. For example, when the location of a gene is known in another species, one can often determine where the gene will be found in humans by comparing the gene map of that species to the human gene map. Knowledge of other mammalian gene maps can aid in the identification or creation of animal models to study disease physiology and the adaptation processes used by other species to overcome disease. These models can provide clues for designing and testing treatments for human disease (O'Brien et al., 1997).

Comparative mapping data are presently available for more than 25 species of mammals. In some pairs of species the number of genes mapped in both species is less than 20. In mouse and human the locations of more than 250 genes have been mapped (http://www.jax.org). The chromosomal distribution of homologous genes between different species can be characterized in three ways, depending on the number and order of genes in each segment (Nadeau, 1989). Homology segments are the fundamental units of comparative gene mapping, because segments can be marked by a single gene localized in the two species. A gene that identifies a homology segment therefore represents the first evidence concerning the location of a homologous chromosomal segment (Nadeau, 1989). Conserved syntenies occur when two genes localize to the same chromosome in the two species, regardless of gene order. An example of a conserved synteny is the pair of genes DHFR and HTRA. The DHFR gene is on human 5q and mouse 13 and the HTRA1 gene is also on human 5q and mouse 13 (Oakey et al., 1991). Conserved linkages are the most rigorously defined segments because both synteny and the gene order must be conserved, which are important for understanding the extent and nature of conservation (Nadeau, 1989).

The aim of this comparative gene mapping study was to localize the NPT1 and NPT2 genes in rabbit and determine whether they mapped to established human-rabbit syntenic groups.

Cytogenet Cell Genet 75:22–24 (1996)

Cytogenetics and Cell Genetics

Comparative mapping of Na⁺-phosphate cotransporter genes, NPT1 and NPT2, in human and rabbit

C.H. Kos,[1] F. Tihy,[2] H. Murer,[3] N. Lemieux,[2] and H.S. Tenenhouse[1,4]

Departments of [1] Biology and [4] Pediatrics, McGill University, Montreal, Québec (Canada); [2] Département de Pathologie, Faculté de Médecine, Université de Montréal, Montréal, Québec (Canada); and [3] Institute of Physiology, University of Zurich, Zurich (Switzerland)

Abstract. The chromosome locations of the rabbit *(Oryctolagus cuniculus)* Na⁺-phosphate cotransporter genes NPT1 and NPT2 were determined by fluorescence in situ hybridization. Our results localize NPT1 to rabbit chromosome 12p11 and NPT2 to rabbit chromosome 3p11. The corresponding genes in the human map to chromosome bands 6p22 and 5q35, respectively. These assignments agree with the previously reported homology between rabbit chromosome 12 and human chromosome 6 and provide the basis for the establishment of a conserved syntenic group between rabbit chromosome 3 and human chromosome 5.

The karyotype of the rabbit *(Oryctolagus cuniculus)* is believed to have remained similar to the ancestral karyotype of eutherian mammals. Earlier cytogenetic studies comparing human and rabbit chromosomes revealed considerable homology in the banding patterns of most of the chromosomes of the two species (Dutrillaux et al., 1980). Comparative gene mapping in these two species has shown that the similarity in banding patterns is reflected in conserved syntenic gene content (Soulié and de Grouchy, 1982, 1983; Xu and Hardison, 1989, 1991).

The genes NPT1 and NPT2 encode two distinct, renal-specific, high-affinity Na⁺-phosphate cotransporter types which display 20% similarity (Murer and Biber, 1996). Both Na⁺-phosphate cotransporters reside at the brush-border membrane of proximal tubular cells, where the bulk of filtered phosphate is reabsorbed (Murer and Biber, 1996). The human NPT1 gene was previously mapped to 6p23→p21.3 using human somatic cell hybrid and chromosome 6 deletion panels (Chong et al., 1993). The NPT2 gene was localized to human chromosome band 5q35 by fluorescence in situ hybridization (FISH) (Kos et al., 1994).

Comparison of the R-band patterns of human and rabbit chromosomes (Dutrillaux et al., 1980) and a previous comparative gene mapping study (Lemieux and Dutrillaux, 1992) showed that the long arm of human chromosome 6 is homologous to the long arm of rabbit chromosome 12. However, to date, no genes mapping to the short arm of human chromosome 6 have been mapped in the rabbit. Moreover, similarities between human chromosome 5 and a rabbit chromosome have not been reported by either comparative banding or gene mapping. Because of the lack of banding similarity between human chromosome 5 and a rabbit chromosome, comparative gene mapping is the only approach so far likely to determine which regions of the rabbit genome are homologous to human chromosome 5. The availability of the corresponding rabbit NPT1 (NaPi-1; Werner et al., 1991) and NPT2 (NaPi-6; Verri et al., 1995) cDNAs made it possible to map these two genes and determine homology segments in the rabbit with the short arm of human chromosome 6 and the long arm of human chromosome 5.

Supported by the Medical Research Council of Canada (MRC Genetics Group Grant to H.S.T.), the Swiss National Science Foundation (to H.M.), and the Recherche et Diagnostic en Cytogenetique (Redex, Inc., grant to N.L.). C.H.K. is the recipient of Studentship Awards from the McGill University–Montreal Children's Hospital Research Institute and The McGill Faculty of Medicine.

Received 20 June 1996; accepted 1 August 1996.

Request reprints from Dr. Harriet S. Tenenhouse, Montreal Children's Hospital, 2300 Tupper Street, Montreal, Quebec H3H 1P3 (Canada); telephone: 514-934-4417; fax: 514-934-4329; e-mail: mdhtt@musica.mcgill.ca.

KARGER E-mail karger@karger.ch Fax + 41 61 306 12 34 http://www.karger.ch

0301–0171/96/0751–0022$10.00/0

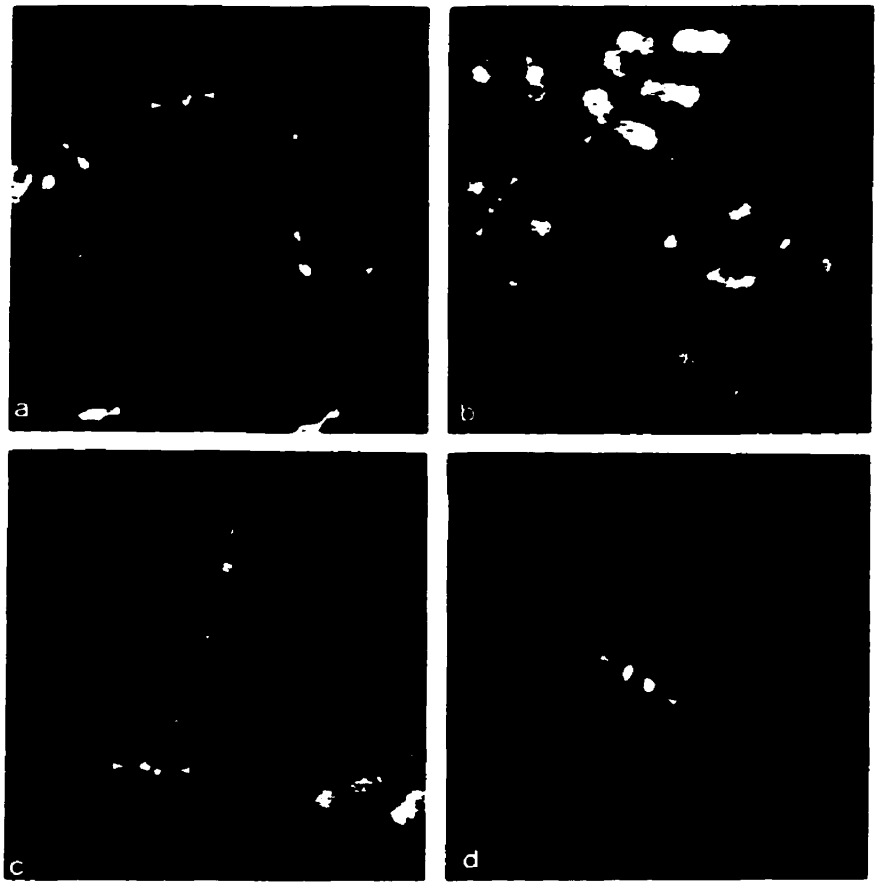

Fig. 1. Localization of the NPT1 and NPT2 genes to human and rabbit BrdU-substituted chromosomes by FISH. Fluorescent signals depict the localization of NPT1 to HSA 6p22 (**a**) and OCU 12p11 (**b**) and of NPT2 to HSA 5q35 (**c**) and OCU 3p11 (**d**), following R-banding. In each case, hybridization of biotinylated, full-length cDNA probes to human or rabbit metaphase and prometaphase chromosomes was performed as described in the Materials and methods.

Materials and methods

Metaphase and prometaphase chromosomes were prepared from human and rabbit lymphoblast cultures as described by Drouin et al. (1988). Prior to harvesting the cultures, 5-bromodeoxyuridine (BrdU) was added to the cultures to reveal early replicating bands. Rabbit NPT1 (NaPi-1; Werner et al., 1991) and NPT2 (NaPi-6; Vern et al., 1995) and human NPT1 (Chong et al., 1993, a gift from Dr. Mark Hughes, National Center for Human Genome Research, Bethesda, MD, USA) and NPT2 (NaPi-3; Magagnin et al., 1993) cDNAs were used in this study. The insert sizes of rabbit NaPi-1 and NaPi-6 cDNAs in pSport were 2.1 and 2.7 kb, respectively. The insert sizes of human NPT1 and NaPi-3 cDNAs in pSport and pBluescript were 2.5 and 2.7 kb, respectively.

The specificity of the rabbit NaPi-1 and NaPi-6 cDNA probes was tested by Northern analysis of total RNA from rabbit kidney. The rabbit NaPi-1 and NaPi-6 cDNAs each hybridized to a single renal transcript of the expected size (Werner et al., 1991; Vern et al., 1995), indicating that each probe is gene specific (data not shown). The probes were biotinylated according to the Bionick protocol (GIBCO BRL). Prior to hybridization, the probes were denatured at 95°C for 8 min. Two hundred nanograms of each denatured probe was hybridized to denatured metaphase spreads at a final concentration of 20 ng/ml. After overnight hybridization at 37°C, the slides were washed and incubated with immunofluorescent agents to produce a signal at the site of hybridization (Lemieux and Dutrillaux, 1992). The chromosomes were counterstained with propidium iodide. The antifade agent *p*-phenylenediamine was added at pH 11 for visualization of R-bands under UV light (Lemieux et al., 1992). Hybridization signals were considered positive when present repeatedly on at least one chromatid.

Results and discussion

Assignments to human (HSA) and rabbit (OCU) chromosomes

The NPT1 gene mapped to HSA 6p22 (Fig. 1a). Localization was established by analysis of 32 metaphase spreads with 76 signals. Twenty-four (75%) of the metaphases showed a signal on each of the two chromatids. These results confirm and refine the previous localization of NPT1 to HSA 6p23→p21.3 (Chong et al., 1993) and place the gene distal to the HLA locus. In the rabbit, NPT1 mapped proximal to the centromere on OCU 12p11 (Fig. 1b). Sixty-seven metaphase spreads with 160 signals were examined. Fifty-one (77%) of the metaphases exhibited two signals.

The NPT2 gene was previously mapped to HSA 5q35 (Kos et al., 1994), which lies above the telomere of the long arm of HSA 5 (Fig. 1c). In the rabbit, NPT2 mapped to OCU 3p11, which is at the proximal end of the short arm above the centromere (Fig. 1d). Thirty-two metaphases exhibited 54 signals. Fourteen (44%) of the metaphase spreads showed a signal on both chromatids.

Comparison between human and rabbit chromosomes

The present localization of NPT1 to HSA 6p22 and OCU 12p11 is consistent with previously reported homologies between HSA 6 and OCU 12 suggested by comparative banding studies (Dutrillaux et al., 1980). In addition, comparative mapping of the superoxide dismutase 2 gene (SOD2) using FISH revealed SOD2-homologous segments at HSA 6q21 and OCU 12q (Lemieux and Dutrillaux, 1992). Thus, markers from both the long and short arms of HSA 6 have been mapped to homologous arms of OCU 12. While the SOD2 and NPT1 genes are syntenic in both human and rabbit, it is believed that a pericentric inversion occurred in the human lineage, producing a longer short arm (Lemieux and Dutrillaux, 1992). The breakpoints of the inversion seem to have been distal to 6q21 and proximal to 6p22.

Comparative banding of human and rabbit chromosomes has not revealed any homology between HSA 5 and OCU 3 (Dutrillaux et al., 1980). This suggests that, unlike the OCU 12/HSA 6 ancestral chromosome, the ancestral chromosome that has given rise to OCU 3 and HSA 5 underwent considerably more rearrangement. The basic unit of comparative gene mapping is a homology segment. It represents the first evidence concerning the location of a homologous chromosomal segment and can be marked by a single gene (Nadeau, 1989). The chromosomal localization of NPT2 to OCU 3p11 now identifies a homologous segment in these two species and provides the basis for establishing whether there exists a syntenic region between HSA 5q35 and OCU 3p11. Closer examination of the R-banding pattern of the distal end of HSA 5q does suggest some similarity to OCU 3p. It will be of interest to assign additional loci from HSA 5q35 in the rabbit to determine the extent and boundaries of the conserved region.

It is clear that a great deal of similarity in the organization of the genome can exist even between divergent mammalian species and that homologous regions can remain conserved over millions of years of evolution. Comparative mapping of the NPT1 and NPT2 Na^+-phosphate cotransporter genes in the human and rabbit helps to determine unassigned syntenic groups in these two species and helps to define regions representing relics of ancestral linkage groups not yet disrupted by chromosomal rearrangements.

Acknowledgements

We thank Dr. Mark Hughes for the human NPT1 cDNA and Jean Leveillé for the photographic work.

References

Chong SS, Kristjansson K, Zoghbi HY, Hughes MR: Molecular cloning of the cDNA encoding a human renal sodium phosphate transport protein and its assignment to chromosome 6p21.3→p23. Genomics 18:355–359 (1993).

Drouin R, Lemieux N, Richer CL: High-resolution R-banding at the 1250-band level: technical considerations on cell synchronization and R-banding (RHG and RBG). Cytobios 56:107–125 (1988).

Dutrillaux B, Viegas-Péquignot E, Couturier J: Très grande analogie de marquage chromosomique entre le lapin *(Oryctolagus cuniculus)* et les primates, dont l'homme. Annls Génét 23:22–25 (1980).

Kos CH, Tihy F, Econs MJ, Murer H, Lemieux N, Tenenhouse HS: Localization of a renal sodium-phosphate cotransporter gene to human chromosome 5q35. Genomics 19:176–177 (1994).

Lemieux N, Dutrillaux B: New gene assignments to rabbit chromosomes: implications for chromosome evolution. Cytogenet Cell Genet 61:132–134 (1992).

Lemieux N, Dutrillaux B, Viegas-Péquignot E: A simple method for simultaneous R- or G-banding and fluorescence in situ hybridization of small single-copy genes. Cytogenet Cell Genet 59:311–312 (1992).

Magagnin S, Werner A, Markovich D, Sorribas V, Stange G, Biber J, Murer H: Expression cloning of human and rat renal cortex Na/Pi-cotransport. Proc natl Acad Sci USA 90:5979–5983 (1993).

Murer H, Biber J: Molecular mechanisms of renal Na-phosphate cotransport. A Rev Physiol 58:607–618 (1996).

Nadeau JH: Maps of linkage and synteny homologies between mouse and man. Trends Genet 5:82–86 (1989).

Soulié J, de Grouchy J: Of rabbit and man: comparative gene mapping. Hum Genet 60:172–175 (1982).

Soulié J, de Grouchy J: New assignments in the rabbit *(Oryctolagus cuniculus)*: comparison with other species. Hum Genet 63:48–52 (1983).

Verri T, Markovich D, Perego C, Norbis F, Stange G, Sorribas V, Biber J, Murer H: Cloning of a rabbit renal Na-Pi cotransporter, which is regulated by dietary phosphate. Am J Physiol 268:F626–F633 (1995).

Werner A, Moore ML, Mantei N, Biber J, Semenza G, Murer H: Cloning and expression of cDNA for a Na/Pi cotransport system of kidney cortex. Proc natl Acad Sci USA 88:9608–9612 (1991).

Xu J, Hardison RC: Localization of the β-like globin gene cluster and the genes for parathyroid hormone and c-Harvey-*ras* 1 to region q14→q21 of rabbit chromosome 1 by in situ hybridization. Cytogenet Cell Genet 52:157–161 (1989).

Xu J, Hardison RC: Localization of the α-like globin gene cluster to region q12 of rabbit chromosome 6 by in situ hybridization. Genomics 9:362–365 (1991).

Chapter 3. NPT2 Gene Structure

"Structure of murine and human renal type II Na^+-phosphate cotransporter genes (*Npt2* and NPT2)", Proceedings of the National Academy of Sciences USA volume 93: 7409-7414 1996.

In this article, the structures of the human NPT2 and mouse *Npt2* genes were determined. Knowledge of the human NPT2 gene structure is necessary for ascertaining whether NPT2 mutations are present in pedigrees segregating autosomally inherited disorders of phosphate homeostasis because NPT2 mRNA expression is kidney-specific and kidney samples are not available for direct mutation analysis of patient NPT2 transcripts. The mouse *Npt2* gene was also characterized so that a knock out vector could be designed for creation of a mouse lacking the *Npt2* gene.

Proc. Natl. Acad. Sci. USA
Vol. 93, pp. 7409–7414, July 1996
Physiology

Structure of murine and human renal type II Na^+-phosphate cotransporter genes (*Npt2* and NPT2)

C. M. HARTMANN*†, A. S. HEWSON*†‡, C. H. KOS†‡, H. HILFIKER*, Y. SOUMOUNOU‡, H. MURER*, AND H. S. TENENHOUSE‡§

*Department of Physiology, University of Zurich, Winterthurerstrasse 190, Zurich, CH-8057, Switzerland; and ‡McGill University–Montreal Children's Hospital Research Institute, Departments of Pediatrics and Biology, McGill University, Montreal, Quebec H3H 1P3, Canada

Communicated by Gerhard Giebisch, Yale University, New Haven, CT, March 25, 1996 (received for review January 5, 1996)

ABSTRACT **Na^+-phosphate (Pi) cotransport across the renal brush border membrane is the rate limiting step in the overall reabsorption of filtered Pi. Murine and human renal-specific cDNAs (NaPi-7 and NaPi-3, respectively) related to this cotransporter activity (type II Na^+-Pi cotransporter) have been cloned. We now report the cloning and characterization of the corresponding mouse (*Npt2*) and human (NPT2) genes. The genes were cloned by screening mouse genomic and human chromosome 5-specific libraries, respectively. Both genes are approximately 16 kb and are comprised of 13 exons and 12 introns, the junctions of which conform to donor and acceptor site consensus sequences. Putative CAAT and TATA boxes are located, respectively, at positions −147 and −40 of the *Npt2* gene and −143 and −51 of the NPT2 gene, relative to nucleotide 1 of the corresponding cDNAs. The translation initiation site is within exon 2 of both genes. The first 220 bp of the mouse and human promoter regions exhibit 72% identity. Two transcription start sites (at positions −9 and −10 with respect to nucleotide 1 of NaPi-7 cDNA) and two polyadenylylation signals were identified in the *Npt2* gene by primer extension, 5′ and 3′ rapid amplification of cDNA ends (RACE). A 484-bp 5′ flanking region of the *Npt2* gene, comprising the CAAT box, TATA box, and exon 1, was cloned upstream of a luciferase reporter gene; this construct significantly stimulated luciferase gene expression, relative to controls, when transiently transfected into OK cells, a renal cell line expressing type II Na^+-Pi cotransporter activity. The present data provide a basis for detailed analysis of cis and trans elements involved in the regulation of *Npt2*/NPT2 gene transcription and facilitate screening for mutations in the NPT2 gene in patients with autosomally inherited disorders of renal Pi reabsorption.**

The mammalian kidney is an important arbiter of extracellular phosphate (Pi) homeostasis. Renal Pi reabsorption occurs predominantly in the proximal tubule where concentrative, Na^+-gradient dependent Pi transport across the brush border membrane is the rate limiting step in the overall Pi reabsorptive process and the site for its regulation (1–6). Although parathyroid hormone and Pi availability are the most important regulators of renal Na^+-Pi cotransport, a variety of hormones including thyroid hormone, 1,25-dihydroxyvitamin D, insulin-like growth factor I, insulin, epidermal growth factor, and glucocorticoids can also modulate cotransporter activity (1–6). However, the molecular mechanisms involved in many of these regulatory processes have not been clearly defined.

Several Mendelian disorders of Pi homeostasis can be attributed to a specific defect in renal Pi reabsorption (7, 8). Autosomal and X-linked forms have been described and both are characterized by reduced growth rate and hypophosphatemic bone disease (7, 8). The mutant genes responsible for the defect in renal Pi transport in these conditions are unknown, with the exception of a candidate gene (PEX) for X-linked hypophosphatemia, recently identified by positional cloning (9).

The cloning of homologous cDNAs encoding high-affinity, renal-specific type II Na^+-Pi cotransporters from several mammalian species has provided structural information about the molecular entities that mediate the cotransport process (10–13). Injection of cloned cRNAs into *Xenopus* oocytes conferred Na^+-dependent Pi transport with kinetic parameters, Na^+-Pi stoichiometry, and pH dependence similar to that seen in isolated renal brush border membrane vesicles (10–13). The cDNAs encode glycosylated proteins of ≈70 kDa with eight putative transmembrane domains (10–13) that have been localized by immunohistochemistry to the apical surface of proximal tubular cells (14).

The human type II Na^+-Pi cotransporter gene (NPT2) was mapped to human chromosome 5q35 by fluorescence *in situ* hybridization (15), thereby ruling it out as a candidate gene for X-linked hypophosphatemia, consistent with the positional cloning of the PEX gene (9). Of interest, however, is the demonstration that in hypophosphatemic (*Hyp*) mice harboring the homologous X-linked mutation, decreased renal Pi reabsorption can be ascribed to a decrease in brush border membrane Na^+-Pi cotransport that is associated with a proportional decrease in type II Na^+-Pi cotransporter mRNA and immunoreactive protein (16). These findings suggest that the PEX gene product plays an important role in the regulation of type II Na^+-Pi cotransporter gene expression. However, the mechanism for this regulation is not understood.

The present study was undertaken to define the structure of the murine (*Npt2*) and human (NPT2) type II Na^+-Pi cotransporter genes. Promoter sequences and intron/exon boundaries were identified for both genes. Our results thus provide a basis for future studies to characterize promoter activity, elucidate the mechanisms underlying the regulation of *Npt2*/NPT2 gene expression, and screen for mutations in patients with Mendelian hypophosphatemias that are autosomally inherited.

MATERIALS AND METHODS

Southern Blot Analysis of Mouse and Human DNA. Genomic DNA from mouse liver and human peripheral blood leukocytes was isolated by the phenol-chloroform method described by Sambrook *et al.* (17). DNA (10 μg) was digested with restriction endonucleases (5 units/μg DNA) under conditions specified by the supplier and electrophoresed on 0.8% agarose gels in 1 × TAE buffer (0.04 M Tris acetate/0.001 M EDTA, pH 8.0). A 1-kb DNA ladder (GIBCO/BRL) was run in parallel with the digested DNA. DNA fragments were capillary transferred to nitrocellu-

The publication costs of this article were defrayed in part by page charge payment. This article must therefore be hereby marked "*advertisement*" in accordance with 18 U.S.C. §1734 solely to indicate this fact.

Abbreviation: RACE, rapid amplification of cDNA ends.

Data deposition: The sequences reported in this paper have been deposited in the GenBank database [accession nos. U56664–U56673, U57491, and U57839 (for mouse) and U56674–U56695 and U57548 (for human)].

†C.M.H., A.S.H., and C.H.K. contributed equally to this publication and are listed alphabetically.

§To whom reprint requests should be addressed at: Montreal Children's Hospital, 2300 Tupper Street, Montreal, Quebec H3H 1P3, Canada. e-mail: mdht@musica.mcgill.ca.

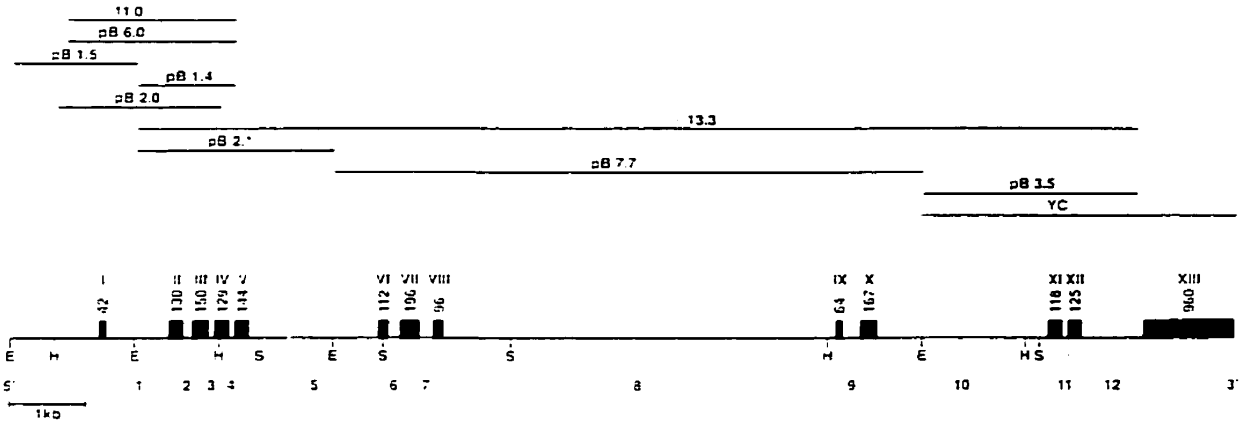

FIG. 1. Organization of the mouse *Npt2* gene. Genomic clones and subclones used for the analysis of *Npt2* gene structure are indicated. The restriction map of the *Npt2* gene was derived by digestion of subcloned genomic fragments with *Eco*RI (E), *Hin*dIII (H), and *Sac*I (S). The position of introns (depicted by dotted vertical lines and numbered 1–12) was determined by sequencing across intron/exon boundaries of subcloned genomic fragments and PCR products amplified from mouse genomic DNA, using exonic primers. Intron size was estimated by restriction analysis, by direct sequencing for small introns, and by estimating the size of PCR amplification products for large introns. Exons are depicted as filled boxes (numbered I–XIII) and their size is indicated by the number above each box.

lose membranes [supported nitrocellulose BA-(S)85, Schleicher & Schuell] or nylon membranes (Biodyne B transfer membrane; Pall) with 20 × SSC as described elsewhere (17). Full-length murine NaPi-7 (13) and human NaPi-3 (10) cDNAs were ^{32}P-labeled to a specific activity of $>1 \times 10^9$ cpm/μg with [α-^{32}P]dCTP (3000 Ci/mmol; 1 Ci = 37 GBq; ICN) using a Radprime DNA labeling kit (GIBCO/BRL). Hybridization was performed at 42°C for 16–18 h in 10% dextran sulfate, 40% formamide, 4 × SSC, 0.02 M Tris·HCl (pH 7.6), 1 × Denhardt's solution and herring sperm DNA (0.1 mg/ml). The membranes were washed several times with 2 × SSC/0.1% SDS at room temperature and with 0.1 × SSC/0.1% SDS at 65°C. Mouse DNA was digested with *Eco*RI, *Hin*dIII, *Bgl*II, *Eco*RV, *Mlu*I, and human DNA with *Eco*RI, *Hin*dIII, *Mlu*I, *Eco*RV, *Kpn*I, *Bam*HI, and *Bam*HI + *Mlu*I.

Murine and Human Genomic DNA Library Screening. A λ DASH II mouse (129SV strain) genomic DNA library (received from A. Karaplis, McGill University) was screened with a full-length rat NaPi-2 cDNA probe (10). Two genomic clones, designated λ 13.3 and λ YC (Fig. 1), were isolated. Digestion of the 13.3-kb clone with *Eco*RI generated 2.1-, 7.7-, and 3.5-kb fragments (designated pB 2.1, pB 7.7, and pB 3.5 in Fig. 1), which were subcloned into pBluescript II (Stratagene). To clone the 5′ flanking region of the *Npt2* gene, a λ Gem 11 library derived from mouse AB-1 embryonic stem cell DNA (a gift from U. Müller, University of Zürich) was screened with a 5′ fragment of the NaPi-7 cDNA (545 bp derived by digestion with *Mlu*I and *Sac*I). One of three positive clones, spanning 11 kb (λ 11.0, in Fig. 1), was digested with *Bam*HI to yield a 6.0-kb fragment (pB 6.0, Fig. 1), which was further digested with *Eco*RI. Two of 3 resulting fragments, designated pB 1.5 (1.5-kb fragment) and pB 1.4 (1.4-kb fragment) (Fig. 1), were subcloned into pBluescript II. A 2.0-kb fragment (pB 2.0, Fig. 1), which overlapped with the sequence of pB 1.5 and pB 1.4 (Fig. 1) was obtained by *Hin*dIII digestion of λ 11.0 and was subcloned into pBluescript II. A human chromosome 5-specific λ library (American Type Culture Collection) was screened with a full-length human cDNA (NaPi-3) probe (10). One of four positive λ clones was digested with *Eco*RI and 3.8- and 4.2-kb fragments were subcloned into pBluescript II.

Nucleotide Sequencing. Genomic *Npt2* and NPT2 subclones were sequenced using the Sequenase Version 2.0 kit (United States Biochemical) with [α-^{35}S]dATP (ICN). The 5′ and 3′ RACE products were sequenced using a T7 Sequencing kit (Pharmacia). DNA fragments, generated by PCR amplification of mouse or human genomic DNA, were sequenced using the double-stranded DNA cycle sequencing system (GIBCO/BRL). Sequencing reactions were resolved on 8% polyacrylamide gels. Sequencing primers were designed from the NaPi-7 (13) and NaPi-3 (10) cDNA sequences.

PCR Amplification. PCR amplification of genomic clones or genomic DNA was performed using forward and reverse primer pairs based on the NaPi-7 and NaPi-3 cDNA sequences. The amplification reactions contained 100–200 ng of DNA, 2.5 units of *Taq* polymerase (GIBCO/BRL) or 1 unit of Elongase (GIBCO/BRL), 10 μl of 10 × PCR buffer (GIBCO/BRL), 200 μM dNTPs, 20 pmol of each primer, and 1–3 mM $MgCl_2$ in a total volume of 100 μl. After an initial 1.5-min denaturation step at 94°C, 30–35 cycles of amplification were performed using a Perkin–Elmer/Cetus DNA thermal cycler. After the last cycle,

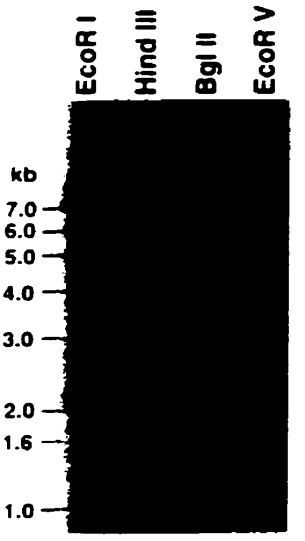

FIG. 2. Southern blot analysis of mouse genomic DNA. Mouse liver DNA (10 μg) was digested with *Eco*RI, *Hin*dIII, *Bgl*II, or *Eco*RV, electrophoresed on 0.8% agarose gels, transferred to supported nitrocellulose, and hybridized with a full-length ^{32}P-labeled rat NaPi-2 cDNA probe (10). The size calibration was obtained by simultaneous loading of a 1-kb DNA ladder.

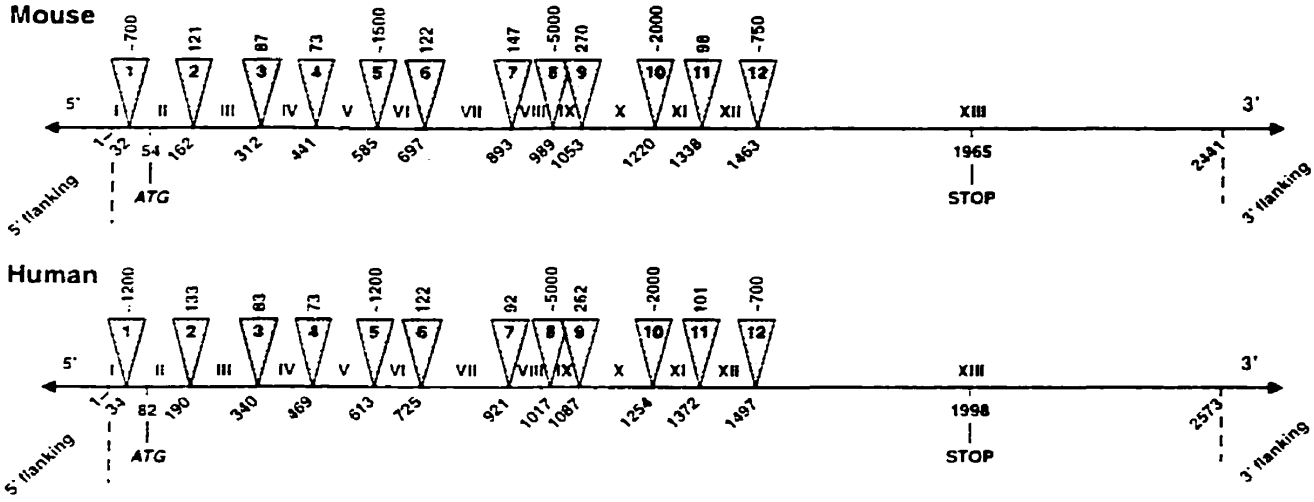

FIG. 3. Comparison of the *Npt2* and NPT2 genes. Location of intron/exon boundaries was determined as described in the legend to Fig. 1 and in *Materials and Methods*. Introns are depicted by triangles and are numbered 1–12. The size of each intron (bp) is shown above each triangle. Exons are numbered I–XIII. Numbers below the line depict the location of introns in the corresponding NaPi-7 and NaPi-3 cDNAs. The vertical dashed lines represent the 5' and 3' ends of the corresponding cDNAs.

elongation was extended to 7 min at 72°C. The primer–template annealing temperatures were approximately 2°C below the T_m of the oligonucleotide primers used. The size of PCR amplified products was estimated by agarose (0.7–2.0%) gel electrophoresis using 100 bp or 1 kb DNA ladders (GIBCO/BRL). PCR products were sequenced as described above to confirm the identity of products. In some cases, PCR amplification products were subcloned into a pCRII vector using a TA cloning system, version 2.2 (Invitrogen) and then sequenced as described above for subcloned fragments.

Intron/Exon Mapping. The location of and sequences at intron/exon boundaries of the *Npt2* and NPT2 genes were determined by sequencing of genomic subclones as described above. To determine whether there are introns downstream from nucleotide 1463 of the NaPi-7 cDNA or downstream from nucleotide 1497 of the NaPi-3 cDNA, PCR amplification reactions were performed with both *Taq* polymerase and Elongase using five different forward and reverse primer pairs with mouse genomic DNA, the mouse λ YC clone (Fig. 1) or human genomic DNA as template. Appropriate water blanks and PCR reactions with cDNA templates were run simultaneously. The identity of PCR products was confirmed by sequencing as described above.

RACE. For 5' RACE mouse kidney total RNA (10 μg) (18) and poly(A)+ RNA (1 μg) [poly(A) Tract System 1000, Promega] were reverse transcribed using 20 units of MuLV reverse transcriptase (Promega) with a NaPi-7-specific primer (nt 195–210 of NaPi-7 cDNA; antisense). The 5' end of the cDNA was extended with polynucleotide transferase (30 units, GIBCO/BRL) in presence of 0.4 mM dATP. PCR was then performed with a second NaPi-7-specific primer (nt 63–78 of NaPi-7 cDNA; antisense), a hybrid dT_{17} adapter primer with a 5' extension containing a *Sal*I recognition site and an adapter primer corresponding to the 5' extension of the dT_{17} adapter primer (19). A second PCR reaction was performed with the adapter primer mentioned above and a third NaPi-7-specific primer (nt 26–41 of NaPi-7 cDNA; antisense). The products were treated with the SureClone ligation kit (Pharmacia), digested with *Sal*I (restriction site located in the adapter primer), subcloned into pBluescript II, and sequenced as described above. For 3' RACE mouse kidney total RNA (10 μg) and poly(A)+ RNA (1 μg) were prepared and reverse transcribed using the dT_{17} adapter primer mentioned above (19). PCR was performed with the adapter primer and a NaPi-7-specific primer (nt 1544–1565 of NaPi-7 cDNA; sense). The products were digested with *Pst*I and *Sal*I, subcloned into pBluescript II, and sequenced.

Primer Extension. A NaPi-7-specific primer, localized within the 5' untranslated region of the cDNA (nt 63–78; antisense), was labeled with 8 units of polynucleotide kinase (Promega) and 50 μCi of [γ-^{32}P]ATP. The labeled primer (≈92,000 cpm) was annealed to 5 μg of total RNA or 4 μg of poly(A)+ RNA, isolated

Table 1. *Npt2*/NPT2 gene intron/exon boundaries

Intron	Location	Donor	Acceptor
		Mouse	
1	32	GTCAAG/gtgag	tgcag/GACTCA
2	162	CACAAG/gtaaa	ctcag/TCCTGC
3	312	AGCCAG/gtagg	tccag/AGCCCA
4	441	CTGGAG/gtagg	tgcag/GGAAGG
5	585	CCGGCT/gtgag	accag/TGTTGG
6	697	CAGGCG/gtgag	ctcag/GGCTTT
7	893	ATCCAG/gtgag	cacag/CTGGAC
8	989	ACAGAG/gtgag	tttag/GCTTCC
9	1053	AGAAAT/gtaag	ttcag/GCAACC
10	1220	ACACAG/gtgag	ttcag/ACTTTC
11	1338	TCATTG/gtgag	accag/GCCTGG
12	1463	TTTCAG/gtaca	ctgag/ATTGCC
		Human	
1	34	TCTAAG/gtgaa	ttcag/CGTTGC
2	190	CTCAGG/gtaag	cctag/TCCTAC
3	340	AGCCAG/gtggg	tccag/AGTCCA
4	469	CTGGAG/gtagg	cccag/GGAAGG
5	613	CTGGCT/gtgta	accag/TGCTGG
6	725	CCGGCG/gtgtg	cccag/GGCCTT
7	921	ATCCAG/gtgac	cacag/CTGGAC
8	1017	TTACAG/gtgag	tctag/GCTCCC
9	1087	AGAAAT/gtaag	gcaag/GCAACC
10	1254	AATACG/gtgtg	ttgag/GACTTC
11	1372	TCATCG/gtgag	cccag/GTCTTG
12	1497	TTCCAG/gtgcg	tgcag/ATTGCC

Location of introns and donor/acceptor site sequences for the *Npt2* and NPT2 genes. The intron location is based on the nucleotide number in the corresponding NaPi-7 and NaPi-3 cDNAs. Exon sequences are depicted in uppercase letters and intron sequences in lowercase letters.

Table 2. *Npt2*/NPT2 gene exon/intron boundary codons

	Mouse		Human	
Intron	Codon phase	Amino acid	Codon phase	Amino acid
2	I	VAL	I	VAL
3	I	GLU	I	GLU
4	I	GLY	I	GLY
5	I	LEU	I	LEU
6	II	ARG	II	ARG
7	0	GLN	0	GLN
8	0	GLU	0	GLN
9	I	CYS	I	CYS
10	I	ASP	0	THR
11	I	GLY	I	GLY
12	0	GLN	0	GLN

Amino acid and codon phase usage at exon/intron boundaries of the *Npt2* and NPT2 genes. The translational start site for both the mouse and human genes lies within exon II (Fig. 3). Introns that do not split codon triplets are indicated by phase 0, interruption after the first nucleotide by phase I, and interruption after the second nucleotide by phase II. Amino acids encoded at the splice sites are indicated.

from mouse kidney as described above. cDNA synthesis was carried out with 20 units of MuLV reverse transcriptase (Promega) as recommended by the supplier. The products of cDNA synthesis were loaded on a 6% sequencing gel along with a sequencing ladder prepared with the above primer and cDNA product.

***Npt2* Promoter Analysis.** A 484-bp *Npt2* fragment was PCR-amplified from the pB 1.5 subclone, using forward and reverse primers corresponding to nucleotides −454 to −435 and 11–30 of the *Npt2* gene, respectively (see Fig. 4). The fragment was subcloned into pBluescript II and the sequence confirmed. The fragment was then excised and inserted immediately upstream of a luciferase reporter gene in a promoterless luciferase expression vector (pGL3-basic, Promega). Correct insertion was verified by sequencing and the right orientation was designated pGL3–484. OK cells that were 40–50% confluent and cultured on 3.5-cm plates as described (20) were transfected with 0.15 μg of the pGL3–484 construct using Ca_2PO_4 (21). pCMV-lacZ (0.2 μg, provided by S. Rusconi, University of Zurich) was cotransfected with the reporter gene construct to control for transfection efficiency. Additional controls were performed by mock-transfection or by transfection with pGL3-basic (0.15 μg). The β-galactosidase assay was done in 0.2 M $NaPO_4$ (pH 7.5), 4 mg/ml *O*-nitrophenyl β-D-galactopyranoside, 1 mM $MgCl_2$ for 30 min at 37°C and the optical density measured at 420 nm. Luciferase was assayed with a luciferase kit and measured in a luminometer (Lumac Biocounter M1500, MBV, Stäfa, Switzerland).

RESULTS AND DISCUSSION

Southern Blot Analysis of Murine and Human Genomic DNA. Southern blot analysis of murine (Fig. 2) and human (not shown) genomic DNA, using full-length NaPi-7 and NaPi-3 cDNA probes, was used to estimate the size and complexity of the *Npt2* and NPT2 genes. Based on digests with at least five restriction endonucleases, or combinations thereof, an approximate size of 16 kb was estimated for both the mouse and human genes. This estimate is in good agreement with the size of the *Npt2* and NPT2 genes determined from genomic cloning (see below). Blots washed at both high and low stringency gave similar results, suggesting that the *Npt2* and NPT2 genes are single copy genes and not part of a larger subfamily of related genes.

Organization of the *Npt2* and NPT2 Genes. Two overlapping *Npt2* clones (λ 13.3 kb and 11.0 kb, Fig. 1) were isolated by screening two mouse genomic DNA libraries. The 13.3-kb clone contained nucleotides 33–1463 of the mouse NaPi-7 cDNA, a portion of the 5′ untranslated region, the ATG translation start site (within exon II), and 12 intron/exon boundaries (Fig. 1). The 11-kb clone contained the first four exons and extended 9 kb into the 5′ flanking region of the gene. The *Npt2* gene did not contain introns downstream of nucleotide 1463 of the cDNA. This was established by PCR amplification of mouse genomic DNA with five different primer pairs, using both *Taq* polymerase and Elongase, which permits amplification of long, single-copy genomic templates (up to 20 kb). In none of the reactions were PCR products detected that exceeded the size expected for the cDNA. The absence of PCR products in corresponding water blanks indicated that contamination with cDNA could not account for our findings. These data were confirmed by PCR amplification of the genomic clone λ YC (Fig. 1).

A single genomic λ clone obtained by screening a human chromosome 5-specific library was digested with *Eco*RI and the 3.8- and 4.2-kb genomic fragments generated were subcloned. The 3.8-kb fragment contained nucleotides 34–1017 of the cDNA, a portion of the 5′ untranslated region, the ATG trans-

```
mouse   gene    gacagtct.g accataggct ccccctgcag aggtgaagat tagCAATtaa ctggaaggaa
                ||    |  | |||||||  | |||| ||||| || ||| ||| ||||||||| |||| |||||
human   gene    gaagaacctg accatagatt ccccatgcag agctgacgat tagCAATtaa ctgggaggaa

mouse   gene    tcttgggggt aaagttaatt taatggggaa aagagggaag gcagctaaag ttcttctagt
                |||  |||||  | |||||||     |||||  |||||||  |  |||||||  | |||
human   gene    tctcaggggt gaggttaatt ...ggggga. cagagggagg gcagctaggg ttc-------

mouse   gene    tcattaagga ctttgccctt gacccgaggg TATAAAgaag agggtcttag ttcct-----
                     | ||| |||||||||| ||||| || | |||||||| | ||||||| || |||
human   gene    ----caggga ctttgccctt gacccaagag TATAAAgagg agggtctcag ttctcctcag

                          * *       +1
mouse   gene    ----ctttag acttccccaA GCAGCCGGGC TGGAGCTGAG CCACAG---
                    ||  ||  ||||    | || || | ||  | ||||||   || ||
human   gene    ggtcctggag gcttcattga gCTGCTGAGC AGAAGCTGAA ACACAG---
                                       +1
```

FIG. 4. Sequence comparison of the 5′ flanking regions of the *Npt2* and NPT2 genes. A comparison of the first 220 bp of the mouse and human promoter sequences revealed an identity of 72%. CAAT and TATA boxes are depicted in boldface, uppercase letters. The transcription start sites of the *Npt2* gene are marked by asterisks. The nucleotides corresponding to the NaPi-7 and NaPi-3 cDNAs are given in uppercase letters. The first nucleotide of each cDNA is labeled as +1. Gaps in the corresponding sequences between the two genes are presented as a dashed line. The sequences were compared and aligned using a program package (Genetics Computer Group, Version 8), which introduces gaps for best fit.

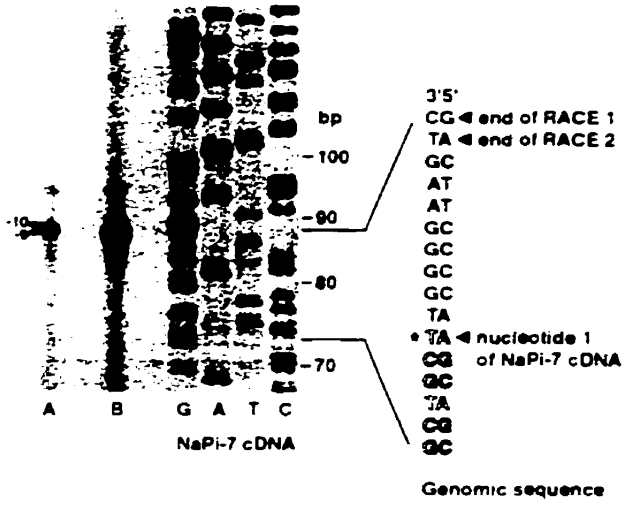

FIG. 5. Determination of the transcriptional start site of the *Npt2* gene by primer extension and 5' RACE. Mouse kidney poly(A)+ RNA (*A*) and total RNA (*B*) were hybridized with a ^{32}P-labeled primer (nt 63–78 of NaPi-7 cDNA) and the primer extension products, generated with reverse transcriptase, were run on 6% polyacrylamide gels. A sequencing ladder prepared with the same primer and the mouse cDNA products was also run on the gel. The extended products were 9 and 10 nucleotides upstream from nucleotide 1 of NaPi-7 cDNA. The double band for total RNA is only visible with longer exposure time. The asterisk depicts the start of the NaPi-7 cDNA sequence and is followed by the sequence of the adaptor used for cloning the cDNA into pSPORT. The boldface letters shown on the right are derived from sequencing two 5' RACE products.

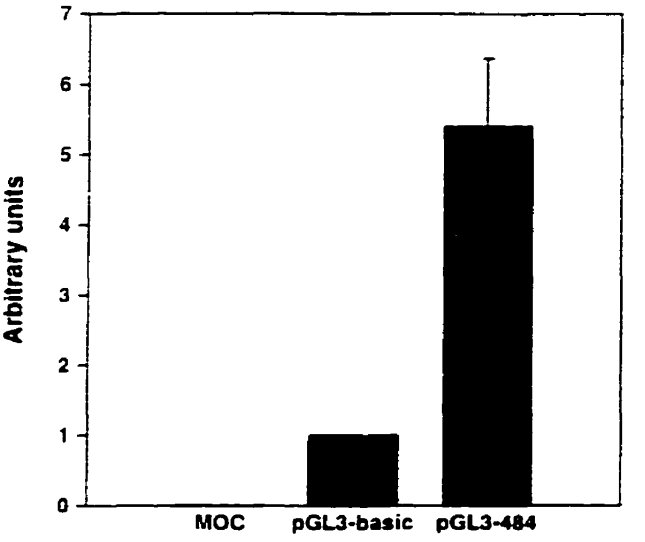

FIG. 7. Expression of a *Npt2* promoter–luciferase construct in OK cells. A 484-bp fragment of the *Npt2* promoter region, comprising exon 1, TATA and CAAT boxes, and 5' sequence, was cloned upstream of a luciferase reporter gene (pGL3–484) as described. OK cells at 40–50% confluency were cotransfected with pGL3–484 and pCMV-lacZ to correct for transfection efficiency. Controls were performed with mock-transfected OK cells and OK cells transfected with the plasmid lacking the *Npt2* promoter fragment (pGL3-basic). After 2 days, the OK cells were harvested and luciferase and β-galactosidase assayed. Luciferase activity was related to β-galactosidase activity. Normalized luciferase activity in OK cells transfected with pGL3-basic was set at one. The data represent the mean ±SD derived from six experiments.

lation initiation site, and eight intron/exon boundaries of the NPT2 gene. Four additional intron/exon boundaries in the NPT2 gene were identified by sequencing PCR products obtained by amplification of human genomic DNA using primers designed from NaPi-3 cDNA sequence. The absence of introns downstream from nucleotide 1497 of the cDNA was confirmed by PCR amplification as described above for the *Npt2* gene.

A comparison of the *Npt2* and NPT2 genes is depicted in Fig. 3. The number, relative position, and size of introns are similar for both murine and human genes. Nucleotide sequences at the intron/exon boundaries of both *Npt2* and NPT2 genes conform to the GT/AG rule for intron donor and acceptor splice sites (Table 1). The amino acids and codon phase usage at exon/intron boundaries are also remarkably similar for both the murine and human genes and differed only in two amino acids and one codon phase usage (Table 2). In addition, a comparison of intronic sequences (introns 2–4) in the *Npt2* and NPT2 genes revealed 68% identity.

Structure of the 5' Flanking Region of the *Npt2* and NPT2 Genes. Sequence analysis of the pB 1.5 subclone (Fig. 1) of the *Npt2* gene revealed a TATA box at position −40 and a CAAT box at position −147, relative to the first nucleotide of NaPi-7 cDNA (Fig. 4). For the NPT2 gene, sequencing the 4.2-kb genomic fragment (see above) revealed a TATA box at position −51 and a CAAT box at position −143, relative to nucleotide 1 of NaPi-3 cDNA (Fig. 4). A comparison of 220 bp from the murine and human promoter regions is depicted in Fig. 4 and shows an overall sequence identity of 72%.

```
2110 acctgtgcat attaagggcc acagtggcat gggcttttgt aattaagagg tagtgtgcac

                              * poly A tail (a)
2170 aaatacatgc taggtactga gcctgtgtga ccattagtgc gggtgtaatg tgagtacact

2230 gtgtgggtac aggcgggtgc agatgcctag ggagtcttca aacttttctg gaaagagtca

2290 gctatacccc ctcattttct cacaactctt gtatcaacag gagggacaga agaacagctg

2350 gccttctgta tacattgggc ttacttctgc caattctgct aactgtgcat agaaaaaaea

                              * poly A tail (b)
2410 aattgaaagt tgc  2422
```

FIG. 6. 3' RACE of mouse kidney mRNA. Two 3' RACE products were obtained with reverse-transcribed mouse kidney poly(A)+ RNA and total RNA as described. The depicted sequence is that of the 3' end and the numbering corresponds to that of NaPi-7 cDNA. Two poly(A) tails were identified, at nucleotide 2189 (*a*) and 2422 (*b*), respectively. Both were preceded by a polyadenylylation signal (underlined).

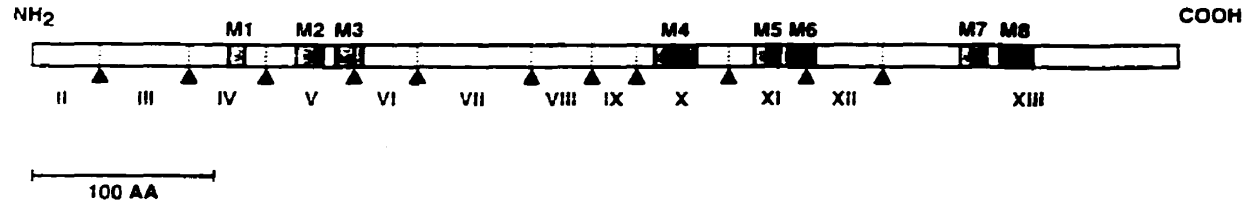

FIG. 8. Superimposition of the exon boundaries with the predicted secondary structure of the *Npt2* protein. The secondary structure was derived from a combination of hydropathy analysis and the inside positive rule. The shaded boxes represent the suggested eight transmembrane regions (numbered M1-M8 in ref. 10). Triangles depict the positions of the exon/intron boundaries. Exons are numbered I-XIII.

Transcription Initiation and Polyadenylylation Sites in the *Npt2* Gene. The transcription initiation site for the mouse gene was determined by primer extension and 5′ RACE. In primer extensions, reverse transcription of poly(A)+ RNA showed two signals, at −9 and −10 (Fig. 5), i.e., 9 and 10 nucleotides upstream from the first nucleotide of the NaPi-7 cDNA (Fig. 4). Similar results were obtained by sequencing the 80-bp amplification product derived from 5′ RACE (Fig. 5).

The 3′ region of the transcribed *Npt2* gene was determined by 3′ RACE. Products of 650 and 900 bp were obtained, subcloned, and sequenced. The larger product ended with a poly(A) tail at nucleotide 2422 and corresponded exactly to the NaPi-7 cDNA (Fig. 6). The shorter 650 bp product was formed from an earlier polyadenylylation signal derived from a cDNA of 2189 bp (Fig. 6). These findings are consistent with the appearance and size of two transcripts (2.6 and 2.4 kb) detected with a full-length, rat NaPi-2 cDNA probe on Northern blots of mouse kidney RNA (10).

Promoter Activity of the 5′ Flanking Region of the *Npt2* Gene. We determined whether a 484 bp 5′ fragment of the *Npt2* gene, containing part of exon I, the TATA and CAAT boxes, could drive the expression of a luciferase reporter gene. The 484-bp fragment functioned as a promoter of luciferase activity following transfection of the pGL3–484 promoter–reporter construct in OK cells (Fig. 7). Correction for transfection efficiency was accomplished by cotransfecting OK cells with the pCMV-lacZ vector. After normalization with respect to β-galactosidase activity, luciferase activity was 5 times greater in OK cells transfected with pGL3–484 than in cells transfected with the same vector lacking the *Npt2* promoter fragment (pGL3-basic) (Fig. 7).

Lack of Correlation Between Exon-Defined Peptide Domains and Predicted Npt2 Secondary Structure. Fig. 8 shows the superimposition of exon boundaries on the *Npt2*/NaPi-7 protein secondary structure model, derived from a combination of hydropathy analysis (22, 23) and the inside positive rule (24, 25). Although previous reports showed that transcripts for several membrane spanning transporter genes and other membrane protein genes are frequently spliced near membrane/aqueous transitions (see ref. 26), no such relationship was apparent with *Npt2*. Moreover, in the case of the *Npt2* gene, exon boundaries are located within predicted transmembrane domains as well as in intracellular and extracellular domains (Fig. 8). Similar findings apply to NPT2.

Conclusions. This study describes the molecular cloning and genomic organization of *Npt2* and NPT2, murine and human type II Na^+-Pi cotransporter genes. The membrane proteins they encode are expressed exclusively in the brush border membrane of renal proximal tubular cells where they mediate the rate limiting step in the renal reabsorption of filtered Pi (1–6). *Npt2*/NPT2 thus play a key role in the overall maintenance of extracellular Pi homeostasis and are crucial for normal bone mineralization and growth. Our data provide a basis for detailed analysis of cis and trans elements involved in the regulation of *Npt2*/NPT2 gene transcription and facilitate screening for mutations in the NPT2 gene in patients with autosomally inherited disorders of renal Pi reabsorption.

Note. In a recent abstract, Taketani *et al.* (27) reported that the human renal type II Na^+-phosphate cotransporter gene spans 8 kb and consists of 10 exons. We have no explanation for the discrepany between those findings and the results of this study.

This work was supported by the Medical Research Council of Canada (MRC Genetics Group Grant to H.S.T.) and the Swiss National Science Foundation (H.M.). C.H.K. is the recipient of Studentship Awards from McGill University–Montreal Children's Hospital Research Institute and The McGill Faculty of Medicine.

1. Mizgala, C. L. & Quamme, G. A. (1985) *Physiol. Rev.* **65**, 431–466.
2. Gmaj, P. & Murer, H. (1986) *Physiol. Rev.* **66**, 36–70.
3. Murer, H., Werner, A., Reshkin, S., Wuarin, R. & Biber, J. (1991) *Am. J. Physiol.* **260**, C885–C899.
4. Murer, H. (1992) *J. Am. Soc. Nephrol.* **2**, 1649–1665.
5. Berndt, T. J. & Knox, F. G. (1992) in *The Kidney: Physiology and Pathophysiology*, eds. Seldin, D. W. & Giebisch, G. (Raven, New York), pp. 2511–2532.
6. Caverzasio, J. & Bonjour, J. P. (1993) *Pediatr. Nephrol.* **7**, 802–806.
7. McKusick, V. A. (1992) *Mendelian Inheritance in Man* (Johns Hopkins Univ. Press, Baltimore).
8. Rasmussen, H. & Tenenhouse, H. S. (1995) in *The Metabolic and Molecular Basis of Inherited Disease*, eds. Scriver, C. R., Beaudet, A. L., Sly, W. S. & Valle, D. (McGraw-Hill, New York), pp. 3717–3745.
9. The HYP Consortium (1995) *Nat. Genet.* **11**, 130–136.
10. Magagnin, S., Werner, A., Markovich, D., Sorribas, V., Stange, G., Biber, J. & Murer, H. (1993) *Proc. Natl. Acad. Sci. USA* **90**, 5979–5983.
11. Sorribas, V., Markovich, D., Hayes, G., Stange, G., Forgo, J., Biber, J. & Murer, H. (1994) *J. Biol. Chem.* **269**, 6615–6621.
12. Verri, T., Markovich, D., Perego, C., Norbis, F., Stange, G., Sorribas, V., Biber, J. & Murer, H. (1995) *Am. J. Physiol.* **268**, F626–F633.
13. Hartmann, C. M., Wagner, C. A., Busch, A. E., Markovich, D., Biber, J., Lang, F. & Murer, H. (1995) *Pflügers Arch.* **430**, 830–836.
14. Custer, M., Lotscher, M., Biber, J., Murer, H. & Kaissling, B. (1994) *Am. J. Physiol.* **266**, F767–F774.
15. Kos, C. H., Tihy, F., Econs, M. J., Murer, H., Lemieux, N. & Tenenhouse, H. S. (1994) *Genomics* **19**, 176–177.
16. Tenenhouse, H. S., Werner, A., Biber, J., Ma, S., Martel, J., Roy, S. & Murer, H. (1994) *J. Clin. Invest.* **93**, 671–676.
17. Sambrook, J., Fritsch, E. F. & Maniatis, T. (1989) *Molecular Cloning: A Laboratory Manual* (Cold Spring Harbor Lab. Press, Plainview, NY).
18. Bertran, J., Werner, A., Strange, G., Markovich, D., Biber, J., Testar, X., Zorano, A., Palacin, M. & Murer, H. (1992) *Biochem. J.* **281**, 717–723.
19. Frohman, M. A. (1990) in *PCR Protocols: A Guide to Methods and Applications*, eds. Innes, M. A., Gelfand, D. H., Sninsky, J. J. & White, T. J. (Academic, New York), pp. 28–38.
20. Malstrom, K. & Murer, H. (1986) *Am. J. Physiol.* **251**, C23–C31.
21. Ausubel, F. M., Brent, R., Kingston, R. E., Moore, D. D., Seidman, J. G., Smith, J. A. & Struhl, K., eds. (1995) *Current Protocols in Molecular Biology*, (Wiley, New York), pp. 9.1.1–9.1.9.
22. Kyte, J. & Doolittle, R. F. (1982) *J. Mol. Biol.* **157**, 105–132.
23. Klein, P., Kanehisa, M. & DeLisi, C. (1985) *Biochim. Biophys. Acta* **815**, 468–476.
24. Hartmann, E., Rapaport, T. A. & Lodish, F. H. (1989) *Proc. Natl. Acad. Sci. USA* **86**, 5786–5790.
25. Cramer, W. A., Engelman, D. M., Von Heijne, G. & Rees, D. C. (1992) *FASEB J.* **6**, 3397–3402.
26. Turk, E., Martin, M. G. & Wright, E. M. (1994) *J. Biol. Chem.* **269**, 15204–15209.
27. Taketani, Y., Miyamoto, K., Tanaka, K., Katai, K., Tatsumi, S., Segawa, H., Yamamoto, H., Chikamori, M., Morita, K., Haga, H. & Takeda, E. (1995) *J. Bone Miner. Res.* **10**, S155 (abstr.).

Chapter 4. A search for the gene responsible for HHRH

INTRODUCTION

The Disorder

Hereditary hypophosphatemic rickets with hypercalciuria is an inherited bone disorder characterized by rickets and osteomalacia, decreased growth rate, bowing of the lower limbs, impaired bone mineralization, decreased renal Pi reabsorption, and hypophosphatemia. The hypophosphatemia in HHRH patients leads to an appropriate increase in serum 1,25(OH)2D levels, secondary to increased renal 1-α-hydroxylase activity, which results in increased intestinal Ca^{2+} absorption and hypercalciuria. All of the phenotypic features of HHRH can be explained by an abnormality in renal Pi conservation. In addition, treatment with Pi supplementation completely corrects all features of the disease phenotype, except the decreased renal Pi reabsorption, suggesting that a defect in a renal Pi transporter may be primarily responsible for HHRH.

Two possible candidate genes for HHRH are the type I and II renal specific Na^+-Pi cotransporter genes, NPT1 and NPT2. Aberrant expression of NPT2 was shown to be associated with X-linked hypophosphatemia, another inherited disorder of Pi homeostasis sharing many phenotypic features with HHRH (Chapter 1, Table 3). *Hyp* and *Gy* mice (the animal models for XLH) exhibit decreased renal expression of *Npt2* mRNA and protein suggesting that decreased *Npt2* expression is responsible for the hypophosphatemia seen in affected animals (Beck et al., 1996; Tenenhouse et al., 1994). In Chapter 2 of my thesis, both types of renal-specific Na^+-Pi cotransporter genes, NPT1 and NPT2, were mapped by fluorescent *in situ* hybridization to autosomes 6p22 (Kos et al., 1996) and 5q35 (Kos et al., 1994), respectively, and polymorphic markers flanking the NPT2 gene were identified (McPherson et al., 1997). Soon afterward, the disorders *Hyp* , *Gy* and XLH were shown to be caused by mutations which inactivate or delete a metalloendopeptidase gene known as PEX (Beck et al., 1997; Strom et al., 1997; The Hyp Consortium, 1995). PEX is believed to regulate NPT2 gene expression. Since PEX is not expressed in the kidney, it must act via an intermediary protein(s). The gene responsible for HHRH could be NPT1, NPT2 or a component of the PEX/ NPT2 regulatory pathway.

The HHRH pedigrees

The first pedigree to be described with HHRH was a large Bedouin kindred with a high prevalence of consanguineous matings (Tieder et al., 1985). We obtained DNA

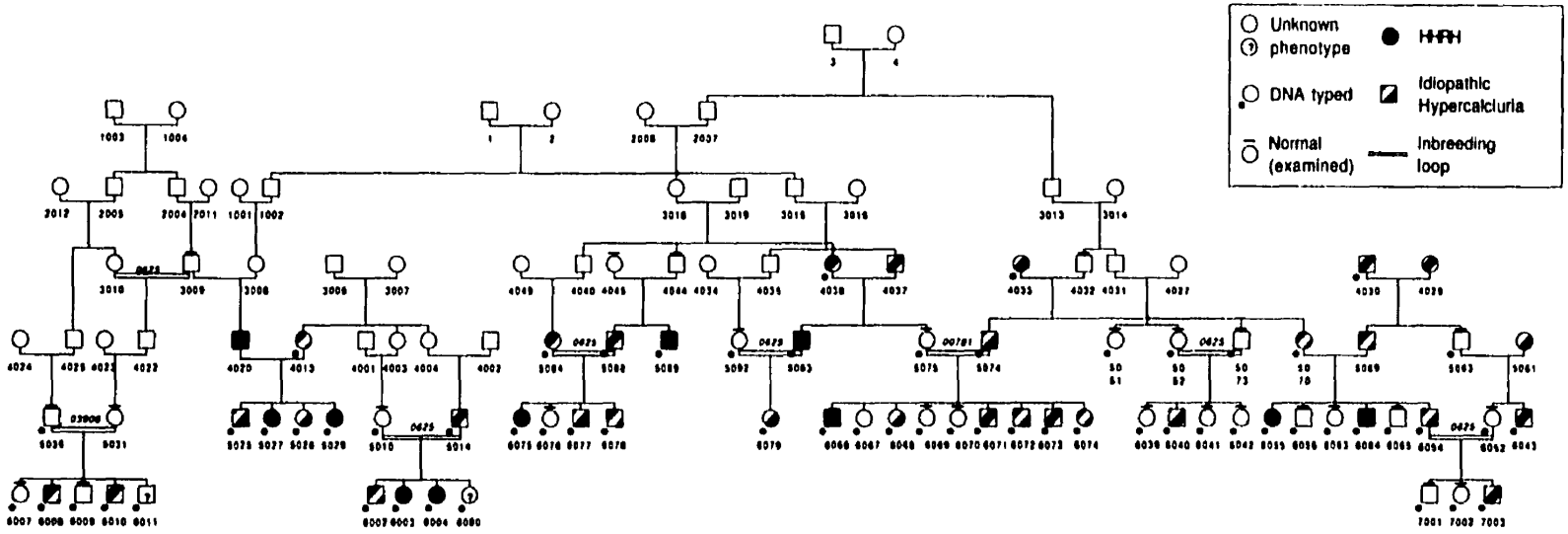

Figure 6. The known genetic relationship of members of the Bedouin HHRH kindred. Male (square) and female (circle) individuals were coded with identification numbers listed below the symbol. Individuals affected with HHRH are designated with a solid black symbol. Individuals with IH are designated by a symbol with black hatched marks. Normal individuals and individuals of unknown phenotype are designated by open symbols. Normal individuals who underwent a thorough examination have a solid line above their symbol. A black dot designates an individual was genotyped for DNA markers.

samples from the original HHRH kindred and additional family members not included in Tieder et al 1985 (Figure 6).

Consanguineous matings are of little importance with respect to a dominantly inherited trait since a dominant trait manifests even if only one disease allele in the heterozygous state is present in an individual. However, for a recessive trait to manifest, an individual needs two disease alleles. The disease alleles can either be different, in which case the individual is referred to as a compound heterozygote or the individual can be homozygous for two identical disease alleles. Consanguineous matings increase the chances that an offspring will inherit two copies of a disease allele homozygous and identical by descent. At the turn of the century, Garrod observed that sixty percent of children affected with a rare disorder born of unaffected parents, were the offspring of consanguineous marriages (Garrod, 1902). Therefore, it was concluded that if the percentage of consanguinity among parents of children exhibiting a trait is increased it is reasonable to assume that the condition is inherited recessively and affected offspring are homozygous and IBD for the mutant allele (Lenz, 1963).

HHRH has only been reported in two other pedigrees (Arie et al., 1982; Tieder et al., 1992) suggesting that HHRH is a rare disorder. Both of these pedigrees are small and of Yemenite Jewish origin. Like the HHRH kindred, the affected children described by Arie et al. (1982) are the offspring of a consanguineous first cousin mating.

Due to the apparent rarity of HHRH and the presence of consanguinity, it is thought that HHRH in the Bedouin kindred is autosomal recessive and due to a single mutant allele inherited identical and homozygous by descent from a common ancestor (Tieder et al., 1985; Tieder et al., 1987). This makes it an ideal pedigree for use in a homozygosity mapping study (Lander and Botstein, 1987). Homozygosity mapping is a powerful strategy for mapping rare, recessive traits in children of consanguineous marriages (Kruglyak et al., 1995) and already has been used to locate genes for several recessive diseases (Farrell, 1993), including, Friedreich ataxia with selective vitamin E deficiency (Ben Hamida et al., 1993), Alkaptonuria (Pollak et al., 1993) and Bloom syndrome (German et al., 1994). Homozygosity mapping studies search for a founding mutant allele and flanking markers present in a homozygous state among affected individuals. In this chapter, my initial aim was to determine if HHRH was linked to either the NPT1 or NPT2 gene. As the project progressed we decided not only to exclude or include NPT1 and/or NPT2 as candidate loci, but to map the HHRH

disease. To do this we allowed for the possibility that the HHRH trait is not transmitted as a recessive disease due to mutation of a single gene.

Phenotypic classifications

Examination of asymptomatic members of the Bedouin kindred revealed that 40% have a biochemical phenotype that is intermediate between that of the patients with bone disease and of the normal individuals (Figure 6) (Tieder et al., 1987). This intermediate phenotype, designated idiopathic hypercalciuria (IH), is assumed to represent the presence of a single mutant allele in heterozygous state. Members of the Bedouin kindred were classified into the following phenotypic groups: individuals with hypophosphatemia, hypercalciuria and bone disease were designated HHRH, individuals with moderate hypophosphatemia and hypercalciuria, but without bone disease were designated IH, and individuals without bone disease who were examined and found to have no decrease in serum Pi levels or elevation in urine Pi and Ca^{2+} excretion were designated normal. Individuals who did not undergo biochemical testing and had no obvious bone abnormality were designated as having an unknown phenotype.

Approaches

Because inbreeding increases the chance of finding homozygosity and the Bedouin kindred has multiple inbreeding loops, there was the possibility that homozygous regions would be prevalent throughout the genome and not just in regions flanking the disease locus. To test for this, data from a set of eight randomly distributed markers (referred to as 'identity markers') known to be highly polymorphic were analyzed.

Next, it was assumed that either the NPT1 or NPT2 gene was the mutated gene responsible for the pathogenesis of HHRH in the Bedouin kindred. Markers closely flanking these candidate genes were typed and the data analyzed for excess homozygosity. The chance of finding a region homozygous by descent in the offspring of a first cousin consanguineous mating is high, 1/16 (Chapter 1, Figure 4a). However, the chance of finding homozygosity in that same region in a second, unrelated individual (Figure 4b) is considerably lower (1/16 X 1/16 = 1/256). Evidence for linkage of a disorder to a locus is detected by locating overlapping regions of homozygosity in affected members of different pedigrees. The homozygosity mapping approach does not work well if more than one disease allele

is segregating in the family, due to the presence of affected individuals that are compound heterozygotes and not homozygous at the disease locus (Chapter 1, Figure 5). Therefore, when the data for the candidate genes were analyzed, it was assumed that HHRH displays autosomal recessive transmission and that a single rare mutant allele was segregating in the kindred. Since HHRH was assumed to be recessive, it was expected that the affected pedigree members would possess two copies of the mutant allele. Because all the affected Bedouin individuals are related and disease alleles are assumed to be rare, the affected individuals would all have the same disease allele at markers showing excess homozygosity (Figure 7).

Methods and Materials

Preparation of DNA samples

Phenotype and pedigree information was collected on a 114 member Bedouin kindred with 8 inbreeding loops (Figure 6). 11 members of this family were diagnosed with HHRH. DNA samples were prepared from peripheral blood lymphocytes from 61 members of the kindred using standard protocols. The 61 DNA samples divide into the following phenotypic categories: 10 individuals were classified as HHRH (severe hypophosphatemia, hypercalciuria and bone disease), 26 as IH (moderate hypophosphatemia and hypercalciuria, no bone disease), 23 were examined and found to be normal and 2 individuals were unexamined and therefore of unknown phenotype.

Markers

Ordered lists of the polymorphic short tandem repeat markers that were typed during this study are provided in Appendices 1 and 2. The lists specify where the markers were typed, and whether fluorescent or radioactive labeling was performed. The three markers flanking the NPT1 candidate region on chromosome 6 and the three markers flanking the NPT2 candidate region on chromosome 5 are depicted in Figure 8. The markers from the genome scan are depicted in Figure 9.

Genotype determinations

Markers Flanking Candidate Genes and Identity Markers

One primer from each of the marker pairs D5S498, D5S469, D6S2238, D6S2237, and D6S2233 (Figure 8) from the candidate regions on chromosome 5 (McPherson et al., 1997) and chromosome 6 (Feder et al., 1996), as well as from nine 'identity markers' (HPRT, FAB2, CD4, CSF1R, TH, PLA2A, F13A1, CYP19, LPL)(Appendix 2. ID Marker List) (Hammond et al., 1994) known to be highly polymorphic in various

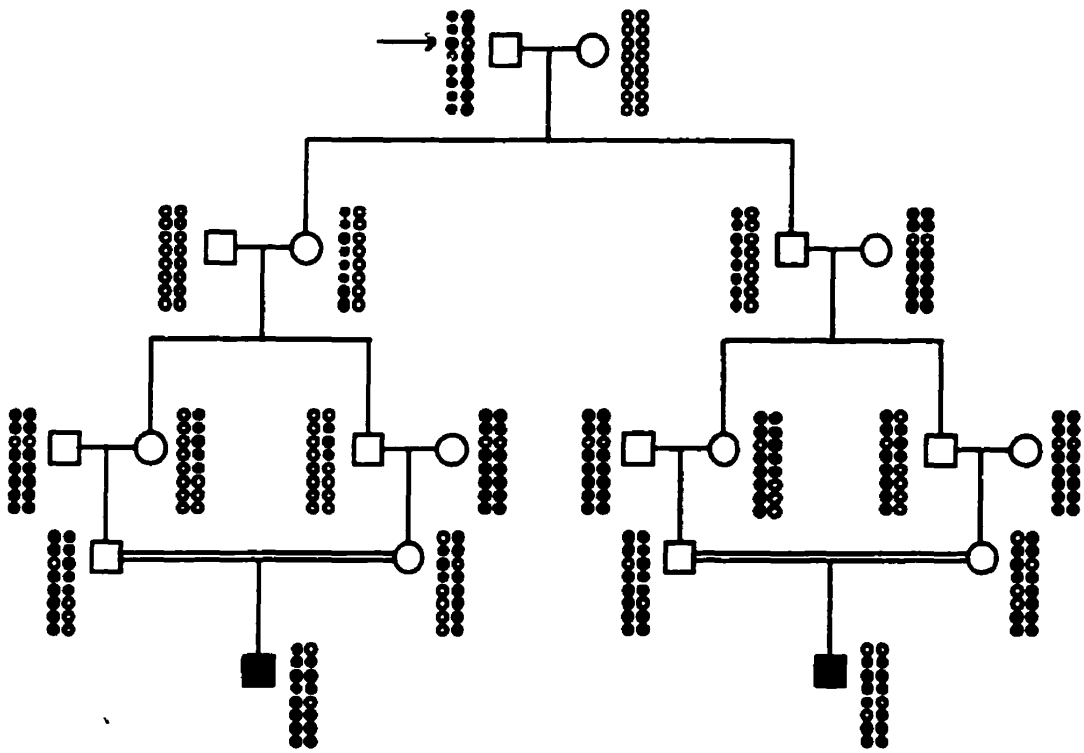

Figure 7. Homozygosity mapping in the HHRH kindred. It is hypothesized that a single mutant allele is segregating in the HHRH kindred. Therefore, all individuals are expected not only to be homozygous at the same markers (third marker and markers flanking it), but to be homozygous by descent for the same allele.

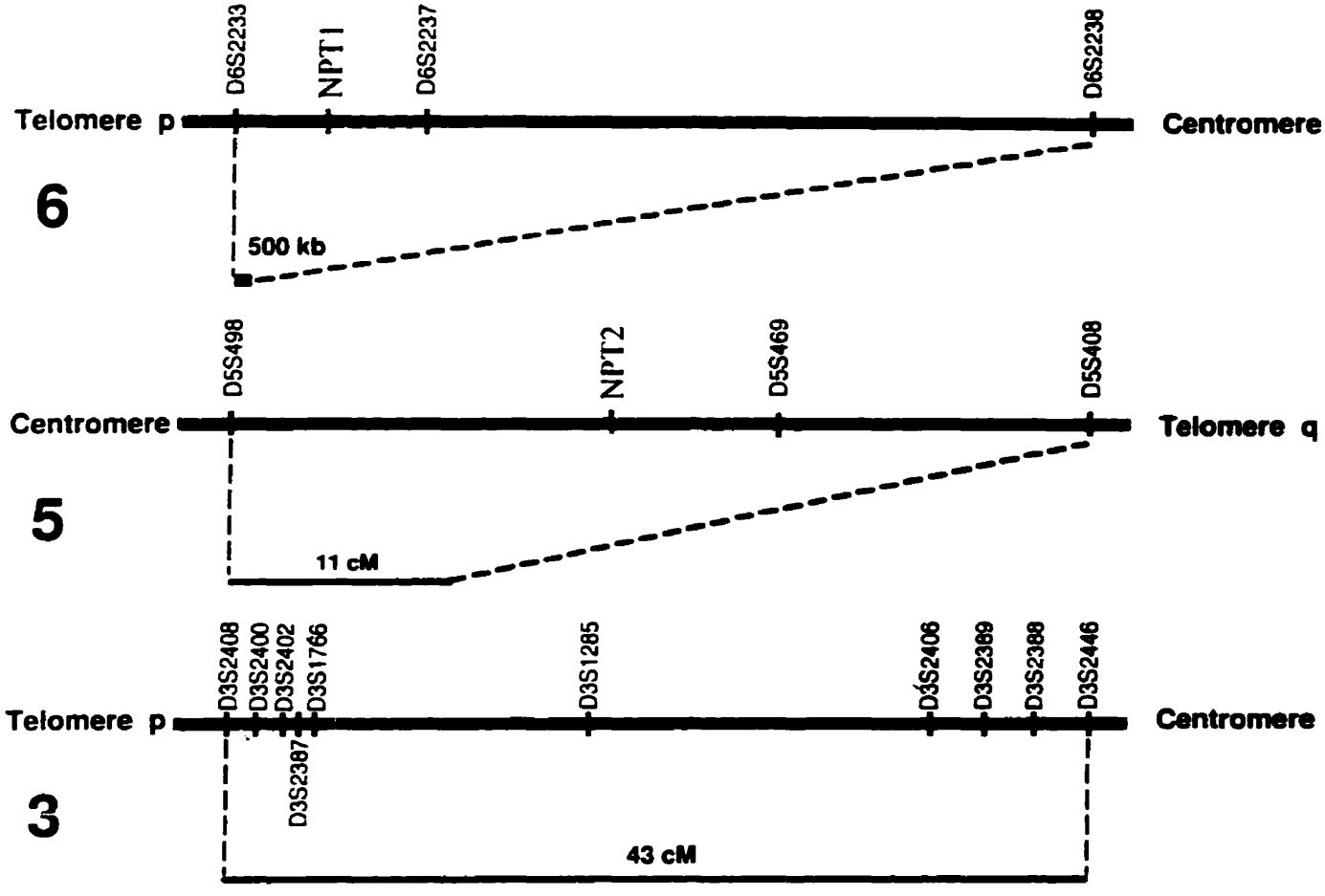

Figure 8. Markers flanking the candidate genes, NPT1 and NPT2, and additional markers from the region of excess allele sharing on chromosome 3.

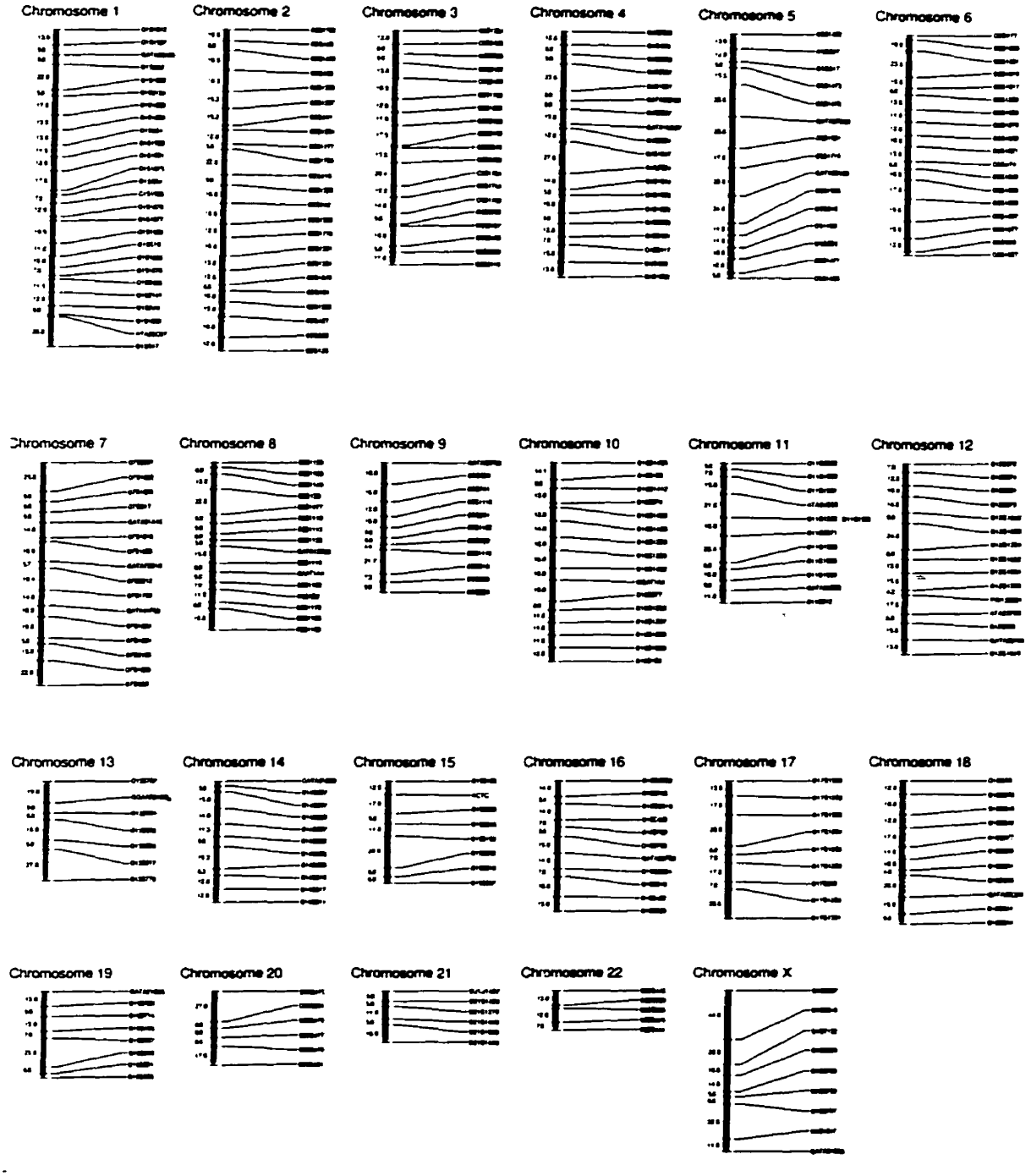

Figure 9. Markers used for genome scan.

ethnic populations, were end-labeled with ^{33}P for genotype detection according to published protocols (Hammond et al., 1994). Briefly, 50ng of genomic DNA was combined with reaction buffer, deoxynucleotide triphosphates and end-labeled primers. The samples were overlaid with mineral oil, denatured at 95°C for 2 min, and subject to 28 cycles of PCR under the following conditions; 95°C for 45 seconds (s), 62°C for 30s, 72°C for 30s. The final extension at 72°C was held for 10 minutes. Three microliters of the reaction mix were combined with 2µl formamide loading dye and electrophoresed on 4% sequencing polyacrylamide gels with size markers. The gels were dried and exposed at room temperature to autoradiographic film. Exposure times ranged from overnight to three days. Two investigators called the alleles by visual examination of the films.

Marker D5S408, closely linked to the candidate gene, NPT2 on chromosome 5, was purchased pre-labeled with a fluorescent tag from Research Genetics. The PCR reactions were prepared by hand using the same solutions, reaction conditions and gel running conditions as the fluorescent genome scan markers below. However, the gel files were processed and the alleles for the D5S408 marker were called using the ABI GENESCAN and GENOTYPER programs along with visual observation of the ABI gel image and not with the MIT programs Bass, Grace and Newcall (see below).

Genome Scan Markers

The sixty-one DNA samples and two control samples were arranged in a 96, 1ml well DNA source plate. Aliquots were removed from DNA source plate and combined with PCR reagents by a ROSYS robotic pipetting station. The genetic markers used for the genome scan were from a marker panel designated "Screening Set One" that was constructed by WICGR staff. This panel contains 300 di-,tri- and tetranucleotide STR markers with an average genome-wide spacing of 10cM (Figure 9) (Appendix 1. Marker List). The markers in the panel were chosen from published genetic maps based on their PIC values and because they gave clean amplification products under the following PCR conditions.

Pre-labeled markers were purchased from Research Genetics. The forward primer from each marker was end-labeled with one of three fluorescent dyes, HEX (yellow), TET (green), 6-FAM (blue). Fifty nanograms of genomic DNA was amplified in 14µl PCR reactions using 20µM labeled primers, overlaid with 25µl mineral oil, and run in 16, 192-well microtiter plates (maximum 3,072 reactions per run) on a waffle-iron thermocycler. 32 cycles of PCR were performed (94°C for 30s, 56°C for 30s, 72°C

Marshfield Medical Research and Education Foundation web site: http://genetics.mflgclin.edu (now found at http://www.marshmed.org/genetics/).

Genome Scan Markers

The genotype data from the genome scan were loaded into a computerized database. The database combined the genotypes for each individual using the individual's identification number, with other information for the individual including gender and disease status. The data from the genome scan were analyzed with the GENEHUNTER program version 1.0 (Kruglyak et al., 1996). GENEHUNTER can perform single point or multipoint analysis and calculate a parametric LOD score or non-parametric sharing statistic (npl-score) as well as generate inheritance vectors and construct haplotypes. The npl score is a measure of the degree of allele sharing among affected individuals and is not dependent on the specific model proposed for the disease as is the parametric LOD score. In this study, GENEHUNTER was used to perform non-parametric multipoint analysis.

Because a large amount of computer memory and time was required to examine multiple markers in pedigrees with inbreeding loops, the large Bedouin HHRH kindred had to be divided into smaller pedigrees in order to run the GENEHUNTER program. This meant that the large family had to be analyzed as separate families. For the first, second and fourth analysis, the kindred was broken into three pedigrees (ABHHRH, DEGHHRH, HHHRH) (Figure 10) consisting of 39 individuals total, 11 of which were affected and only 26 of which were genotyped. For the third analysis, the kindred was broken into eight pedigrees (AHHRH-HHHRH) (Figure 11) consisting of all but three genotyped individuals and additional non-genotyped family members were specified to incorporate the inbreeding loops.

In the first analysis, the npl scoring function measured the degree of allele sharing among individuals affected with the HHRH. In the second analysis, members of the kindred displaying hypercalciuria, i.e. individuals with either HHRH or IH, were coded as affected. In order to include additional family members displaying IH, the original large kindred was divided again, this time into eight separate pedigrees. As in the second analysis above, in the third analysis, family members displaying hypercalciuria were coded as affected. Two family members (6075 and 5027) (Figure 10) were found to have an unusually high frequency of segregation errors in their typing data. Their data were excluded and the analysis of the three pedigrees with all

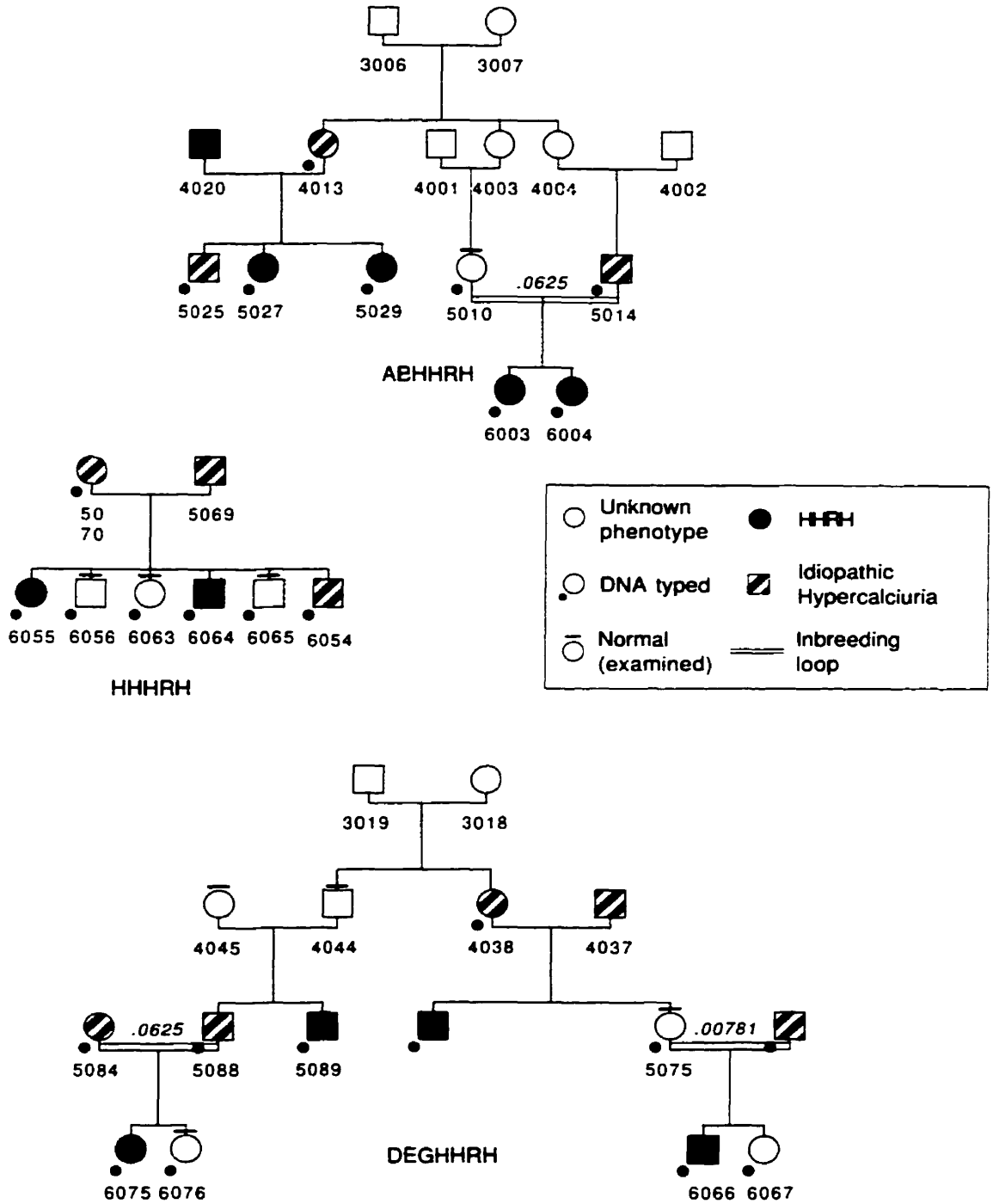

Figure 10. Three small portions of Bedouin kindred used for GENEHUNTER analysis.

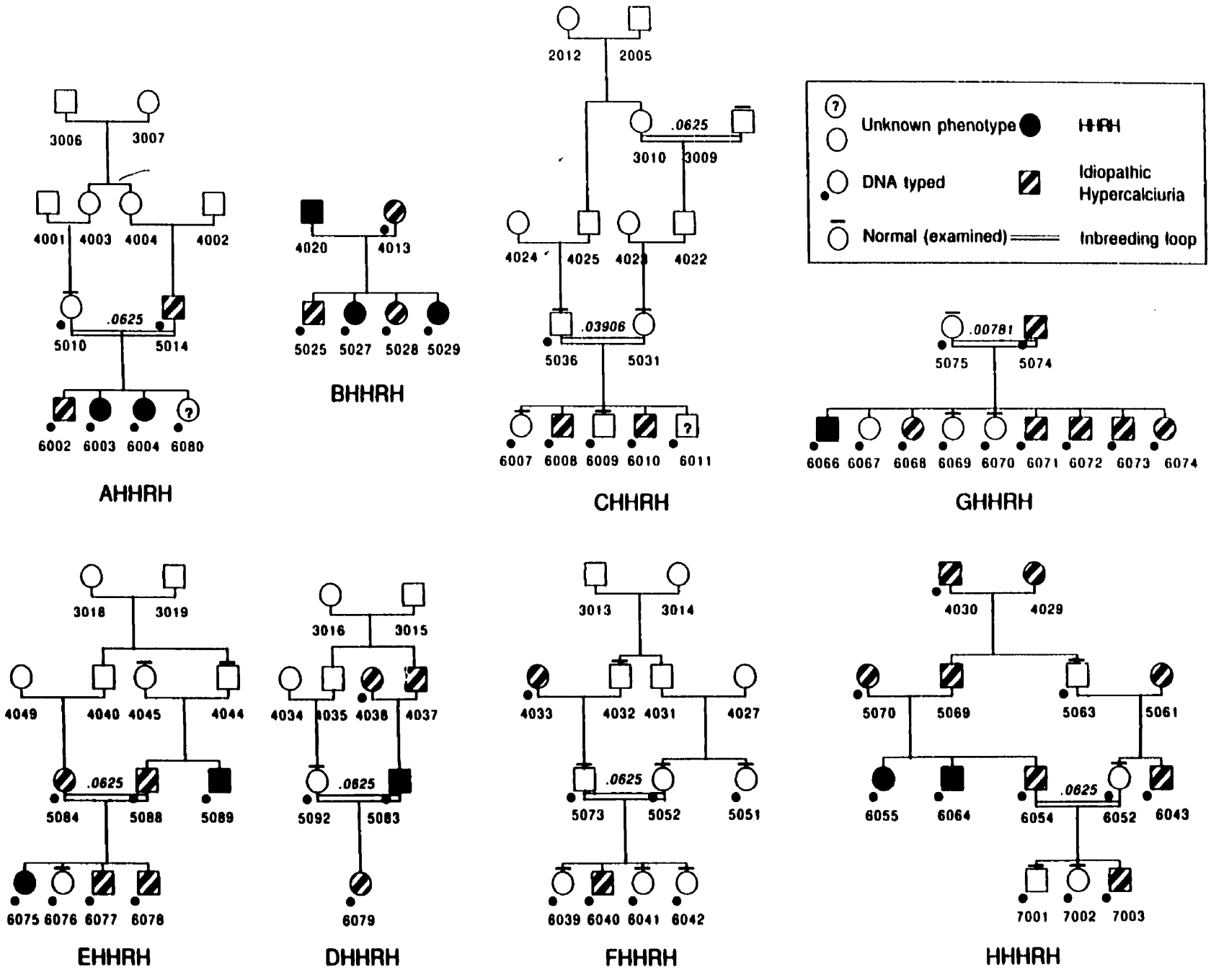

Figure 11. Eight small portions of Bedouin kindred used for GENEHUNTER analysis.

forms of hypercalciuria coded as affected was repeated. No formal LINKAGE calculations were performed with the genotype data.

RESULTS

Markers flanking candidate genes

Based on the data for the eight identity markers from all typed individuals, the observed frequency of homozygotes in the Bedouin kindred was apparently not significantly greater than expected. Inbreeding in the kindred did not increase the frequency of homozygosity to the extent that multiple false positives would be detected using the homozygosity mapping approach (Figure 12a). Likewise, the data for the candidate gene markers on chromosomes 6 and 5 shown in Figure 12b and 12c, did not show a higher than expected frequency of homozygotes in the HHRH affected category.

Only one individual (5027) was homozygous at all markers on chromosome 6 (Figure 13). Her affected sister (5029) did not share any alleles with 5027 nor was 5029 homozygous at any of the three chromosome 6 markers (Figure 13). The homozygous, 105-129-157 haplotype was seen in only one other individual, 6055.

A single individual (6064) was homozygous at all markers on chromosome 5 (Figure 13). Individual 6064's homozygous, 189-142-256 haplotype was not seen in his affected sister (6055), but was seen in three other affected individuals; 5027, 5089, 6066 in the heterozygotic state (Figure 13). All of the HHRH affected individuals were homozygous for allele 142 at marker D5S469. However, D5S469 is believed to be uninformative since every member of the Bedouin kindred that was typed had at least one copy of allele 142 at marker D5S469 and 80% of the IH individuals, and 86% of the normal individuals were also homozygous for allele 142.

Genome scan markers

The results of the PEDMANAGER program showed that three of the individuals (6075, 5025 and 5027), all affected with either IH or HHRH had a rate of segregation errors >10%.

The GENEHUNTER results can be summarized as follows. In the first analysis, where only the individuals with HHRH patients were coded as affected, a peak npl score was **2.25** and a p-value 0.03 found on chromosome 3 at distance 79cM from the telomere of the short arm. In the second analysis, where members of the kindred

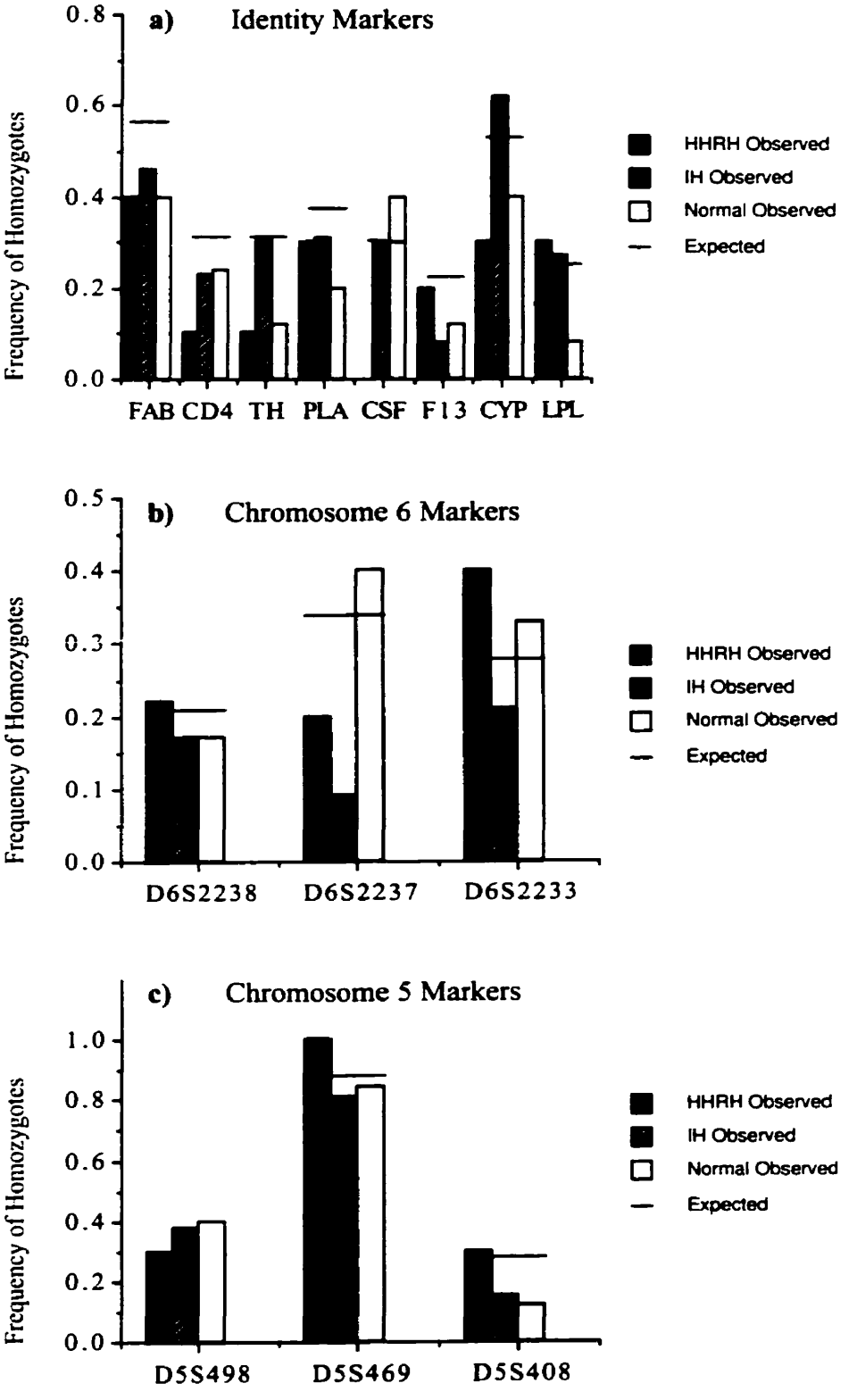

Figure 12. The expected and observed frequency of homozygotes for different markers in each of three phenotypic classifications.

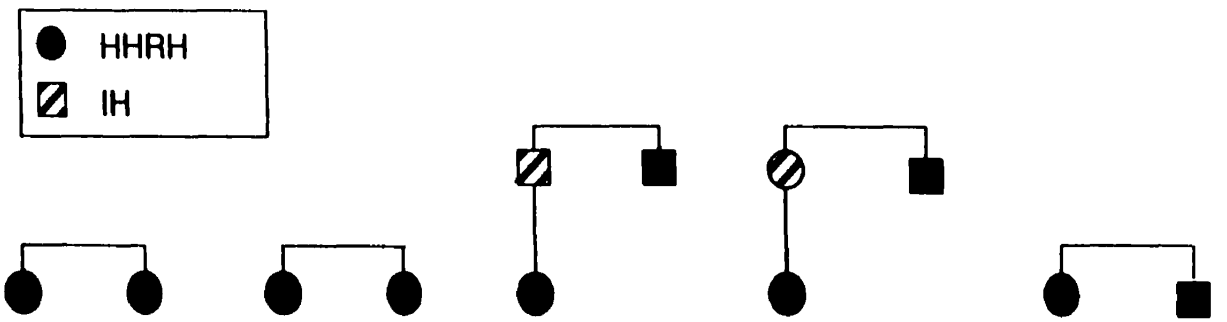

	5027	5029	6003	6004	6075	5089	5083	6066	6055	6064
D6S2238	105 |105	95 |109	101 |105	107 |109	105 |109	105 | 95	107 |107	107 | 95	105 |105	105 |109
D6S2237	129 |129	131 |123	129 |129	131 |123	129 |131	129 |131	131 |129	129 |131	129 |131	129 |131
D6S2233	157 |157	153 |149	151 |155	157 |149	155 |155	155 |153	159 |159	159 |155	157 |155	155 |157
	D6S2238	**- 500 Kb -**	**D6S2233**							
D5S498	189 |179	189 |175	179 |175	179 |175	189 |189	189 |189	179 |173	189 |179	189 |175	189 |189
D5S469	142 |142	142 |142	142 |142	142 |142	142 |142	142 |142	142 |142	142 |142	142 |142	142 |142
D5S408	256 |256	252 |254	256 |256	252 |256	254 |264	264 |256	256 |254	256 |260	254 |264	256 |256
	D5S498	**- 11 cM -**	**D5S408**							
D3S2408	181 |191	197 |191	197 |188	194 |188	203 |188	188 |188	188 |197	188 |188	188 |191	188 |191
D3S2400	· |(210)	210 |210	· |·	201 |219	· |·	210 |210	(210 |210)	210 |210	210 |204	199 |207
D3S2402	234 |238	238 |238	238 |238	234 |238	234 |242	242 |242	238 |242	242 |238	242 |234	238 |242
D3S2387	205 |169	201 |169	201 |193	201 |193	181 |181	· |·	193 |201	205 |193	205 |201	201 |205
D3S1766	219 |223	223 |223	219 |223	223 |223	219 |215	· |·	223 |223	219 |223	219 |227	· |·
D3S1285	241 |237	241 |237	241 |239	· |·	233 |·	233 |231	233 |233	237 |233	237 | ·	235 |237
D3S2406	· |341	341 |341	341 |341	341 |341	317 |317	321 |317	349 |349	321 |345	321 |353	353 |321
D3S2389	280 |256	272 |256	256 |256	256 |256	248 |248	272 |248	256 |272	260 | ·	260 |280	· |·
D3S2388	113 |113	113 |113	113 |113	113 |113	113 |113	113 |113	117 |113	113 |113	113 |113	113 |113
D3S2446	239 |247	243 |247	243 |247	243 |247	243 |243	243 |247	243 |243	239 |243	239 |239	239 |239
D3S2459	190 |174	190 |174	194 |198	190 |198	198 | ·	198 | ·	198 |186	190 | ·	198 |190	198 |190
D3S3045	192 |192	192 |192	192 |183	192 |183	· |200	192 |200	192 |179	179 |179	183 |179	183 |192
D3S2460	158 |162	162 |162	158 |158	158 |158	154 |146	162 |158	166 |162	162 |154	166 |162	166 |158
	D3S2408	**- 43 cM -**	**D3S2389**							
	D3S2408	**- 85 cM -**	**D3S2460**							

Figure 13. Marker haplotypes for chromosomes 6, 5 and 3 of 10 HHRH affected individuals.

displaying either IH or HHRH were coded as affected, the highest npl score of **3.01** and a p-value 0.01 was also at 79cM on chromosome 3. Evidence for allele sharing on chromosome 3 decreased when additional members of the kindred displaying IH were included and a peak npl score of **2.20** occurred on chromosome 9 at distance 35cM. When the two HHRH family members (6075 and 5027) with the unusually high amount of segregation errors were excluded, a peak npl score of **1.78** occurred on chromosome 17 at distance 13cM.

Because of the suggestion of excess allele sharing on chromosome 3, additional markers from around the 79cM region were typed at Montreal General Hospital (MGH).

Data from markers on chromosome 3 were analyzed in a similar fashion to the markers flanking the candidate genes on chromosomes 6 and 5 (Appendix 6). Haplotype analysis produced evidence for allele sharing at multiple markers. For example, individuals 5027 and 5029, share the 238-169-223-237-341-256-113-247 haplotype. Individuals 6003 and 6004 share with 5027 and 5029, the 341-256-113-247 portion of that haplotype. However, only one marker D3S2388 showed excess homozygosity (Figure 13). No conclusions regarding linkage of HHRH to markers on chromosome 3 can be made without a denser set of markers.

Discussion

These studies aimed to determine by genetic analysis whether HHRH in the Bedouin kindred is linked to region p22 of chromosome 6 containing the NPT1 gene or to region q35 of chromosome 5 containing the NPT2 gene. As the project progressed, it became obvious that the mode of transmission of HHRH in the Bedouin kindred was not entirely clear and that analyzing our data would be more complex than was originally anticipated. In addition to looking at data for markers near the candidate Na^+-Pi cotransport genes we looked at markers spanning the genome and analyzed this data using less stringent, model-independent methods.

Close examination of the pedigree, based on the reported information, reveals at least six instances where disease alleles are entering the kindred, suggesting that the disease alleles may not be rare. Four of these individuals displaying the IH trait (4029, 4030, 4033 and 5061) are specified as having married into the kindred, and therefore would have brought in disease alleles of independent origin. At least two other disease alleles

segregate within the kindred, although it is not possible to determine where these two alleles entered into the kindred. If HHRH is a very rare recessive disorder, and IH represents the heterozygous state, then it is unlikely that so many additional disease alleles entered the kindred from unrelated individuals. What is more likely is that we are missing complete pedigree information and additional unidentified inbreeding loops are present which link those "unrelated individuals" to the kindred making those individuals related and the six disease alleles not of independent origin, but identical by descent (personal communication with Dr. M. Tieder).

In addition, the IH trait seems to display incomplete penetrance. For example, individuals 5010 and 5075 are reported to be normal, yet both gave birth to HHRH affected children (6003, 6004 and 6066). If two mutant alleles are required for presentation of HHRH, then 5010 and 5075 must be carriers of a mutant allele but non-penetrant for IH. Another more complicated example is individual 3009, who is also reported to be normal but must be a carrier nonpenetrant for IH. A son (4020) and two granddaughters (5027 and 5029) of 3009 are affected with HHRH. Individual 3009 is reported to be related to the central part of the pedigree by marriage only. If this is true, then in order for 4020, 5027 and 5029 to be homozygous IBD for the same alleles as the other affected members in the kindred, 3009 must be related not simply by marriage but also by kinship to central part of the kindred.

The extensive inbreeding and incomplete penetrance make interpretation of the inheritance pattern of HHRH in the Bedouin kindred difficult. Yet, the rarity of the disorder, and the presence of consanguinity and of several instances of male-to-male transmission of the IH trait argues in favor of an autosomal recessive model. Assuming that HHRH is a single-gene autosomal recessive disorder and that all the affected individuals possess two copies of the same mutant allele inherited identical by descent from a common ancestor, if mutation of either the NPT1 gene, the NPT2 gene, or a gene on chromosome 3 was responsible for HHRH, one would expect that all the affected individuals would be homozygous by descent for the same haplotype at markers closely linked to the disease gene. The results of these experiments did not show this to be the case. Instead, multiple haplotypes were seen in the 10 HHRH affected individuals who were genotyped. The distance between markers flanking the NPT2 gene is sufficiently large that if an old mutation underwent multiple recombination events homozygosity might not be detected. However, such a scenario is unlikely to have resulted in so many different disease haplotypes. In the case of the NPT1 gene the marker interval is so small (less than 1cM) that even if there was a very

old NPT1 mutation, the occurrence of multiple recombination events between NPT1 and the flanking markers would be highly unlikely.

In summary, homozygosity mapping and allele sharing studies failed to provide evidence for linkage of HHRH in the Bedouin kindred to the renal Na^+-Pi cotransporter genes NPT1 or NPT2. This could be due to insufficient power to detect linkage because of there being only 10 HHRH affected individuals with HHRH, to the presence of gaps in the genotyping data or due to a combination of both insufficient power and incomplete data. The results do not exclude the possibility that these genes play a role in the disease phenotype under a more complicated genetic model. The genome scan data showed that there was excess allele sharing at markers on chromosome 3 and point to chromosome 3p as a possible site of further investigations into a gene responsible for HHRH. A computer search of expressed sequences from this region was done to see if there existed any known genes in this region that if mutated could result in a HHRH phenotype.

The only gene in this region that struck us as interesting was the calcium sensing receptor gene. Activating mutations of this gene result in a decreased ability of the parathyroid gland to sense low serum Ca^{2+} levels and have been implicated in autosomal dominant hypocalcemia/hypoparathyroidism (ADH) (Pollak et al., 1996). Although ADH patients like HHRH patients exhibit hypercalciuira, ADH patients also have moderate hypocalcemia and normal PTH levels which are inappropriately low relative to the degree of hypocalcemia (Pearce et al., 1996). Additional markers from this region of excess allele sharing on chromosome 3 were typed. However, no conclusions regarding linkage of HHRH to this region can be made without further typing of a denser set of markers because of the large genetic distances between the markers.

Chapter 5. General Discussion

The kidney is the major site of regulation of serum Pi levels. Failure of the kidney to properly reabsorb Pi was believed to be the primary cause of several inherited disorders of Pi homeostasis (Chapter 1, Table 2). Renal BBM Na^+-Pi cotransport is the rate-limiting step of the Pi reabsorption process. The overall aim of this thesis was to assess the role of the NPT1 and NPT2 renal Na^+-Pi cotransporter genes in inherited hypophosphatemic disorders. Specifically, there were three goals. The first was to map the two genes in human and rabbit to determine their chromosomal localization. The second was to characterize the structure of the NPT2 gene to gain information necessary to perform mutation detection studies in patients with inherited hypophosphatemias. The final goal was to map the disorder hereditary hypophosphatemic rickets with hypercalciuria to determine if either NPT1 or NPT2 was involved in the pathophysiology.

Three physical mapping experiments presented in Chapter 2 localized the NPT1 and NPT2 genes in human to chromosomes 6p22 and 5q35, and in rabbit to chromosomes 12p11 and 3p11, respectively. These assignments agree with the previously reported homology between human chromosome 6 and rabbit chromosome 12 and provide the basis for the establishment of a conserved syntenic group between human chromosome 5 and rabbit chromosome 3. The localization of the two cotransporter genes to autosomes excludes them as candidate genes for X-linked hypophosphatemia. In order to evaluate by genetic mapping whether autosomal disorders of Pi homeostasis are linked to the NPT2 gene, polymorphic markers flanking the NPT2 gene were identified.

The third chapter described the cloning, sequencing and characterization of the structure of the human NPT2 gene and similar experiments performed on the mouse *Npt2* gene. In both species, the type II renal Na^+-Pi cotransporter gene is approximately 16kb in length and is comprised of 13 exons and 12 introns. The results of this work enabled the design of intronic primers for the amplification of NPT2 exons in order to screen DNA from patients with autosomal disorders of renal Pi reabsorption for mutations in the NPT2 gene. The information also provided the basis for studying the regulation of type II renal Na^+-Pi cotransporter transcription and for the construction of a *Npt2* knockout vector.

Chapter 4 describes the efforts to genetically map the autosomal disorder hereditary hypophosphatemic rickets with hypercalciuria (HHRH) in an inbred Bedouin kindred.

These studies did not provide conclusive evidence for linkage of HHRH to a chromosomal region. Investigation into whether HHRH shows linkage to either the NPT1 or NPT2 genes was carried out both nonparametrically and under the assumption that HHRH is a rare autosomal recessive disorder. Haplotype analysis showed that the affected individuals have several different haplotypes at markers flanking the NPT1 and NPT2 genes. Analysis failed to reveal excess homozygosity or allele sharing on either chromosome 6 or 5, where the NPT1 and NPT2 genes are located, but suggested chromosome 3p as a possible starting point for further searches for a gene responsible for HHRH. These results do not provide support for the hypothesis that mutation of either the NPT1 or NPT2 gene is responsible for HHRH.

Interestingly however, homozygous *Npt2* knock-out mice (*Npt2*$^{-/-}$) lacking functional *Npt2* protein, display biochemical characteristics typical of HHRH patients (Beck et al., 1998). The *Npt2*$^{-/-}$ mice exhibit increased Pi excretion, hypophosphatemia, and an appropriate elevation in serum $1,25(OH)_2D$ levels resulting in hypercalciuria (Beck et al., 1998). Given the striking similarity of the HHRH and *Npt2*$^{-/-}$ biochemical phenotypes, it was somewhat of a surprise that the *Npt2*$^{-/-}$ mice do not have rickets or osteomalacia. Rather, the newborn *Npt2*$^{-/-}$ mice exhibit a complex bone phenotype which is not only reversed after weaning, but is overcompensated for with increasing age (Beck et al., 1998).

Although the results of the genetic mapping of HHRH presented earlier and the phenotype of the NPT2 knockout mouse (Beck et al., 1998) appear contradictory, they are not irreconcilable. The multiple haplotypes and lack of evidence for excess allele sharing in the Bedouin kindred could be because HHRH alleles are in fact not rare but common (Tieder et al., 1992). Other possible reasons could be because the founding mutation is very old, the founder was a compound heterozygote or some combination of all these reasons. The discordant bone abnormalities seen in HHRH patients and *Npt2*$^{-/-}$ mice could be due to species differences in the amount of Pi required for proper skeletal mineralization or differences in response to elevated $1,25(OH)_2D$ levels (Beck et al., 1998). Similarly these differences could be do to the genetic background of the mice. Reported differences in vitamin D metabolism between *Hyp* and *Gy* mice (Davidai et al., 1990)were not found when the two mice were studied on the same genetic background (Meyer et al., 1996). Characteristic features of the *Gy* mutation such as circling behavior were also seen in mice harboring the *Hyp* mutation when it was transferred to the same background as the original *Gy* strain. Breeding the *Npt2*$^{-/-}$

mice onto another genetic background may result in mice with a phenotype closer to that of human patients.

Another attractive explanation for why there are so many different haplotypes at markers near the candidate genes is that common mutations or polymorphisms in the NPT2 gene could act in combination with a rare allele of another gene to cause HHRH. This is not unreasonable given that multiple genes have been speculated to contribute to hypercalciuria in the normal population (Scheinman, 1998). An example of a digenic disorder is autosomal recessive Limb girdle muscular dystrophy (LGMD2A) (Allamand et al., 1995; Richard et al., 1995).

On the island of La Réunion there is a founding population with a high prevalence of LGMD2A showing linkage to a region of chromosome 15q. This region of chromosome 15q contains the muscle-specific gene calpain3, which was felt to be a good candidate gene for LGMD2A. The calpain3 gene was sequenced using DNA from La Réunion LGMD2A patients and mutations were identified. Despite the isolated population and rarity of the disorder, haplotypes seen in the affected individuals from the island were not IBD for markers flanking the calpain3 gene. Rather, six different haplotypes were identified, each harboring a different calpain3 mutation. To explain the perplexity of many rare recessive disease alleles of independent origin in the founder population, a two-gene model for LGMD2A was postulated (Allamand et al., 1995; Richard et al., 1995). Mutations of the calpain3 gene are believed to be very common. Yet, for homozygous or compound heterozygous mutations to result in manifestation of the disease phenotype, a second rare allele of another polymorphic gene is also required (van Ommen, 1995). For example in the La Réunion population it is speculated that the second yet-to-be-identified gene has become fixed.

Such a digenic model is an appealing explanation for why multiple haplotypes were seen at markers flanking the NPT2 gene in the Bedouin population and for why the phenotype of HHRH patients is different from the phenotype of the *Npt2*$^{-/-}$ mouse. NPT2 mutations may be common, and a mutation at an unknown gene could be fixed in the Bedouin HHRH population due to a founder effect. However, this explanation is not supported by any concrete evidence. Unlike in LGMD2A where evidence for linkage was found to calpain3, there is no evidence for linkage of HHRH to 5q35 or 6p22.

The only gene that has been shown to cause a hypophosphatemic disorder is PEX. PEX was surprising because the way in which it functions to bring about the XLH disease phenotype is not obvious. PEX is a membrane bound protein and is not expressed in the kidney. It is believed to be indirectly involved in the regulation of renal NPT2 Na^+-Pi cotransporter gene expression, and therefore serum Pi levels. Of the many mechanisms this could involve, the most imaginable is one where a mutation decreases the amount of functional PEX protein (haploinsufficiency) and leads to a disease phenotype (Econs and Francis, 1997). In this situation there would not be enough of the normal PEX protein to activate a humoral phosphate conserving hormone or to inhibit the expression and/or action of the putative phosphate wasting factor, phosphatonin. Either of the two hormones would act on the kidney to regulate renal NPT2 Na^+-Pi cotransporter gene expression.

Low serum Pi levels resulting from PEX mutations do not seem to be the primary cause of the bone disease seen in the XLH, *Hyp* and *Gy* disorders. Several studies have provided evidence for an intrinsic bone defect in *Hyp* mice (Ecarot-Charrier et al., 1988; Rifas et al., 1997; Rifas et al., 1995). These studies revealed that Hyp mice show a higher rate of glucose production and decreased casein kinase II activity compared with normal mice (Rifas et al., 1997; Rifas et al., 1995). In addition, it has been shown that *Hyp* osteoblasts continue to produce abnormally mineralizing bone when transplanted into mice displaying normal serum Pi levels (Ecarot-Charrier et al., 1988) and that these cells have normal Na^+-Pi cotransport activity (Ecarot et al., 1994; Ecarot-Charrier et al., 1988; Rifas et al., 1994) This means the bone disease is not simply a result of low serum Pi levels, but that PEX which is expressed in bone (Beck et al., 1997) plays a direct role in bone metabolism.

Another uncommon disorder of renal proximal tubular reabsorptive failure is X-linked hypercalciuric nephrolithiasis (XLHN) (Scheinman, 1998). XLHN is an umbrella term used to refer to four syndromes: X-linked recessive nephrolithiasis, Dent's disease, X-linked recessive hypercalciuric rickets (XLRHR) and Low-molecular-weight proteinuria with hypercalciuria and nephrocalcinosis (Scheinman, 1998). Each is caused by mutations in the same chloride channel gene CLCN5 (Fisher et al., 1995). Although the XLHN syndromes were at no time believed to be due to a problem in renal Pi reabsorption, they are worthy of mention.

One of the earliest and most consistent features of XLHN is hypercalciuria. The XLHN syndromes display high-normal to high serum $1,25(OH)_2D$ levels. Two

syndromes, Dent's disease and XLRHR present with rickets and osteomalacia. Although, the role of the CLCN5 channel in Ca^{2+} reabsorption is unknown, for a time the CLCN5 gene was speculated to contribute to IH in the normal population and be a possible candidate for HHRH. To date no CLCN5 mutation has been found in either normal IH individuals (Scheinman, 1998).or members of the Bedouin HHRH kindred (personal communication with Dr. R. Thakker). Like PEX, CLCN5 is a novel gene identified by positional cloning and mutation of the gene does not immediately explain the clinical phenotype observed in patients.

The signaling mechanisms that link the known regulators of Na^+-Pi cotransport (PEX, dietary Pi intake, serum Pi concentrations and serum PTH levels), to changes in NPT2 activity are unknown. A differential display-PCR experiment, comparing renal mRNA from rats fed low- and high-Pi diets, resulted in the identification of a new gene product associated with increased BBM NPT2 cotransport activity called dietary Pi-regulated RNA-1 or diphor-1 (Custer et al., 1997). Two possibilities were postulated for how diphor-1 acts to increase NTP2 cotransport activity. The first is that it increases the number of NPT2 cotransporters present in the BBM by promoting cotransporter incorporation into the membrane or decreasing the removal and degradation of cotransporters from the membrane. The second is that diphor-1 increases the activity of the NPT2 cotransporters already present in the membrane. Circumstantial evidence also exists for a circulating factor which down-regulates renal Pi reabsorption, phosphatonin, but no gene has been isolated.

If HHRH is truly an autosomal recessive disorder, whether or not it is due to a single gene or to two genes, typing of a denser marker set and filling in the gaps between markers should enable one to identify a gene using the methods we have employed. Collecting DNA samples from more affected individuals would aid in the above study and in identification of the gene(s) assuming a different mode of transmission. Since HHRH was not mapped, the question of whether or not mutations of the NPT2 gene contribute to the HHRH phenotype is still unanswered. Sequencing the NPT2 gene and finding a mutation in the HHRH kindred would answer the question. Mutation detection experiments carried out by another laboratory member using the information gathered in Chapter 3, have so far failed to uncover NPT2 mutations in the Bedouin HHRH patients. However not finding a NPT2 mutation does exclude the possibility of NPT2 involvement in disease.

Eventually, the locus or loci causing HHRH will be discovered. It may turn out to be diphor-1, phosphatonin or an entirely new component of the renal Pi reabsorption regulatory pathway. Nevertheless, what makes the disorder HHRH so interesting despite all of its problems, is that identifying the gene(s) will not only increase our understanding of the specific pathophysiology of HHRH, but of renal Pi reabsorption and possibly Ca^{2+} homeostasis in general.

Contributions to Original Knowledge

The following is a list of experiments and results that to my knowledge had not yet been published by another author prior to publication by our group.

1) The localization of the NPT2 gene to a human chromosome region 5q35.

2) The localization of the NPT2 gene to a rabbit chromosome region 3p11.

3) Comparative mapping of a human chromosome 5 marker in rabbit.

4) The identification of a rabbit chromosome 3 marker.

5) The cytogenetic localization of the NPT1 gene to a human chromosome 6p22.

6) The localization of the NPT1 gene to a rabbit chromosome 12p11.

7) Comparative mapping of a human chromosome 6p marker in rabbit.

8) The results of experiments which eliminate the NPT1 and NPT2 genes as candidate genes for X-linked hypophosphatemia.

9) The identification of markers flanking the human NPT2 gene.

10) The gene structure of the human and mouse renal type II Na^+-Pi cotransporter genes.

11) The results of genetic mapping experiments investigating the disorder hereditary hypophosphatemic rickets with hypercalciuria (HHRH).

12) The suggestion that a locus on human chromosome 3p may have a role in HHRH.

References

Abraham, M.I., J.A. McAteer & S.A. Kempson. Insulin stimulates phosphate transport in opossum kidney epithelial cells. *American Journal of Physiology* 258:F1592-F1598 (1990).

Albright, F., A.M. Butler & E. Bloomberg. Rickets resistant to vitamin D therapy. *American Journal of Diseases of Children* 54:529-547 (1937).

Allamand, V., O. Broux, I. Richard, F. Fougerousse, N. Chiannilkulchai, N. Bourg, L. Brenguier, C. Devaud, P. Pasturaud, et al. Preferential localization of the Limb-girdle muscular dystrophy type 2A gene in the proximal part of a 1-cM 15q15.1-q15.3 interval. *American Journal of Human Genetics* 56:1417-1430 (1995).

Arar, M., M. Baum, J. Biber, H. Murer & M. Levi. Epidermal growth factor inhibits Na-Pi cotransport and mRNA in OK cells. *American Journal of Physiology* 268:F309-F314 (1995).

Arie, R., R. Samuel, A. Halabe & U.A. Liberman. Hereditary familial syndrome of renal phosphate leak with hypercalciuria, nephrolithiasis and bone lesions. In:Current Advances in Skeletogenesis, Development, Biomineralization, Mediators and Metabolic Bone Disease. M. Silbermann & H.C. Slavkin Ed(s). Excerpta Medica, Amsterdam-Oxford-Princeton, 1982, pg. 537-543.

Beck, L., R.A. Meyer, M.H. Meyer, J. Biber, H. Murer & H.S. Tenenhouse. Renal expression of Na^+-phosphate cotransporter mRNA and protein: effect of the Gy mutation and low phosphate diet. *Pflügers Archiv-European Journal of Physiology* 431:936-941 (1996).

Beck, L.P., A.C. Karaplis, N. Amizuka, A.S. Hewson, H. Ozawa & H. Tenenhouse. Targeted inactivation of *Npt2* in mice leads to severe renal phosphate wasting, hypercalciuria and skeletal abnormalities. *Proceedings of the National Academy of Sciences of the United States of America* 95:5372-5377 (1998).

Beck, L.P., Y. Soumounou, J. Martel, G. Krishnamurthy, C. Gauthier, C.G. Goodyear & H.S. Tenenhouse. *Pex/PEX* tissue distribution and evidence for a deletion in the 3' region of the*Pex* gene in X-linked hypophosphatemic mice. *Journal of Clinical Investigation* 99:1200-1209 (1997).

Bell, C.L., H.S. Tenenhouse & C.R. Scriver. Primary cultures of renal epithelial cells from X-linked hypophosphatemic (Hyp) mice express defects in phosphate transport and vitamin D metabolims. *American Journal of Human Genetics* 43:293-303 (1988).

Ben Hamida, C., N. Doerflinger, S. Delal, A. Linder, L. Reutenauer, C. Dib, G. Gyapay, A. Vignal, D. Le Paslier, et al. Localization of Friedreich ataxia phenotype with selective vitamin E deficiency to chromosome 8q by homozygosity mapping. *Nature Genetics* 5:195-200 (1993).

Berry, C.A. Transport functions of renal tubules. In:Renal Physiology in Health and Disease. B. Brenner, F.L. Coe & F.C. Rector Ed(s). Saunders Company, PA., 1987, pg. 27-56.

Biber, J., M. Custer, A. Werner, B. Kaissling & H. Murer. Localization of NaPi-1, Na/Pi cotransporter, in rabbit kidney proximal tubules. II. Localization by immunohistochemistry. *Pflügers Archiv-European Journal of Physiology* 424:210-215 (1993).

Botstein, D., R.L. White, M. Skolnick & R. Davis. Construction of a genetic linkage map in man using restriction fragment length polymorphisms. *American Journal of Human Genetics* 32:314-331 (1980).

Cai, Q., S.F. Hodgson, P.C. Kao, V.A. Lennon, G.G. Klee, A.R. Zinsmiester & R. Kumar. Brief report: Inhibition of renal phosphate transport by a tumor product in a patient with oncogene osteomalacia. *New England Journal of Medicine* 330:1645-1649 (1994).

Castle, W.E. & W.L. Wachter. Variations of linkage in rats and mice. *Genetics* 9:1-12 (1924).

Caverzasio, J. & J.P. Bonjour. Insulin-like growth factor I stimulates Na-dependent Pi transport in cultured kidney cells. *American Journal of Physiology* 257:F712-F717 (1989).

Chan, J.C.M. & N.H. Bell. Disorders of Phosphate Metabolism. In:Kidney Electrolyte Disorders. J.C.M. Chan & J.R.J. Gill Ed(s). Churchill Livingston Inc., New York, NY., 1990, pg. 223-260.

Chen, C., T. Carpenter, N. Steg, R. Baron & C. Anast. Hypercalciuric hypophosphatemic rickets, mineral balance, bone histomorphometry, and therapeutic implications of hypercalciuria. *Pediatrics* 84(2):276-280 (1989).

Chong, S.S., K. Kristjansson, H.Y. Zoghbi & M.R. Hughes. Molecular cloning of the cDNA encoding a human renal sodium phosphate transport protein and its assignment to chromosome 6p21.3-p23. *Genomics* 18:355-359 (1993).

Clark, F.H. Linkage of pink-eye and albinism in the deer-mouse. *Journal of Heredity* 27:256-260 (1936).

Cole, J.A., A.L. Eber, R.E. Poelling, P.K. Thorne & L.R. Forte. A dual mechanism for regulation of kidney phosphate transport by parathyroid hormone. *American Journal of Physiology* 253:E221-E227 (1987).

Cox, D.R., M. Burmeister, E.R. Price, S. Kim & R.M. Myers. Radiation hybrid mapping: A somatic cell genetic method for constructing high resolution maps of mammalian chromosomes. *Science* 250:245-250 (1990).

Custer, M., F. Meier, E. Schlatter, R. Greger, A. Garcia-Perez, J. Biber & H. Murer. Localization of NaPi-1, a Na-Pi-cotransporter, in rabbit kidney proximal tubules. I. mRNA localization by reverse transcription/polymerase chain reaction. *Pflügers Archiv-European Journal of Physiology* 424:203-209 (1993).

Custer, M., B. Spindler, F. Verrey, H. Murer & J. Biber. Identification of a new gene product (diphor-1) regulated by dietary phosphate. *American Journal of Physiology* 273:F801-F806 (1997).

D'Eustachio, P.D. & F.H. Ruddle. Somatic cell genetics and gene families. *Science* 220:919-924 (1983).

Davidai, G.A., T. Nesbitt & M.K. Drezner. Normal regulation of calcitriol metabolism in Gy mice. Evidence for biochemical heterogeneity in the X-linked hypophosphatemic diseases. *Journal of Clinical Investigation* 85:334-339 (1990).

Dixon, P.H., C. Wooding, D. Trump, D. Schlessinger, M.P. Whyte & R.V. Thakker. Eleven novel mutations in the PEX gene indicate molecular heterogeneity for X-linked hypophosphatemic rickets. *American Journal of Human Genetics* (Abstract 1477) Supplement 59(4)(1996).

Du, L., M. Desbarats, J. Viel, F.H. Glorieux, C. Cawthorn & B. Escarot. cDNA Cloning of the Murine PEX Gene Implicated in X-linked Hypophosphatemia and Evidence for Expression in Bone. *Genomics* 36:22-28 (1996).

Ecarot, B., J. Caverzasio, M. Desbarats, J.P. Bonjour & F.H. Glorieux. Phosphate transport by osteoblasts from X-linked hypophosphatemic mice. *American Journal of Physiology* 266:E33-E38 (1994).

Ecarot-Charrier, B., F.H. Glorieux, R. Travers, M. Desbarats, F. Bouchard & A. Hinek. Defective bone formation by transplanted Hyp mouse bone cells into normal mice. *Endocrinology* 123:768-773 (1988).

Econs, M.J. & M. . Drezner. Tumor-induced osteomalacia - unveiling a new hormone. *New England Journal of Medicine* 330:1679-1681 (1994).

Econs, M.J. & F. Francis. Positional cloning of the PEX gene: new insights into the pathophysiology of X-linked hypophosphatemic rickets. *American Journal of Physiology* 273(42):F489-F498 (1997).

Econs, M.J. & P.T. McEnery. Autosomal Dominant Hypophosphatemic Rickets/Osteomalacia: Clinical characterization of a novel renal phosphate-wasting disorder. *Journal of Clinical Endocrinology and Metabolism* 82:674-681 (1997).

Econs, M.J. & M.C. Speer. Genetic studies of complex diseases: Let the reader beware. *Journal of Bone and Mineral Research* 11(12):1835-1840 (1996).

Eicher, E.M., J.L. Southard, C.R. Scriver & F.H. Glorieux. Hypophosphatemia: Mouse model for human familial hypophosphatemic (vitamin D-resistant) rickets. *Proceedings of the National Academy of Sciences of the United States of America* 73:4667-4671 (1976).

Farrell, M. Homozygosity mapping : Familiarity breeds debility. *Nature Genetics* 5:107-108 (1993).

Feder, J.N., A. Gnirke, W. Thomas, Z. Tsuchihashi, D.A. Ruddy, A. Basava, F. Dormishian, R. Domingo, M.C. Ellis, et al. A novel MHC class 1-like gene is mutated in pateints with hereditary haemochromatosis. *Nature Genetics* 13:399-408 (1996).

Fisher, S.E., I.V. Bakel, S.E. Lloyd, S.H.S. Pearce, R.V. Thakker & I.W. Craig. Cloning and characterization of CLCN5, the human kidney chloride channel gene implicated in Dent disease (an X-linked hereditary nephrolithiasis). *Genomics* 29:598-606 (1995).

Garrod, A.E. The incidence of alkaptonuria: A study in chemical individuality. *The Lancet* December:1616-1620 (1902).

Gastier, J.M., P.J. C., S. Sunden, T. Brody, K.H. Buetow, J.C. Murray, J.L. Weber, T.J. Hudson, V.C. Sheffield & G.M. Duyk. Survey of trinucleotide repeats in the human genome: Assessment of their utility as genetic markers. *Human Molecular Genetics* 4(10):1829-1836 (1995).

Gazit, D., M. Tieder, U.A. Liberman, L. Passi-Even & I.A. Bab. Osteomalacia in hereditary hypophosphatemic rickets with hypercalciuria: A correlative clinical-histomorphometric study. *Journal of Clinical Endocrinology and Metabolism* 72:229-235 (1991).

German, J., A.M. Roe, M.F. Leppert & N.A. Ellis. Bloom syndrome: An analysis of consanguineous families assigns the locus mutated to chromosome band 15q26.1. *Proceedings of the National Academy of Sciences of the United States of America* 91:6669-6673 (1994).

Ghishan, F., S. Knobel, M. Dasuki, M. Butler & J. Phillips. Chromosomal localization of the human renal sodium phosphate transporter to chromosome 5: Implications for X-linked hypophosphatemia. *Pediatric Research* 35:510-513 (1994).

Glorieux, F.H., K.L. Insogna, R. Travers, J. Bibeau, E.E. Delvin, J.M. Gertner & R. Baron. Hypophosphatemic rickets with or without osteomalcia in correlation with circulating calcitriol levels. *Journal of Bone and Mineral Research* (Abstract 131) 1:91 (1986).

Goss, S.J. & H. Harris. New methods for mapping genes in human chromosomes. *Nature* 255:680-684 (1975).

Haldane, J.B.S., A.D. Sprunt & N.M. Haldane. Reduplication in mice. *Journal of Genetics* 5:133-135 (1915).

Hammond, H.A., L. Jin, Y. Zhong, C.T. Caskey & R. Chakraborty. Evaluation of 13 short tandem repeat loci for use in personal identification applications. *American Journal of Human Genetics* 55:175-189 (1994).

Heiskanen, M., L. Peltonen & A. Palotie. Visual mapping by high resolution FISH. *Trends in Genetics* 12(10):377-431 (1996).

Holm, I.A., X. Huang, N.M. Zacconi & L.M. Kunkel. Mutations in the PEX gene in X-linked hypophosphatemic rickets (HYP). *American Journal of Human Genetics* (Abstract 214) Supplement 59(4)(1996).

Hsu, T.C. Human and Mammalian Cytogenetics. Springer-Verlag, New York, NY., 1979.

Hudson, T.J., L.D. Stein, S.S. Gerety, J. Ma, A.B. Castle, J. Silva, D.K. Slonim, R. Baptista, L. Kruglyak, et al. An STS-based map of the human genome. *Science* 270:1945-1954 (1995).

Jeffereys, A.J., V. Wilson & S.L. Thein. Hypervariable 'minisatellite' regions in human DNA. *Nature* 314(6006):67-73 (1985).

Kavanaugh, M.P. & D. Kabat. Identification and characterization of a widely expressed phosphate transporter/retrovirus receptor family. *Kidney International* 49(4):959-963 (1996).

Kavanaugh, M.P., D.G. Miller, W. Zhang, W. Law, S.L. Kozak, D. Kabat & A.D. Miller. Cell-surface receptors for gibbon ape leukemia virus and amphotropic murine retrovirus are inducible sodium-dependent phosphate symporters. *Proceedings of the National Academy of Sciences of the United States of America* 91(15):7071-7075 (1994).

Kempson, S.A., A.L. Ying, J.A. McAteer & H. Murer. Endocytosis and Na+/solute cotransport in renal epithelial cells. *Journal of Biological Chemistry* 264:18451-18456 (1989).

Knochel, J.P. & R. Agarwal. Hypophosphatemia and hyperphosphatemia. In:Brenner and Rector's The Kidney. 5th ed., B.M. Brenner Ed(s). W.B. Saunders Company, Philadelphia, PA., 1996, pg. 1086-1133.

Knox, F.G. & A. Haramati. Renal regulation of phosphate excretion. In:The Kidney: Physiology and pathophysiology. D.W. Seldin & G. Giebisch Ed(s). Raven Press, New York, NY., 1985, pg. 1381-1396.

Kos, C.H., F. Tihy, M.J. Econs, H. Murer, N. Lemieux & H.S. Tenenhouse. Localization of a renal sodium-phosphate cotransporter gene to human chromosome 5q35. *Genomics* 19:176-177 (1994).

Kos, C.H., F. Tihy, H. Murer, N. Lemieux & H.S. Tenenhouse. Comparative mapping of Na^+-phosphate cotransporter genes, NPT1 and NPT2, in human and rabbit. *Cytogenetics and Cell Genetics* 75:22-24 (1996).

Kruglyak, L., M. Daly & E.S. Lander. Rapid multipoint analysis of recessive traits in nuclear families, including homosygosity mapping. *American Journal of Human Genetics* 56:519-527 (1995).

Kruglyak, L., M.J. Daly, M.P. Reeve-Daly & E.S. Lander. Parametric and Nonparametric Linkage Analysis: A Unified Multipoint Approach. *American Journal of Human Genetics* 58:1347-1363 (1996).

Laan, M., O.P. Kallioniemi, E. Hellsten, K. Alitalo, L. Peltonen & A. Palotie. Mechanically stretched chromosomes as targets for high-resolution FISH mapping. *Genomic Research* 5:13-20 (1995).

Lander, E.S. Mapping complex genetic traits in humans. In:Genome Analysis: A practical approach. K.E. Davies Ed(s). IRL Press Limited, Oxford, 1988, pg. 171-189.

McPherson, J.D., M.C. Krane, C.B. Wagner-McPherson, C.H. Kos & H.S. Tenenhouse. High resolution mapping of the renal sodium-phosphate cotransporter gene (SLC17A2) confirms its localization to human chromosome 5q35. *Pediatric Research* 41(5):632-634 (1997).

Meyer, R.A., M.h. Meyer & P.L. Morgan. Effects of altered diet on serum levels of 1,25-dihydroxyvitamin D and parathyroid hormone in X-linked hypophosphatemic (Hyp and Gy) mice. *Bone* 18(1):23-28 (1996).

Meyer, R.A.J., M.H. Meyer & R.W. Gray. Parabiosis suggests a humoral factor is involved in X-linked hypophosphatemia in mice. *Journal of Bone and Mineral Research* 4:493-500 (1989).

Mokrycki, A.K., M. Tassabehji, M. Davies, P. Rowe, E.B. Mawer & A.P. Read. PEX mutations in families with X-linked hypophosphatemic rickets. *American Journal of Human Genetics* (Abstract 1579) Supplement 59(4)(1996).

Murer, H. Cellular mechanisms in proximal tubular Pi reabsorption: Some answers and more questions. *Journal of the American Society of Nephrology* 2:1649-1665 (1992).

Murer, H. & J. Biber. Molecular mechanisms of renal apical Na/phosphate cotransport. *Annual Review of Physiology* 58:607-618 (1996).

Murer, H. & J. Biber. A molecular view of proximal tubular inorganic phosphate (Pi) reabsorption and its regulation. *Pflügers Archiv-European Journal of Physiology* 433(4):379-389 (1997).

Murer, H., M. Lotscher, B. Kaissling, M. Levi, S.A. Kempson & J. Biber. Renal brush border membrane Na/Pi-cotransport: Molecular aspects in PTH-dependent and dietary regulation. *Kidney International* 49(6):1769-1773 (1996).

Murer, H., A. Werner, S. Reshkin, R. Wuarin & J. Biber. Cellular mechanisms in proximal tubular reabsorption in inorganic phosphate. *American Journal of Physiology* 260:C885-C899 (1991).

Nadeau, J.H. Maps of linkage and synteny homologies between mouse and man. *Trends in Genetics* 5(3):82-86 (1989).

Nakai, M., M. Fukase, Y. Kinoshita & T. Fujita. Atrial natriuretic factor inhibits phosphate uptake in opossum kidney cells: As a model of renal proximal tubules. *Biochemical and Biophysical Research Communications* 152:1416-1420 (1988).

Nakamura, Y., M. Leppert, P. O'Connell, R. Wolff, T. Holm, M. Culver, C. Martin, E. Fujimoto, M. Hoff & E. Kumlin. Variable number of tandem repeat (VNTR) markers for human gene mapping. *Science* 235:1616-1622 (1987).

Nesbitt, T., T.M. Coffman, R. Griffiths & M.K. Drezner. Cross-transplantation of kidneys in normal and Hyp mice: Evidence that the Hyp phenotype is unrelated to an intrinsic renal defect. *Journal of Clinical Investigation* 89:1453-1459 (1992).

Nishiyama, S., F. Inoue & I. Matsuda. A single case of hypophosphatemic rickets with hypercalciuria. *Journal of Pediatric Gastroenterology and Nutrition* 5(5):826-829 (1986).

Noronha-Blob, L., V. Lowe & B. Sacktor. Stimulation by thyroid hormone of phosphate transport in primary cultured renal cells. *Journal of Cellular Physiology* 137:95-101 (1988).

O'Brien, S.J., H.N. Seuanez & J.E. Womack. Mammalian genome organization: An evolutionary view. *Annual Review of Genetics* 22:323-351 (1988).

O'Brien, S.J., J. Weinberg & L.A. Lyons. Comparative genomics: Lesson from cats. *Trends in Genetics* 13(10):393-399 (1997).

Oakey, R.J., M.G. Caron, R.J. Lefkowitz & M.F. Seldin. Genomic organization of adrenergic and serotonin receptors in the mouse: Linkage mapping of sequence-related genes provides a method for examining mammalian chromosome evolution. *Genomics* 10:338-344 (1991).

Ohno, S. Sex Chromosomes and Sex-linked Genes. Springer-Verlag, Berlin, 1967.

Ott, J. Analysis of human genetic linkage. Revised ed., The Johns Hopkins University Press, Baltimore, MD., 1991.

Paraiso, M.S., J.A. McAteer & S.A. Kempson. Parathyroid hormone inhibits plasma membrane Pi transport without changing endocytic activivty in opossum kidney cells. *Biochimica et Biophysica Acta* 1266:143-147 (1995).

Pearce, S.H.S., C. Williamson, O. Kifor, M. Bei, M.G. Coulthard, M. Davies, N. Lewis-Barned, D. McCredie, H. Powell, et al. A familial syndrome of hypocalcemia with hypercalciuria due to mutations in the calcium-sensing receptor. *New England Journal of Medicine* 335(15):1115-1122 (1996).

Pfister, M.F., E. Lederer, J. Forgo, U. Ziegler, M. Lotscher, E.S. Quabius, J. Biber & H. Murer. Parathyroid hormone-induced degradation of type II Na+/Pi cotransporters. *Journal of Biological Chemistry* 272(32):20125-20130 (1997).

Pizurki, L., R. Rizzoli, J. Caverzasio & J.-P. Bonjour. Effect of transforming growth factor-α and parathyroid hormone-related protein on phosphate transport in renal cells. *American Journal of Physiology* 259:F929-F935 (1990).

Pizurki, L., R. Rizzoli, J. Moseley, T.J. Martin, J. Caverzasio & J.-P. Bonjour. Effect of synthetic tumoral PTH-related peptide on cAMP production and Na-dependent Pi transport. *American Journal of Physiology* 255:F957-F961 (1988).

Pollak, M.R., C.E. Seidman & E.M. Brown. Three inherited disorders of calcium sensing. *Medicine* 75(3):115-123 (1996).

Pollak, M.R., Y.-H. Wu Chou, J.J. Cerda, B. Steinmann, B.N. La Du, J.G. Seidman & C.E. Seidman. Homozygosity mapping of the gene for alkaptonuria to chromosome 3q2. *Nature Genetics* 5:201-204 (1993).

Quamme, G.A. Effect of parathyroid hormone and dietary phosphate on phosphate transport in renal outer cortical and outer medullary brush-border membrane vesicles. *Biochimica et Biophysica Acta* 1024:122-130 (1990).

Rasmussen, H. & H.S. Tenenhouse. Mendelian hypophosphatemias. In:The Metabolic and Molecular Basis of Inherited Disease. 7th ed., C.R. Scriver, A.L. Beaudet, W.S. Sly & D. Valle Ed(s). McGraw-Hill Book Co., New York, NY., 1995, pg. 3717-3745.

Reichel, H., H.P. Koeffler & A.W. Norman. The role of the vitamin D endorine system in health and disease. *New England Journal of Medicine* 320(15):980-991 (1989).

Renwick, J.H. Progress in mapping human autosomes. *British Medical Journal* 25:65-73 (1969).

Richard, I., O. Broux, V. Allamand, F. Fougerousse, N. Chiannilkulchai, N. Bourg, L. Brenguier, C. Devaud, P. Pasturaud, et al. Mutations in the proteolytic enzyme calpain 3 cause Limb-girdle muscular dystrophy type 2A. *Cell* 81:27-40 (1995).

Rifas, L., S.L. Cheng, L.R. Halstead, A. Gupta, K.A. Hruska & L.V. Aviolo. Skeletal casein kinase activity defect in the *Hyp* mouse. *Calcified Tissue International* 61:256-259 (1997).

Rifas, L., L. Dawson, L.R. Halstead, M. Roberts, L.V. Avioli & . Phosphate transport in osteoblasts from normal and X-linked hypophosphatemic mice. *Calcif Tissue Int* 54:505-510 (1994).

Rifas, L., A. Gupta, K.A. Hruska & L.V. Aviolo. Altered osteoblast gluconeogenesis in X-linked hypophophatemic mice is associated with a depressed intracellular pH. *Calcified Tissue International* 57:60-63 (1995).

Ritz, E., W. Kreusser & J. Bommer. Effects of hormones other than parathyroid hormone on renal handling of phosphate. In:Renal Handling of Phosphate. S.G. Massry & H. Fleisch Ed(s). Plenum Medical Book Company, New York, NY., 1980, pg. 137-195.

Rowe, P.S.N., C.L. Oudet, F. Francis, C. Sinding, S. Pannetier, M.J. Econs, T.M. Strom, T. Meitinger, M. Garabedian, et al. Distribution of mutations in the *PEX* gene in families with X-linked hypophosphataemic rickets (HYP). *Human Molecular Genetics* 6(4):539-549 (1997).

Royle, N.J., R.E. Clarkson, Z. Wong & A.J. Jeffreys. Clustering of hypervariable minisatellites in the proterminal regions of human autosomes. *Genomics* 3(4):352-360 (1988).

Scheinman, S.J. X-linked hypercalciuric nephrolithiasis: Clinical syndromes and chloride channel mutations. *Kidney International* (In Press) 53:3-17 (1998).

Schork, N.J. & A. Chakravarti. A nonmathematical overview of modern gene mapping techniques applied to human diseases. In:Molecular Genetics and Gene Therapy of Cardiovascular Diseases. S.C. Mockrin Ed(s). Marcel Dekker, Inc., New York, NY., 1996, pg. 79-109.

Schrier, R.W. & C.W. Gottschalk. Diseases of the Kidney. 4th ed., Little, Brown and Company, Boston, MA., 1988.

Shipp, M.A., G.E. Tarr, C.-Y. Chen, S.N. Switzer, L.B. Hersh, H. Stein, M.E. Sunday & E.L. Reinherz. CD10/ neutral endopeptidase 24.11 hydrolyzes bombesin-like peptides and regulates the growth of small cell carcinomas of the lung. *Proceedings of the National Academy of Sciences of the United States of America* 88:10662-10666 (1991).

Shugart, Y.Y. Precision of marker heterozygosity estimates. *Genetic Epidemiology* 12:671-674 (1995).

Smith, C.L. & C.R. Cantor. Approaches to physical mapping of the human genome. *Cold Spring Harbor Symposia on Quantitative Biology* 51:115-122 (1986).

Stallings, R.L.. A.F. Ford, D. Nelson, D.C. Torney, C.E. Hildebrand & R.K. Moyzis. Evolution and distribution of (GT)n repetitive sequences in mammalian genomes. *Genomics* 10(3):807-815 (1991).

Strom, T.M., F. Francis, B. Lorenz, A. Böddrich, M.J. Econs, H. Lehrach & T. Meitinger. Pex gene deletions in Gy and Hyp mice provide mouse models for X-linked hypophosphatemia. *Human Molecular Genetics* 6(2):165-171 (1997).

Sturtevant, A.H. The linear arrangement of six sex-linked factors in drosophila, as shown by their mode of association. *Journal of Experimental Zoology* 14:43-59 (1913).

Tenenhouse, H.S. Cellular and molecular mechanisms of renal phosphate transport. *Journal of Bone and Mineral Research* 12(2):159-164 (1997).

Tenenhouse, H.S. & L. Beck. Renal Na^+-phosphate cotransporter gene expression in X-linked *Hyp* and *Gy* mice. *Kidney International* 49:1027-1032 (1996).

Tenenhouse, H.S., A.H. Klugerman & J.L. Neal. Effect of phosphonoformic acid, dietary phosphate and the Hyp mutation on kinetically distinct phosphate transport processes in mouse kidney. *Biochimica et Biophysica Acta* 984:207-213 (1989).

Tenenhouse, H.S., R.A.J. Meyer, S. Mandla, M.H. Meyer, R.W. Gray & . Renal phosphate transport and vitamin D metabolism in X-linked hypophosphatemic Gy mice: Responses to phosphate deprivation. *Endocrinology* :- (1992).

Tenenhouse, H.S. & C.R. Scriver. Minireview. X-linked hyphosphatemia. A phenotype in search of a cause. *International Journal of Biochemistry* 24:685-691 (1992).

Tenenhouse, H.S., A. Werner, J. Biber, S. Ma, J. Martel, S. Roy & H. Murer. Renal Na^+-phoshate cotransport in murine X-linked hypophosphatemic rickets. *Journal of Clinical Investigation* 93:671-676 (1994).

The Hyp Consortium. A gene (PEX) with homologies to endopeptidases is mutated in patients with X-linked hypophosphatemic rickets. *Nature Genetics* 11:130-136 (1995).

Tieder, M., R. Arie, I. Bab, J. Maor & U.A. Liberman. A new kindred with hereditary hypophosphatemic rickets with hypercalciuria: Implications for correct diagnosis and treatment. *Nephron* 62:176-181 (1992).

Tieder, M., D. Nodai, R. Samuel, R. Arie, A. Halabe, I. Bab, D. Gabizon & U.A. Luberman. Hereditary hypophosphatemic rickets with hypercalciuria. *New England Journal of Medicine* 312:611-616 (1985).

Tieder, M., D. Nodai, U. Shaked, R. Samuel, R. Arie, A. Halabe, J. Maor, J. Weissgarten, Z. Averbukh, et al. Idiopathic hypercalciuria and hereditary hypophosphatemic rickets. *New England Journal of Medicine* 316:125-129 (1987).

Trask, B.J. Fluorescence *in situ* hybridization: Applications in cytogenetics and gene mapping. *Trends in Genetics* 7(5):149-154 (1991).

Trohler, U., T.P. Bonjour & H. Fleish. Renal tubular adaptation to dietary phosphorus. *Nature* 261:145-146 (1976).

Turner, A.J. & K. Tanzawa. Mammalian membrane metallopeptidases: NEP, ECE, KELL, and PEX. *FASEB Journal* 11:355-364 (1997).

Van De Graaf, K.M. & S.I. Fox. Concepts of Human Anatomy and Physiology. 3rd ed., Wm. C. Brown Pub., Dubuque, IA., 1992.

van Ommen, G.J. A foundation for limb-girdle muscular dystrophy. *Nature Medicine* 1(5):412-414 (1995).

Verri, T., D. Markovich, C. Perego, F. Norbis, G. Stange, V. Sorribas, J. Biber & H. Murer. Cloning of a rabbit renal Na-Pi cotransporter, which is regulated by dietary phosphate. *American Journal of Physiology* 268:F626-F633 (1995).

Walker, J.J., T.S. Yan & G.A. Quamme. Presence of multiple sodium-dependent phosphate transport processes in proximal brush-border membranes. *American Journal of Physiology* 252:F226-F231 (1987).

Walling, M.W. Intestinal Ca and phosphate transport: Differential responses to vitamin D3 metabolites. *American Journal of Physiology* 233:E488-E494 (1977).

Weber, J.L. & P.E. May. Abundant class of human DNA polymorphisms which can be typed using the polymerase chain reaction. *American Journal of Human Genetics* 44:388-396 (1989).

Weidner, N. Review and update: Oncogenic osteomalacia-rickets. *Ultrastructural Pathology* 15:317-333 (1991).

Werner, A., M.L. Moore, N. Mantei, J. Biber, G. Semenza & H. Murer. Cloning and expression of cDNA for a Na/Pi cotransport system of kidney cortex. *Proceedings of the National Academy of Science USA* 88:9608-9612 (1991).

Winters, R.W., J.B. Graham, T.F. Williams, V.W. McFalls & C.H. Burnett. A genetic study of familial hypophosphatemia and vitamin D-resistant rickets with a review of the literature. *Medicine* 37:97-142 (1958).

Womack, J.E. Comparative Gene Mapping: A valuable new tool for mammalian developmental studies. *Developmental Genetics* 8:281-293 (1987).

Xu, D., N. Emoto, A. Giaid, C. Slaughter, S. Kaw, D. deWit & M. Yanagisawa. ECE-1: A membrane-bound metalloprotease that catalyzes the proteolytic activation of big endothelin-1. *Cell* 78:473-485 (1994).

Yusufi, A.N.K., T.J. Berndt, N. Murayama, F.G. Knox & T.P. Dousa. Calcitonin inhibits Na+ gradient-dependent phosphate uptake across renal brush-border membranes. *Americal Journal of Physiology* 252:F598-F604 (1987).

Appendices

Appendix 1. Marker List

The following is a list of marker information as it appeared at WICGR-MIT during the time of the study (discrepancies with other sources may exist). Additional information for the markers flanking the candidate genes on chromosomes 5 and 6 and the additional markers typed on chromosome 3 were based on information obtained from WICGR, Dr. Feder, Dr. McPherson and from the Marshfield Center for Medical Genetics: http://www.marshmed.org/genetics/maps/

Chr-Chromosome where marker is located
Marker-The name or ID for the primer pair or polymorphic locus
Placed typed-Location where the genotyping was performed either at WICGR-MIT (MIT) or at the Montreal General Hospital (MGH)
Label-Abbreviation for the type of radioactive isotope or fluorescent dye used to label primers
cM to next-The distance in centimorgans to the next marker
Het.-The Heterozygosity value
Allele range-The range of allele sizes in basepairs
Panel-The MIT marker panel name
Robot run-The MIT robot panel name
Type-The type of polymorphic repeat

Chr	Marker	Placed typed	Label	cM to next	Het.	Allele range	Panel	Robot run	Type
1	D1S1612	MIT	F	13	0.83	88-130	1	A	tetra
1	D1S1597	MIT	T	8.9	0.71	155-181	3	A	tetra
1	GATA29A05	MIT	F	9.3	0.73	171-215	27	E	tetra
1	D1S552	MIT	H	22	0.72	240-264	1	A	tetra
1	D1S1622	MIT	F	4.8	0.72	252-275	33	D	tri
1	D1S2134	MIT	F	17.2	0.84	256-301	27	E	tetra
1	D1S1669	MIT	F	13.2	0.74	372-410	4	A	tetra
1	D1S1665	MIT	H	12.4	0.74	219-241	16	C	tetra
1	D1S551	MIT	T	11.2	0.67	166-186	10	C	tetra
1	D1S1588	MIT	F	11.5	0.68	114-139	8	C	tri
1	D1S1631	MIT	F	17.4	0.77	125-156	12	B	tri
1	D1S1675	MIT	F	3.8	0.62	220-255	12	B	tetra
1	D1S534	MIT	H	6.9	0.83	196-218	38	E	tetra
1	D1S1595	MIT	T	11.6	0.78	260-297	8	C	tetra
1	D1S1679	MIT	F	4.2	0.84	148-170	38	E	tetra
1	D1S1677	MIT	F	19.2	0.68	180-214	8	C	tetra
1	D1S1589	MIT	T	10	0.76	194-220	33	D	tri
1	D1S518	MIT	T	9.3	0.84	191-224	12	B	tetra
1	D1S1660	MIT	H	7.4	0.78	226-252	30	D	tetra
1	D1S1678	MIT	H	3.5	0.68	288-313	8	C	tetra
1	D1S3465	MIT	H	11.5	0.62	121-133	31	E	tetra
1	D1S2141	MIT	F	11.6	0.84	235-265	8	C	tetra

Chr	Marker	Placed typed	Label	cM to next	Het.	Allele range	Panel	Robot run	Type
1	D1S549	MIT	T	8.3	0.77	157-194	8	C	tetra
1	D1S1656	MIT	H	2.2	0.90	125-165	8	C	tetra
1	ATA29C07	MIT	F	25.7	0.75	248-270	4	A	tri
1	D1S547	MIT	T	7.6	0.79	280-310	35	C	tetra
2	D2S1780	MIT	F	9.9	0.73	307-338	33	D	tetra
2	D2S423	MIT	T	7.9	0.70	110-135	10	C	tetra
2	D2S1400	MIT	H	17.9	0.66	107-140	1	A	tetra
2	D2S405	MIT	T	17.8	0.67	233-262	23	D	tetra
2	D2S1356	MIT	F	14.4	0.76	236-256	23	D	tri
2	D2S1337	MIT	T	10.2	0.66	123-163	31	E	tetra
2	D2S441	MIT	H	4	0.75	127-159	10	C	tetra
2	D2S1394	MIT	T	11.8	0.70	158-175	37	E	tetra
2	D2S1777	MIT	F	5.3	0.65	190-215	23	D	tetra
2	D2S1790	MIT	F	21.8	0.80	278-328	12	B	tetra
2	D2S410	MIT	T	9	0.80	152-182	23	D	tetra
2	D2S1328	MIT	F	15.5	0.75	135-168	3	A	tetra
2	D2S442	MIT	H	18.1	0.65	194-228	2	A	tetra
2	D2S1353	MIT	F	12.3	0.80	136-164	23	D	tri
2	D2S1776	MIT	F	15.7	0.72	286-308	1	A	tetra
2	D2S1391	MIT	F	13.3	0.79	109-133	30	D	tetra
2	D2S1384	MIT	F	11.9	0.80	141-167	34	E	tetra
2	D1S1649	MIT	F	5.6	0.80	106-136	2	A	tetra
2	D2S434	MIT	T	9.6	0.77	256-286	21	D	tetra
2	D2S1363	MIT	T	12.6	0.79	172-192	5	C	tetra
2	D2S427	MIT	H	17.4	0.76	215-263	34	E	tetra
2	D2S338	MIT	T	11.6	0.81	271-291	12	B	di
2	D2S125	MIT	T		0.82	82-103	25	E	di
2	tel-2q44	MIT	F			175-183	36	E	di
				18.8					
3	D3S1304	MIT	F	16.5	0.80	253-275	29	D	di
3	D3S2403	MIT	F	28.3	0.70	248-292	14	B	tetra
3	D3S2432	MIT	F	13.2	0.83	117-170	14	B	tetra
3	D3S2409	MIT	T	8.1	0.75	111-127	12	B	tri
3	D3S1766	MIT	T	12.9	0.76	207-232	3	A	tetra
3	D3S1285	MIT	H	11.8	0.73	230-243	4	A	di
3	D3S2406	MIT	T	17.5	0.87	306-370	38	E	tetra
3	D3S2459	MIT	H	6.5	0.84	174-204	31	E	tetra
3	D3S3045	MIT	H	11.2	0.82	175-208	14	B	tetra
3	D3S2460	MIT	T	20.7	0.76	143-174	14	B	tetra
3	D3S1764	MIT	T	13.6	0.80	218-260	29	D	tetra
3	D3S1744	MIT	F	17.7	0.80	131-167	4	A	tetra
3	D3S1763	MIT	T	6.3	0.78	260-282	28	E	tetra
3	D3S3053	MIT	H	9.2	0.72	223-246	26	E	tetra

Chr	Marker	Placed typed	Label	cM to next	Het.	Allele range	Panel	Robot run	Type
3	D3S2427	MIT	T	14.2	0.87	203-250	4	A	tetra
3	D3S2436	MIT	T	5.7	0.66	164-181	1	A	tetra
3	D3S2398	MIT	H	6.7	0.79	266-298	12	B	tetra
3	D3S2418	MIT	T	8.9	0.71	87-117	14	B	tri
4	D4S2366	MIT	H	11.8	0.79	120-144	12	B	tetra
4	D4S403	MIT	F	8.1	0.77	214-234	3	A	di
4	D4S2639	MIT	T	8.6	0.85	160-192	29	D	tetra
4	D4S2397	MIT	F	23.8	0.78	126-144	24	D	tri
4	D4S1627	MIT	H	8.4	0.81	177-202	1	A	tetra
4	GATA28F03	MIT	H	8.1	0.73	231-257	22	D	tetra
4	D4S2367	MIT	F	12.9	0.78	125-147	18	C	tetra
4	GATA10G07	MIT	T	4.2	0.66	161-179	24	D	tetra
4	D4S2361	MIT	F	12.2	0.74	149-164	36	E	tri
4	D4S1647	MIT	F	26.4	0.75	130-156	27	E	tetra
4	D4S2394	MIT	T	13.5	0.79	235-259	24	D	tetra
4	D4S1644	MIT	F	4.6	0.72	188-210	4	A	tri
4	D4S1625	MIT	F	16.3	0.74	182-210	24	D	tetra
4	D4S1629	MIT	H	8.6	0.72	137-158	24	D	tetra
4	D4S2368	MIT	T	11.6	0.75	299-328	9	B	tetra
4	D4S2431	MIT	H	6.5	0.82	234-258	20	C	tetra
4	D4S2417	MIT	F	14.6	0.68	251-273	24	D	tetra
4	D4S408	MIT	H	12.7	0.76	225-248	15	B	tetra
4	D4S1652	MIT	H		0.71	136-150	2	A	di
5	D5S1492	MIT	T	12.3	0.60	114-126	24	D	tetra
5	D5S807	MIT	H	4.8	0.76	166-203	22	D	tetra
5	D5S817	MIT	H	14.6	0.66	260-272	2	A	tetra
5	D5S1473	MIT	F	11.9	0.72	240-320	37	E	tetra
5	D5S1470	MIT	H	28.2	0.82	173-199	21	D	tetra
5	GATA67D03	MIT	T	16.5	0.82	149-181	28	E	tetra
5	D5S1501	MIT	T	11.5	0.78	98-144	21	D	tetra
5	D5S1719	MIT	F	24.2	0.81	81-108	7	A	di
5	GATA68A03	MIT	H	11.2	0.75	305-334	2	A	tetra
5	D5S1505	MIT	F	11.2	0.80	215-275	28	E	tetra
5	D5S816	MIT	T	9.6	0.83	225-251	38	E	tetra
5	D5S1480	MIT	F	12	0.79	218-240	5	C	tetra
5	D5S820	MIT	F	18.7	0.77	188-210	32	E	tetra
5	D5S1471	MIT	T	5.1	0.68	151-172	20	C	tetra
5	D5S1456	MIT	H	10	0.78	191-211	18	C	tetra
5	**D5S498**	MGH	P32	5	0.81	173-189	NA	Manual	di
5	**D5S469**	MGH	P32	6	0.48	142-146	NA	Manual	di
5	**D5S408**	MIT	H		0.73	247-266	NA	Manual	di
6	D6S477	MIT	T	14.5	0.82	213-237	17	D	tetra

Chr	Marker	Placed typed	Label	cM to next	Het.	Allele range	Panel	Robot run	Type
6	D6S1006	MIT	F	23	0.61	192-202	6	A	tri
6	D6S1281	MIT	H	0.13	0.72	176-212	17	D	tetra
6	**D6S2238**	MGH	P32	0.13	0.81	87-113	NA	Manual	di
6	**D6S2237**	MGH	P33	0.13	0.77	113-137	NA	Manual	di
6	**D6S2233**	MGH	P34	9.81	0.81	139-161	NA	Manual	di
6	D6S1019	MIT	F	5.4	0.67	212-236	17	D	di
6	D6S1017	MIT	F	13.3	0.68	151-171	32	E	tetra
6	D6S1280	MIT	T	10.8	0.78	168-192	17	D	tetra
6	D6S1053	MIT	T	12.7	0.81	295-325	15	B	tetra
6	D6S1270	MIT	H	9.5	0.62	111-137	13	B	tetra
6	D6S1056	MIT	H	12.6	0.85	236-273	14	B	tetra
6	D6S1021	MIT	F	5.5	0.73	140-156	39	E	tri
6	D6S474	MIT	F	10.3	0.77	151-167	17	D	tetra
6	D6S1040	MIT	H	10	0.75	257-285	32	E	tetra
6	D6S1009	MIT	H	7.2	0.80	237-273	5	C	tetra
6	D6S1003	MIT	T	19.9	0.77	292-319	14	B	tri
6	D6S1007	MIT	T	15.1	0.60	283-303	22	D	tetra
6	D6S1277	MIT	T	12.1	0.72	282-311	17	D	tetra
6	D6S503	MIT	H	3.4	0.71	247-263	11	B	tetra
6	D6S1027	MIT	T		0.77	115-138	17	D	tri
7	D7S2201	MIT	T	25	0.62	100-117	15	B	tetra
7	D7S1802	MIT	H	9.3	0.73	177-201	20	C	tetra
7	D7S1808	MIT	F	8.9	0.78	251-276	15	B	tetra
7	D7S817	MIT	F	8.5	0.78	156-180	1	A	tetra
7	GATA31A10	MIT	T	14	0.76	172-196	2	A	tetra
7	D7S1818	MIT	T	3.3	0.71	180-202	30	D	tetra
7	D7S1830	MIT	T	17.4	0.76	200-230	20	C	tetra
7	GATA73D10	MIT	T	5.7	0.81	217-269	15	B	tetra
7	D7S2212	MIT	T	19.4	0.8	196-216	28	E	tetra
7	D7S1799	MIT	H	14.4	0.72	171-199	15	B	tetra
7	GATA44F09	MIT	H	9.9	0.86	174-201	4	A	tetra
7	D7S1804	MIT	F	19.1	0.86	210-290	35	C	tetra
7	D7S1824	MIT	H	5	0.83	163-199	28	E	tetra
7	D7S2195	MIT	H	15.4	0.79	237-292	23	D	tetra
7	D7S1826	MIT	F	21.6	0.76	142-164	15	B	tetra
7	D7S559	MIT	H		0.81	190-235	24	D	di
8	D8S1130	MIT	H	4.3	0.80	130-162	18	C	tetra
8	D8S1106	MIT	F	5.4	0.73	126-155	20	C	tetra
8	D8S1145	MIT	T	12.5	0.73	261-293	20	C	tetra
8	D8S136	MIT	F	21.9	0.88	63-89	6	A	di
8	D8S1477	MIT	F	8.1	0.86	137-180	5	C	tetra
8	D8S1110	MIT	F	8.7	0.77	262-286	2	A	tetra
8	D8S1113	MIT	T	6.1	0.81	215-245	16	C	tetra

Chr	Marker	Placed typed	Label	cM to next	Het.	Allele range	Panel	Robot run	Type
8	D8S1136	MIT	F	4.7	0.72	235-268	20	C	tetra
8	GATA12B06	MIT	T	15.1	0.84	260-288	5	C	tetra
8	D8S1119	MIT	H	8.3	0.80	173-199	13	B	tri
8	GAAT1A4	MIT	H	9.2	0.66	140-157	19	C	tetra
8	D8S1132	MIT	F	6.6	0.86	134-171	35	C	tetra
8	D8S592	MIT	T	11.1	0.67	150-164	12	B	tetra
8	D8S1179	MIT	H	6	0.82	162-194	23	D	tetra
8	D8S1128	MIT	H	14	0.76	240-268	17	D	tetra
8	D8S1100	MIT	T		0.65	183-193	15	B	tri
9	GATA62F03	MIT	F	18.8	0.64	272-295	22	D	tetra
9	D9S925	MIT	H	16.2	0.82	167-199	29	D	tetra
9	D9S741	MIT	F	13.4	0.79	190-208	20	C	di
9	D9S1118	MIT	T	9.8	0.81	139-177	36	E	tetra
9	D9S301	MIT	T	8.6	0.80	208-241	37	E	tetra
9	D9S1122	MIT	H	5.9	0.71	190-210	8	C	tetra
9	D9S922	MIT	H	4.4	0.78	251-272	9	B	tetra
9	D9S1119	MIT	H	21.7	0.92	151-175	39	E	tetra
9	D9S910	MIT	T	7.3	0.5	105-129	26	E	tru
9	D9S938	MIT	F	9.1	0.79	390-414	3	A	tetra
9	D9S930	MIT	T		0.78	278-307	19	C	tetra
10	D10S1435	MIT	H	14.1	0.69	256-276	26	E	tetra
10	D10S189	MIT	T	8.4	0.72	178-189	4	A	di
10	D10S1412	MIT	F	12.4	0.73	108-170	25	E	tri
10	D10S674	MIT	T	3.6	0.76	218-258	18	C	tetra
10	D10S1423	MIT	F	12.3	0.74	218-242	39	E	tetra
10	D10S1426	MIT	T	13.8	0.74	152-180	13	B	tetra
10	D10S1220	MIT	H	12.2	0.62	230-252	13	B	tri
10	D10S1225	MIT	T	15.9	0.76	168-204	27	E	tri
10	D10S1432	MIT	T	9.8	0.74	159-185	39	E	tetra
10	GGAT1A4	MIT	T	18.7	0.66	198-230	22	D	tetra
10	D10S677	MIT	F	7.9	0.81	195-225	2	A	tetra
10	D10S1239	MIT	T	10.8	0.75	158-184	25	E	tetra
10	D10S1237	MIT	F	11.4	0.82	363-436	1	A	tetra
10	D10S1230	MIT	H	11.1	0.74	110-138	14	B	tri
10	D10S1223	MIT	F	13.5	0.74	269-296	13	B	tri
10	D10S169	MIT	T		0.75	95-117	23	D	di
11	D11S2362	MIT	T	7.1	0.81	208-232	13	B	tri
11	D11S1999	MIT	H	15.2	0.80	108-137	3	A	tetra
11	D11S1981	MIT	F	21	0.83	134-178	28	E	tetra
11	ATA34E08	MIT	F	0.1	0.76	152-172	29	D	tri
11	D11S1392	MIT	F	16	0.77	198-220	13	B	tetra
11	D11S1985	MIT	H	11.8	0.87	234-286	37	E	tetra

Chr	Marker	Placed typed	Label	cM to next	Het.	Allele range	Panel	Robot run	Type
11	D11S2371	MIT	H	22	0.67	192-213	19	C	tetra
11	D11S1366	MIT	T	7.9	0.71	198-262	31	E	tetra
11	D11S1986	MIT	T	9.6	0.79	184-248	32	E	tetra
11	D11S1998	MIT	F	9	0.68	129-165	13	B	tetra
11	GATA64D03	MIT	H	11.1	0.78	225-253	19	C	tetra
11	D11S912	MIT	T		0.81	99-123	13	B	tetra
12	D12S372	MIT	T	7.2	0.76	173-190	18	C	tetra
12	D12S374	MIT	T	12.2	0.71	274-294	13	B	tetra
12	D12S391	MIT	H	9.6	0.88	209-251	3	A	tetra
12	D12S373	MIT	T	14.2	0.76	173-228	26	E	tetra
12	D12S1042	MIT	T	8.7	0.81	118-136	4	A	tri
12	D12S1090	MIT	H	23.5	0.87	217-258	7	A	tetra
12	D12S1294	MIT	F	8.5	0.84	168-204	18	C	tetra
12	D12S1052	MIT	T	12.8	0.72	138-165	22	D	tetra
12	D12S1064	MIT	F	14.7	0.82	167-197	30	D	tetra
12	D12S1300	MIT	H	4.2	0.63	108-135	15	B	tetra
12	PAH.30361	MIT	H	17	0.79	228-260	28	E	tetra
12	ATA25F09	MIT	H	7.7	0.79	86-104	7	A	tri
12	D12S395	MIT	H	15.3	0.76	223-247	39	E	tetra
12	GATA32F05	MIT	F	13.2	0.81	250-283	18	C	tetra
12	D12S1045	MIT	T		0.80	76-103	16	C	tri
13	D13S787	MIT	F	18.9	0.72	245-267	26	E	tetra
13	GGAA29H03	MIT	T	8.7	0.80	217-245	11	B	tetra
13	D13S894	MIT	T	6.4	0.64	180-205	19	C	tetra
13	D13S325	MIT	F	18.2	0.80	195-235	25	E	tetra
13	D13S800	MIT	T	8.8	0.75	292-319	18	C	tetra
13	D13S317	MIT	H	27	0.79	175-199	33	D	tetra
13	D13S779	MIT	H		0.71	180-199	30	D	tri
14	GATA31B09	MIT	T	3.5	0.70	288-301	3	A	tetra
14	D14S597	MIT	H	5.1	0.78	177-193	35	C	tri
14	D14S297	MIT	T	14.5	0.62	84-112	11	B	tetra
14	D14S306	MIT	F	14	0.79	188-214	15	B	tetra
14	D14S587	MIT	F	11.3	0.84	245-278	19	C	tetra
14	D14S592	MIT	H	8.9	0.75	228-240	25	E	tri
14	D14S588	MIT	H	18.9	0.67	114-141	9	B	tetra
14	D14S606	MIT	T	6.3	0.69	266-278	26	E	tetra
14	D14S610	MIT	H	11.7	0.71	355-376	6	A	tetra
14	D14S617	MIT	F	11.5	0.78	137-173	22	D	tetra
14	D14S611	MIT	F		0.67	151-174	19	C	tetra
15	D15S165	MIT	H	12.2	0.79	180-217	9	B	di
15	ACTC	MIT	T	17	0.87	67-96	5	C	di

Chr	Marker	Placed typed	Label	cM to next	Het.	Allele range	Panel	Robot run	Type
15	D15S659	MIT	H	9	0.84	161-206	25	E	tetra
15	D15S643	MIT	F	10.7	0.86	193-223	29	D	tetra
15	D15S153	MIT	F	27.9	0.87	194-228	9	B	di
15	D15S652	MIT	H	8.4	0.80	283-309	3	A	tri
15	D15S816	MIT	F	6.1	0.66	123-148	9	B	tetra
15	D15S657	MIT	F		0.82	329-360	2	A	tetra
16	D16S2622	MIT	T	14.3	0.67	71-91	7	A	tetra
16	D16S748	MIT	F	6.4	0.82	181-214	26	E	tri
16	D16S2619	MIT	T	14.3	0.79	143-163	34	E	tetra
16	D16S403	MIT	H	7.3	0.85	132-155	27	E	di
16	D16S769	MIT	F	7.5	0.69	255-272	9	B	tetra
16	D16S753	MIT	T	15.2	0.79	250-278	9	B	tetra
16	GATA22F09	MIT	H	14	0.71	167-188	16	C	tetra
16	D16S2624	MIT	H	7.1	0.70	131-150	17	D	tetra
16	D16S518	MIT	H	18.2	0.83	272-290	4	A	di
16	D16S422	MIT	H	13.2	0.79	184-212	5	C	di
16	D16S539	MIT	T		0.76	144-172	9	B	tetra
17	D17S1308	MIT	F	13	0.67	304-316	26	E	tetra
17	D17S1298	MIT	F	16.9	0.60	246-260	11	B	tetra
17	D17S1303	MIT	T	27.5	0.70	227-245	14	B	tetra
17	D17S1294	MIT	F	8	0.68	244-272	21	D	tetra
17	D17S1293	MIT	T	6.5	0.83	262-296	2	A	tetra
17	D17S1299	MIT	F	16.7	0.73	185-209	21	D	tetra
17	D17S809	MIT	H	6.5	0.71	229-249	6	A	di
17	D17S1290	MIT	H	25.7	0.84	168-210	11	B	tetra
17	D17S1301	MIT	F		0.65	141-164	21	D	tetra
18	D18S59	MIT	F	12.3	0.80	142-165	7	A	di
18	D18S976	MIT	T	17.7	0.86	166-194	7	A	tetra
18	D18S843	MIT	H	12	0.75	179-195	7	A	tri
18	D18S542	MIT	H	16.5	0.79	178-198	12	B	di
18	D18S877	MIT	T	10.7	0.68	116-137	27	E	tetra
18	D18S535	MIT	H	10	0.76	130-157	5	C	tetra
18	D18S851	MIT	F	4.4	0.73	250-277	7	A	tetra
18	D18S858	MIT	F	19.8	0.75	188-208	7	A	tri
18	GATA26C03	MIT	T	15.3	0.83	272-300	16	C	tetra
18	D18S541	MIT	T	8.5	0.76	266-289	7	A	tetra
18	D18S844	MIT	H		0.76	182-201	36	E	tri
19	GATA21G05	MIT	F	13.1	0.72	222-245	30	D	tetra
19	D19S586	MIT	T	8.8	0.83	222-250	27	E	tetra
19	D19S714	MIT	H	12.7	0.79	220-258	33	D	tetra
19	D19S433	MIT	F	7.3	0.77	192-221	11	B	tetra

Chr	Marker	Placed typed	Label	cM to next	Het.	Allele range	Panel	Robot run	Type
19	D19S587	MIT	F	24.8	0.62	138-156	11	B	tetra
19	D19S246	MIT	F	5.7	0.82	184-233	34	E	tetra
19	D19S601	MIT	F	4.4	0.78	197-237	22	D	tetra
19	D19S589	MIT	T		0.72	161-186	11	B	tetra
20	D20S473	MIT	T	26.6	0.68	169-187	6	A	tri
20	D20S604	MIT	F	5.9	0.72	131-147	6	A	tetra
20	D20S470	MIT	T	7.5	0.87	266-314	11	B	tetra
20	D20S477	MIT	F	8.3	0.71	221-268	6	A	tetra
20	D20S478	MIT	T	9.5	0.81	240-275	39	E	tetra
20	D20S481	MIT	T		0.83	217-253	6	A	tetra
21	D21S1437	MIT	H	9.4	0.73	110-143	6	A	tetra
21	D21S1435	MIT	T	5.3	0.81	163-191	16	C	tetra
21	D21S1270	MIT	H	11.3	0.83	172-198	6	A	tetra
21	D21S1440	MIT	F	5	0.74	153-175	16	C	tri
21	D21S1809	MIT	H	15.8	0.75	210-222	27	E	tetra
21	D21S1446	MIT	T		0.69	200-226	9	B	tetra
22	D22S446	MIT	F	13.4	0.81	182-233	33	D	di
22	D22S689	MIT	F	3.3	0.76	197-230	16	C	tetra
22	D22S685	MIT	T	12.6	0.79	168-209	21	D	tetra
22	D22S445	MIT	T	6.9	0.65	110-130	1	A	tetra
22	D22S444	MIT	H		0.53	123-131	28	E	tetra
X	DXS6807	MIT	F	48	0.68	253-273	3	A	tetra
X	DXS6810	MIT	T	19	0.66	212-225	10	C	tetra
X	DXS7132	MIT	F	9	0.73	282-303	11	B	tetra
X	DXS6800	MIT	F	10	0.76	195-221	14	B	tetra
X	DXS6789	MIT	F	14	0.76	118-153	10	C	tetra
X	DXS6799	MIT	F	5	0.70	241-274	10	C	tetra
X	DXS6797	MIT	T	24	0.76	240-274	1	A	tetra
X	DXS1047	MIT	F		0.81	177-211	10	C	di
3	GATA31E08	MIT	H	not used	0.73	226-256	10	C	tetra
XY	GATA2A12	MIT	H	not used	0.65	230-250	21	D	tetra
Y	DYS389	MIT	F	not used	0.66	248-264	17	D	tetra
Y	DYS390	MIT	F	not used	0.76	205-224	19	C	tetra

Appendix 2. Identity Marker List

Genbank Locus[STR]$_n$/ GDB Designation	Gene (chromosome location)	PCR Primers	Product Length (bp)
HUMHPRTB[AGAT]$_n$/ HPRT	Hypoxanthine phosphoribosyltransferase (Xq26)	A: atg cca cag ata ata cac atc ccc B: ctc tcc aga ata grt aga tgt agg	259–299
HUMFABP[AAT]$_n$/ FABP2	Intestinal fatty acid-binding protein (4q28–q31)	A: gta gta tca grt tca tag ggt cac c B: cag ttc grt tcc art gtc tgt ccg	199–220
HUMCD4[AAAAG]$_n$/ CD4	Recognition / surface antigen (cd4) (12p12-pter)	A: ttg gag tcg caa gct gaa cta gcg B: cca gga agt tga ggc tgc agt gaa	125–175
HUMCSF1PO[AGAT]$_n$/ CSF1R	c-fms proto-oncogene for CSF-1 receptor (5q33.3-q34)	A: aac ctg agt ctg cca agg act agc B: ttc cac aca cca ctg gcc atc ttc	295–327
HUMTH01[AATG]$_n$/TH	Tyrosine hydroxylase (11p15.5)	A: grg ggc tga aaa gct ccc gat tat B: art caa agg gta tct ggg ctc tgg	179–203
HUMPLA2A1[AAT]$_n$/PLA2A	Pancreatic phospholipase A-2 (12q23-qter)	A: ggt tgt aag ctc cat gag grt aga B: ttg agc act tac tat grg cca ggc t	118–139
HUMF13A01[AAAG]$_n$/F13A1	Coagulation factor XIII (6p24-p25)	A: gag grt gca ctc gag cct ttg caa B: ttc ctg aat cat ccc aga gcc aca	281–331
HUMCYAR04[AAAT]$_n$/CYP19	Aromatase cytochrome P-450 (15q21.1)	A: ggt aag cag gta ctt agt tag cta c B: grt aca grg agc caa ggt cgt gag	173–201
HUMLIPOL[AAAT]$_n$/LPL	Lipoprotein lipase (8p22)	A: ctg acc aag gat agt ggg ata tag B: ggt aac tga gcg aga ctg tgt ct	125–175

Table reproduced from Hammond et al., 1994.

This table lists the markers used to estimate the frequency of homozygotes and degree of inbreeding in the HHRH kindred. In addition, confirmation of the reported gender specification was performed as described in Bailey et al., 1992 (see Appendix 4). PCR amplification of human male DNA using a pair of primers that spans the first intron of the X-Y homologous gene amelogenin results in two different size fragments. A fragment of 542bp is amplified from the X chromosome and a fragment of 358bp from the Y chromosome. Consequently, when a single 542bp band is amplified the individuals is designated female. When two bands are amplified the individuals is designated male (Bailey et al., 1992).

Bailey, D.M.D., N.A. Affara & M.A. Fergson-Smith. The X-Y homologous gene amelogenin maps to the short arms of both the X and Y chromosomes and is highly conserved in primates. *Genomics* 14:203-205 (1992).

Hammond, H.A., L. Jin, Y. Zhong, C.T. Caskey & R. Chakraborty. Evaluation of 13 short tandem repeat loci for use in personal identification applications. *American Journal of Human Genetics* 55:175-189 (1994).

Appendix 3. Description of Programs

The following is a list and very brief description of the programs used in Chapter 4 of my thesis that I have written based on my experience at the Center for Genome Research at MIT's Whitehead Institute for Biomedical Research (WICGR). The programs and additional information on their applications can be obtained from the Center for Genome Research web site at: www-genome.wi.mit.edu. A description of the GENEHUNTER commands can also be found at: http://bimas.dcrt.nih.gov/linkage/ghcmds.html.

The ABI GENESCAN/GENOTYPER gel and data processing programs were used to call the alleles for the fluorescent marker D5S408. The GENESCAN program was used to call the alleles for the seven additional fluorescent markers typed on chromosome 3. These programs were used according the instructions supplied with the sequencers.

The gel and data processing programs used for the genome scan were written at the WICGR and run on the Unix operating system using Digital Equipment Corporation, Alpha workstations. ABI produced gel files were transferred to the UNIX machine and processed by the programs BASS/GRACE.

BASS produces a UNIX readable version of the gel image and 48 files corresponding the individual lanes of the gel. These files contain the information from the 4 color traces in each lane.

GRACE displays the gel image and allows for tracking of the lanes. Information from each lane is extracted into the 48 BASS produced files and each lane is examined by the allele calling program NEWCALL.

NEWCALL checks that there is no leakage between lanes, checks that there are no more than two alleles per marker for each sample and calls the allele sizes. The NEWCALL program generates tables of lanes and allele sizes that can be used to check whether a lane has been successfully called. If a lane was not called it gives a reason i.e., suspected leakage, size standards problems, multiple alleles or no sample present. Marker performance can be obtained by checking how often markers were and were not called. Several files are generated by NEWCALL including a "calls.db" file listing the alleles for each marker in each lane.

INTERCALL is similar to newcall, but designed to analyze gels containing PCR samples from different marker panels.

Additional files needed to run NEWCALL and INTERCALL:
mendel.in file- when present NEWCALL does a simple check for Mendelian segregation i.e., that each child receives one allele from each parent. This warns if plate was inverted during loading, or if a gel was misnamed.
lane.panel file- specifies which individual and marker panel sample is in which lane.

Files loaded into database:
Pedigree file- lists all members of the pedigree including all additional individuals created to specify marriage and consanguinity loops. Specifies the pedigree name, individual's identification number (ID), father's ID, mother's ID, and gender.
DNA Panel files- tells which individual is in which lane for the a-gel and b-gel. Specifies the name of the panel, lane no., pedigree name and individual's ID.
Phenotype file- specifies the pedigree name, individual's ID, affection status and liability class (optional).
calls.db- lists markers, gel name, DNA panel name and the alleles called in each lane of the gel.
intercalls.db - is similar to calls.db, but larger and with slightly different format. Lists marker, gel name, lane no., pedigree name, individual's ID, allele for that individual.

The file DATABASE.LOG is generated when the above files are loaded into the database. This log reports any discrepancies detected between the allele values that are currently being loaded into the database and any allele values already stored in the database.

Files needed to extract (dump) information from the database:
Marker list- specifies which markers to dump from database. A separate list was used for each chromosome.
Individual file- specifies which of the individuals in the pedigree should be listed in the dump file.

The dump file for each chromosome is obtained from the database and loaded into the PEDMANAGER program.

The PEDMANAGER program zeros segregation errors, bins the alleles by size, rounds off the allele sizes to integers, calculates the allele frequencies and generates a pedigree file (.ped) and a parameter file (.data) in LINKAGE format (Terwilliger & Ott,

1994). The PEDMANAGER program flags segregation errors by family and marker. Several checks of data quality were done, before linkage data analysis was performed.

The GENEHUNTER program can perform single point or multipoint, linkage analysis and calculate a parametric LOD score and non-parametric Z-score.

INDIV. I.D.	Phenotype	Amelogenin*	HPRT		FABP2		CD4		CSF1R		TH		PLA2A		F13A1		CYP19		LPL	
5027	~~HHH~~	F	291	287	214	205	275	260	315		195	187	121	121	291	287	181	177	121	117
5029	~~HHH~~	F	287	287	205	205	260	240	315		195	187	121	121	291	291	177	177	121	117
5083	~~HHH~~	M	283	283	214	205	240	240	315	307	199	195	121	121	303	295	177	177	121	113
5089	~~HHH~~	M	283	283	205	205	260	240	315	307	195	187	133	121	291	279	201	177	125	117
6003	~~HHH~~	F	287	287	211	205	260	240	311	307	187	187	136	121	291	279	193	177	129	121
6004	~~HHH~~	F	287	287	214	205	260	240	311	307	187	183	136	121	291	291	197	177	117	117
6055	~~HHH~~	F	287	287	214	205	265	240	307	299	199	195	136	127	295	291	185	177	121	117
6064	~~HHH~~	M	291	291	214	205	265	240	319	299	199	195	127	121	291	287	177	165	117	125
6066	~~HHH~~	M	287	287	205	205	275	240	315	307	195	187	133	121	303	279	177	177	121	121
6075	~~HHH~~	F	287	275	205	205	260	235	315	307	199	195	127	121	295	279	181	177	125	125
4013	IH	F	287	283	205	205	260	240	315	311	187	187	121	121	291	287	181	177	129	121
4030	IH	M	287	287	205	205	240	235	315	307	199	187	124	121	295	295	185	181	125	125
4033	IH	F	291	287	205	205	260	240	319	315	199	195	121	121	295	291	177	177	117	117
4038	IH	F	287	283	214	205	240	235	315	307	199	199	133	121	303	291	177	177	125	121
5014	IH	M	287	287	214	211	260	260	311	307	187	187	136	124	303	291	181	177	129	117
5025	IH	M	287	287	214	205	260	240	315	299	195	187	130	121	287	279	181	177	129	117
5028	IH	F	287	287	214	205	260	240	311	299	187	187	130	121	291	279	177	177	121	117
5070	IH	F	291	287	214	205	240	240	319	307	195	195	127	121	291	279	177	177	121	117
5074	IH	M	291	291	214	205	275	260	315	307	199	195	133	121	291	279	181	177	121	113
5084	IH	F	287	283	205	205	235	235	315	311	199	195	130	121	295	291	177	177	125	121
5088	IH	M	275	275	205	205	260	240	315	307	195	187	133	127	291	279	181	177	125	117
6002	IH	M	287	287	214	205	260	240	311	311	187	183	124	121	291	279	193	177	117	117
6008	IH	M	287	287	205	205	240	240	315	311	195	195	121	121	291	287	177	177	129	117
6010	IH	M	283	283	205	205	240	240	315	311	195	183	121	121	291	287	177	177	117	117
6040	IH	M	283	283	214	205	260	235	315	307	199	195	121	121	295	279	177	177	125	121
6043	IH	M	291	291	214	205	240	235	315	307	199	195	136	121	295	287	181	177	125	121
6054	IH	M	287	287	205	205	240	235	307	307	199	195	127	121	291	287	185	177	121	121
6066	IH	F	287	291	214	205	275	240	307	307	199	195	133	121	295	279	177	177	121	113
6071	IH	M	287	287	214	205	275	240	319	307	195	187	121	121	295	291	177	177	117	113
6072	IH	M	287	287	214	205	260	240	307	307	199	195	133	133	295	279	177	177	121	113
6073	IH	M	287	287	205	205	275	240	315	307	199	195	133	121	303	291	177	177	121	113
6074	IH	F	291	287	214	205	261	240	307	307	199	195	121	121	295	279	177	177	121	121
6077	IH	M	287	287	205	205	260	235	315	307	199	187	133	121	291	291	181	177	125	117
6078	IH	M	283	283	205	205	260	235	315	315	195	195	127	121	295	291	177	177	125	125
6079	IH	F	283	283	214	205	240	235	315	315	195	195	124	121	295	283	177	177	121	113
7003	IH	M	287	287	205	205	235	235	307	307	199	199	136	121	291	283	177	177	125	121
5010	normal	F	287	287	205	205	240	240	311	311	187	183	121	121	291	279	197	193	121	117
5036	normal	M	287	287	214	205	240	240	315	311	195	187	130	121	291	279	177	177		129
5051	normal	F	291	287	214	205	240	235	315	307	195	183	136	121	295	279	197	177	125	117
5052	normal	F			205	205	275	235	315	307	195	183	133	121	291	279	197	177	125	117
5063	normal	M	287	287	205	205	265	235	307	299	199	195	121	121	295	287	185	177	125	125
5073	normal	M	287	287	214	205	260	240	319	307	199	195	127	121	295	279	177	177	121	117
5075	normal	F	287	287	205	205	240	240	307	307	199	187	133	121	303	295	177	177	121	113
5082	normal	F	283	295	214	205	260	235	315	303	195	187	124	121	291	283	177	177	121	113
6007	normal	F	287	287	205	208	240	240	311	311	187	183	121	121	279	279	177	177	121	117
6009	normal	M	283	283	205	205	240	240	315	311	195	187	121	121	291	279	177	177	117	129
6011	unknown	M	287	287	214	208	240	240	315	315	195	187	121	121	291	287	177	177	129	117
6039	normal	F	291	287	214	205			319	315	195	183	133	121	295	279	197	177	125	117
6041	normal	F	287	283	214	205	275	260	307	307	199	195	133	121	295	291	177	177	121	117
6042	normal	F	287	283	214	205	240	235	307	307	199	195	133	127	295	279	197	177	125	121
6052	normal	F	291	287	205	205	240	235	315	307	199	199	136	121	287	283	181	177	125	117
6056	normal	M	287	287	214	205	265	240	319	319	199	195	127	121	295	291	185	177	121	117
6063	normal	F	291	287	214	205	240	235	307	307	199	195	136	127	287	279	185	177	121	121
6065	normal	M	291	291	205	205	240	235	307	299	199	195	127	121	287	279	185	177	125	117
6067	normal	F	291	287	214	205	275	240	307	307	195	187	133	121	303	279	181	177	121	113
6069	normal	F	291	287	214	205	260	240	315	307	195	187	133	121	295	291	177	177	117	113
6070	normal	F	291	287	214	205	275	240	315	307	199	195	121	121	303	291	181	177	117	113
6076	normal	F	287	275	205	205	260	235	315	315	195	187	133	130	291	291	177	177	117	125
6080	unknown	F	287	287	211	205	260	240	311	311	187	187	136	121	303	291	197	177	129	117
7001	normal	M	287	287	205	205	240	235	315	307	199	195	136	121	287	283	185	181	125	121
7002	normal	F	287	287	205	205	240	235	315	307	199	199	136	127	287	287	185	177	125	121

Blank spaces mean that genotype information is unavailable

*Refer to Appendix 2 for explanation of amelogenin marker.

INDIV. I.D.	Phenotype	D3S2388		D3S2360		D3S2387		D3S2406		D3S2400		D3S2402		D3S2403	
5027	H+/H+	113	113	260	256	205	160	186	191			234	236	247	239
5029	H+/H+	113	113	272	256	201	160	191	197	210	210	238	238	247	243
5063	H+/H+	117	113	272	256	193	201	197	186			242	238	243	243
5089	H+/H+	113	113	272	248			186	186	210	210	242	242	247	243
6003	H+/H+	113	113	256	256	201	193	186	197			238	238	247	243
6004	H+/H+	113	113	256	256	201	193	186	194	219	201	234	238	247	243
6055	H+/H+	113	113	260	260	205	201	186	191	210	204	234	242	238	239
6064	H+/H+	113	113			205	201	191	191	207	199	238	242	239	239
6066	H+/H+	113	113	321	260	205	193	186	186	210	210			243	239
6075	H+/H+	113	113	248	248	181	181	186	203			234	242	243	243
4013	IH	113	113	272	256	193	160	186	191	210	210	238	238	247	247
4030	IH	113	113	260	256	193	201	191	186	204	204			239	
4033	IH	113	113	280	260	201	205	186	186	210	210	234	234	239	239
4038	IH	117	113	260	256	193	193	186	186	210	210	242	238	243	243
5014	IH	113	113	268	256	201	201	186	200	210	187			247	243
5025	IH	113	113	272	256	201	160	191	197	210	210			243	243
5028	IH	113	113	272	256	193	201	197	186	210	210	238	238	243	247
5070	IH	113	113	260	260	205	205	186	191	210	210	234	238	238	239
5074	IH	113	113	280	260	205	205	191	186	210	210			239	239
5084	IH	113	113	272	248	181	205	203	186	210	213			235	243
5088	IH	117	113	272	248	181	201	186	186	210	210			243	247
6002	IH	109	113	268	256	186	201	200	194	197	219			243	243
6008	IH	105	113	268	260	205	197	186	186	210	210				
6010	IH	113	113	272	256	197	193	186	197	210	210	238	238	243	239
6040	IH	105		280	272	205		203	186	210	210	238	234	239	239
6049	IH	113	113	274	256	205	197	186	194	210	210	234	234	239	239
6054	IH	113	113	280	260	206	201	191	191	210	204	238	242	239	239
6068	IH	113	113	280	272	201	206	186	186	210	210	238	234	238	243
6071	IH	113	113	272	260	193	205	191	186	210	210	242	238	238	243
6072	IH	113	113	260	260	193	205	186	186	210	210	238	234	239	243
6073	IH	113	113	272	260	205	201	186	186	210	210	234	236	239	236
6074	IH	113	113	272	260	193	205	191	186	210		238	234	239	243
6077	IH	117	113	272	272	181	201	203	186	210	213			235	247
6078	IH	117	113	272	248	201	205	203	186	210	213			243	247
6079	IH	109	117	272	256	193	201	197	186	210	210	242	238	243	243
7003	IH	113	113	280	256	205	197	186	191	204	204	234	242	239	239
5010	normal	109	113	268	256	160	193			210	210	236	234	243	243
5038	normal	113	113	272	272	197	193	197	197	219	210			243	243
5051	normal	113	105	272	268	205	205	191	186	210	210	236	236	239	239
5052	normal	105	113	272	260	205	205	203	186	210	213			239	239
5063	normal	113	113	268	256	205	205	186	186	210	204	234	234	243	239
5073	normal	105	113			205	201	186	186	216	210	234		239	239
5075	normal	113	113	272	260	201	193	186	186	210	210			243	243
5082	normal	109	109	272	272	193	193	197	197	210	210			243	243
6007	normal	113	105	272	260	193	197	197	197	210	210	236	234	243	243
6009	normal	113	113	256	272	197	193	186	197	210	210	234	238	243	239
6011	unknown	113	113	272	256	193	205	197	186	210	210	238	234	239	243
6039	normal	105	105	268	260	205	205	197	186	210	210	238	234	239	243
6041	normal	113	105	280	272	201	205	203	186	210	210	238	234	239	239
6042	normal	105	113	272	260	205	201	186	203	210	210	234	234		
6052	normal	113	113	268	256	201	197	186	197	210	204	234		239	239
6056	normal	113	113	258	280	205	201	186	191	207	202	234	238	243	239
6063	normal	113	113	260	256	201	205	186	191	210	210	238	234	239	243
6065	normal	113	113	256	280	205	201	186	191	210	210	234	238	243	239
6067	normal			260	260	201	205	191	186	210	210	238	238	239	243
6069	normal	113	113	260	260	201	205	191	186	210	210	242	238	239	243
6070	normal	113	113	280	260	193	205	186	186	210	210	242	234	239	243
6076	normal	113	113	248	248	181	205	186	186	210	210	240	240	243	243
6080	unknown	109	113	268	258	193	201	200	194	197	218	234	234	243	243
7001	normal	113	113	280	256	197	205	197	191	210	210	238	236	239	239
7002	normal	113	113	280	248	205	201	186	191	210	204			239	239

Blank spaces mean that genotype information is unavailable.

INDIV. LD.	Phenotype	D5S498		D5S469		D5S408		D6S2238		D6S2237		D6S2233	
5027	~~HHH~~	189	179	142	142	256	256	105		129	129/27	157	157
5029	~~HHH~~	189	175	142	142	252	254	95	109	131	123	153	149
5083	~~HHH~~	179	173	142	142	254	256	107	107	131	129		159
5089	~~HHH~~	189	189	142	142	256	264	95	105	131	129	155	155/153
6003	~~HHH~~	179	175	142	142	256	256	101	105	129	129	155	151
6004	~~HHH~~	179	175	142	142	252	256	107	109	131	123	157	149
6055	~~HHH~~	189	175	142	142	254	264	105	105	131	129	157	155
6064	~~HHH~~	189	189	142	142	256	256	95	105	129	113	157	155
6066	~~HHH~~	189	179	142	142	256	260	95	107	131	129	159	155
6075	~~HHH~~	189	189	142	142	254	264	105	109	129	113	155	155
4013	H	179	175	142	142	252	256	105	109	129	123	157	149
4030	H	175	173	142	142	254	254	105	105				
4033	H	189	189	144	142	256	256	105	105				
4038	H	189	173	142	142	254	264	107	107			159	155
5014	H	175	175	142	142	252	256	105	107	131	129	157	155
5025	H	177	173	142	142	252	254	95	105	131	129	157	153
5028	H	177	175	142	142	254	256	95	109			153	149
5070	H	189	189	142	142	256	264	95	105			157	155
5074	H	189	189	142	142	256	260	95	105			157	155
5084	H	189	173	142	142	254	264	107	109	131	113	155	155
5088	H	189	173	142	142	254	256	105		129	129/117	155	155
6002	H	175	175	142	142	256	256	107	109				
6008	H	179	175	142	142	244	254	101	109	131	131	155	151
6010	H	189	175	142	142	244	254	101	103	131	129	157	155
6040	H	179	189	142	142	252	260	95	105				
6043	H	189	189	144	142	254	256	101	105	129	117	157	153
6054	H	189	189	142	142	256	264	105	105	131	129	157	155
6068	H	189	179	144	142	256	260	95				159	155
6071	H	189	189	144	142	254	256	105	107			159	157
6072	H	189	189	142	142	254	256	95	107			159/61	155
6073	H	189	179	144	142	256	256	105	107	131	129	159	157
6074	H	189	179	142	142	254	256	95	107			159	155
6077	H	189	173	142	142	254	256	105	109	129	113	155	155
6078	H	189	173	142	142	254	264	95	109			155	155
6079	H	177	173	142	142	254	256		107				
7003	H	189	189	142	142	256	256	101	105	131	117	155	153
5010	normal	179	175	142	142	256	256	101	109				
5036	normal	175	175	142	142	244	256	103	109	133	129	157	151
5051	normal	175	175	142	142	246	246	95	109			153	153
5052	normal	189	179	142	142	252	256	95	109				
5063	normal	189	173	142	142	254	256	105		129	129	157	155
5073	normal	179	189	144	142	256	260	95	105				
5075	normal	189	179	142	142	254	256	107	107	131	129	159	157
5092	normal	187	175	142	142	254	254	101	105	131	129	155	155
6007	normal	175	189	142	142	254	256	103	107			157	155
6009	normal	189	175	142	142	254	256	101	109				
6011	unknown	175	189	142	142	244	254	103	107				
6039	normal	179	189			256	260	105	109				
6041	normal	189	179	142	142	252	260	95	95				
6042	normal	179	179	142	142	256	260	95	105				
6052	normal	187	177	142	142	254	256	101	105	129	117	157	153
6056	normal	189	189	142	142	254	264	95	105			157	155
6063	normal	189	189	142	142	256	264	105	105			155	155
6065	normal	189	189	142	142	256	264	95	105			157	155
6067	normal	189	189	142	142	254	260	95	107			159	157
6069	normal	189	179	144	142	256	256	105	107			159	157
6070	normal	189	189	144	142	254	256	95	107			159/61	155
6076	normal	173	189	142	142	254	264	105	107			155	155
6080	unknown	175	175	142	142	256	256		105				
7001	normal	189	173	142	142	254	264	101	105				
7002	normal	189	189	142	142	256	264	105	105	129	129	157	157

Blank spaces mean that genotype information is unavailable.